Characterization of the *Arabidopsis thaliana* homologue of NBR1

By

Steingrim Svenning

Master thesis in Molecular Biology

Section of Biochemistry
Department of Medical Biology
University of Tromsø
2006

Acknowledgements

This work was performed at the Molecular Cancer Research Group, Section of Biochemistry, Department of Medical Biology, University of Tromsø.

I extend my sincere thanks to my supervisor Professor Terje Johansen for giving me the opportunity to work on such an interesting project and for providing guidance throughout the project. Thank you also to my co-supervisor Associate professor Trond Lamark for all the help in the lab. Your willingness to share from your depth of knowledge is an inspiration.

Thanks to all the people in the Molecular cancer research group for a wonderful working atmosphere: Turid, Endalk, Julianne, Jennifer, Serhiy, Toril-Anne, Halvard, Kenneth and Eva. Everyone is happy to help, and the daily dose of delightful nerdy humor helps to endure pulldown after pulldown. I want to extend special appreciations to Aud Øvervatn for carrying out all the HeLa cell transfections.

Extended thanks to Professor Kirsten Krause for all the help with the plant experiments, and for enthusiastically contributing with your knowledge to the project. I also want to extend my gratitude to all the people who assisted me at the plant physiology department, especially Ullrich Herrmann and Ania Gorska.

Finally, thanks to my family for their unquestionable support, and to Hanne for keeping me on the straight and narrow path=)

Tromsø, 15.05.09

-Steingrim

Summary

It is now well established that p62 and NBR1 are selectively degraded by autophagy and can act as cargo receptors or adaptors for the autophagic degradation of ubiquitinated substrates. Research on autophagy in plants is also well under way, but the mechanism by which target substrates are sequestered for autophagic degradation has not been elucidated. The uncharacterized plant protein Q9SB64 shares several important functional properties with p62 and NBR1, which indicates that it could act as a cargo receptor for the autophagic degradation of ubiquitinated substrates in plants. Results from this study show that Q9SB64 polymerize via an N-terminal PB1 domain, binds ubiquitin through a C-terminal UBA domain and interacts with the Arabidopsis family of ATG8 proteins. Based on sequence similarity Q9SB64 can be viewed as the Arabidopsis orthologue of vertebrate NBR1 and named AtNBR1. Plants do not seem to have a p62 orthologue. However, with regard to the functional properties studied here AtNBR1 behaves more similar to mammalian p62 than to NBR1.

Abbreviations

At – *Arabidopsis thaliana*

ATG – AuTophaGy

BF – Bright Field

CFP - Cyan Fluorescent Protein

Co-IP – Co-Immunoprecipitation

DTT – Dithiothreitol

GFP – Green Fluorescent Protein

GST - Glutathione-S-Transferase

HeLa – cervical cancer cell line isolated from Henrietta Lacks

HRP- Horse Radish Peroxidase

IP - Immunoprecipitation

LC3 – Light Chain 3

LIR – LC3-interacting region

LSCM - Laser Scanning Confocal Microscopy

mCherry – monomeric Cherry

NBR1 – Neighbor of BRCA1 gene 1

PAGE – PolyAcrylamide Gel Electrophoresis

PAS – Phagophore Assemby Site

PB1 – Phox and Bem 1

PEG – PolyEthylene Glycol

PVDF – PolyVinyliDine Fluoride

RFP - Red Fluorescent Protein

SDS – Sodium Dodecyl Sulphate

UBA – Ubiquitin Associated Domain

Ub - Ubiquitin

UPS – Ubiquitin proteasome system

WT – Wild Type

Table of contents

1.0 Introduction

In the last decade we have witnessed an increased focus on two degradation systems, the Ubiquitin-Proteasome System (UPS) and autophagy. These systems are known to be very important in eukaryotic organisms, in which they play a role in numerous biological processes, from basic cellular functions to human pathophysiology (Klionsky 2007, Reinstein and Ciechanover 2006). The discovery of both systems dates back to the middle half of the last century, but with the development of modern molecular genetics we have now begun to understand the complexity of these systems.

Plants are sessile organisms that require a unique proteomic plasticity to cope with changing environmental conditions. Also, plants go through a series of metamorphic changes during their lifecycle that involves a broad reorganization of cells and tissue. This involves large scale degeneration of biomolecules, which requires a large pool of genes devoted to the proteolytic machinery (Schwechheimer and Schwager 2004). The list of proteins and genes that are thought to be involved in these systems continues to grow, and this study focuses on the uncharacterized plant protein Q9SB64, which is thought to be related to two mammalian proteins acting as cargo receptors for degradation of ubiquitinated targets by autophagy.

1.1 The UPS and Autophagy

Degradation of cellular constituents serves two purposes, which is to remove unwanted or damaged components and to provide the cell with metabolic substrates to maintain energy homeostasis. The proteome of any cell is in a dynamic state of synthesis and degradation, and the turnover of proteins is regulated by specific and general mechanisms of protein degradation. There are sometimes errors in the production of proteins, or damage can occur from external stress such as heat shock or free radicals. These damaged proteins need to be removed since they can cause harm to the cell, and they are also a source of amino acids that the cell can re-use (Meusser *et al.* 2005, Nakamura and Lipton 2007). The UPS is the main route of specific protein degradation in the cell, and is thought to regulate protein lifetime as well as degrade damaged proteins (Hershko and Ciechanover 1998). Ubiquitin (Ub) is a highly conserved 8.5 kDa protein that can be conjugated to lysine residues of other proteins by Ub-conjugating enzymes (Hershko *et al.* 2000, Schlesinger *et al.* 1975). The Ub-marker

signals the fate of the protein, and polyubiquitin chains (poly-Ub) usually target the protein for degradation (Chau et al. 1989). Poly-Ub chains are formed when additional Ub is attached to lysine residues on a previously attached Ub, and several different poly-Ub chains can be formed depending on which lysine is connected. In principal, all the lysines can be used for making chains (Lys6, Lys11, Lys27, Lys29, Lys33, Lys48 and Lys63), but the two most studied chains are the Lys63 and Lys48 linked chains. Lys63 linked Poly-Ub chains are thought to be mainly involved in non-catabolic processes, while Lys48 linked Poly-Ub chains are known as a tag for protein degradation by the proteasome (Hochrainer and Lipp 2007). The proteasome is a multiprotein complex that binds ubiquitinated proteins and degrades them in a proteolytic core. The following figure illustrates the process of ubiqutination and degradation by the proteoasome.

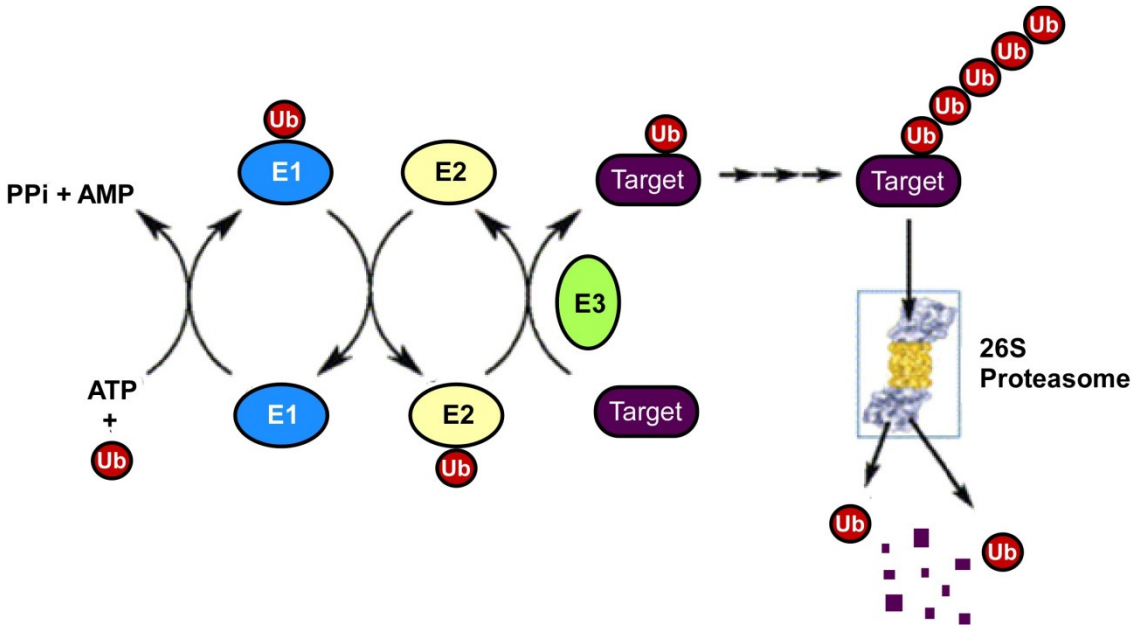

Figur 1.1: Ubiquitination of proteins targeted to the proteasome. Ub-activating enzyme (E1) binds Ub, which is then transferred to an Ub-conjugating enzyme (E2); a Ub–protein ligase (E3) helps transfer Ub to the target substrate. Polyubiquitinated proteins are transported to the 26S proteasome where the Ub tags dissociate and the target protein is degraded.

In addition to targeting proteins for degradation, ubiquitination is thought to partake in several other regulation systems, like endocytic sorting (Hicke 2001) and DNA repair (Hoege et al. 2002).

Autophagy (or “self eating”) is the term for lysosomal degradation of cytoplasmic components. The term autophagy was introduced at the CIBA Foundation Symposium on Lysosomes in 1963 by Christian De Duve, and then clearly defined in a review article in 1966 (De Duve and Wattiaux 1966). “Auto” and “phagein” literally means self-eating, referring to degradation of material from within the cell, and is made to distinguish this process from heterophagy, where a cell degrades material that is taken up by endocytosis (from outside).

The general mechanism has been named macroautophagy. In a recent paper, D. Klionsky tries, together with other researchers in this field, to define a nomenclature for all the autophagic processes that have been identified (see appendix, table 6.1), and this is their definition of macroautophagy; “Macroautophagy is the largely nonspecific autophagic sequestration of cytoplasm into a double- or multiple-membrane-delimited compartment (an autophagosome) of nonlysosomal/vacuolar origin. Note that certain proteins may be selectively degraded via macroautophagy, and, conversely, some cytosolic components such as cytoskeletal elements are selectively excluded” (Klionsky *et al.* 2007). Following this description, several forms of macroautophagy were discussed, including the sequestering of organelles (the mitochondrion, peroxisome and endoplasmatic reticulum), protein aggregates and microbes. Common for all of these processes is the formation of an autophagosome, which forms around the target structure and delivers it to the lysosome (see figure 1.2).

In another type of autophagy, microautophagy, the lysosome/vacuole itself engulfs a part of the cytosol. This process is not well understood, but seems to be involved in degrading peroxisomes and mitochondria (micropexo/mitophagy) and portions of the nucleus (piecemeal microatuophagy) (Kanki and Klionsky 2008, Kvam and Goldfarb 2007, Sakai *et al.* 1998). Furthermore, some autophagic pathways have been discovered that falls outside these categories. Cytoplasm to vacuole targeting (Cvt) is a unique pathway in yeast that that transports resident hydrolases to the vacuole, while chaperone mediated autophagy (CMA) and vacuole import and degradation (Vid) are selective forms of autophagy that proceeds without the formation of autophagosomes (Kim and Klionsky 2000, Majeski and Dice 2004, Shieh and Chiang 1998).

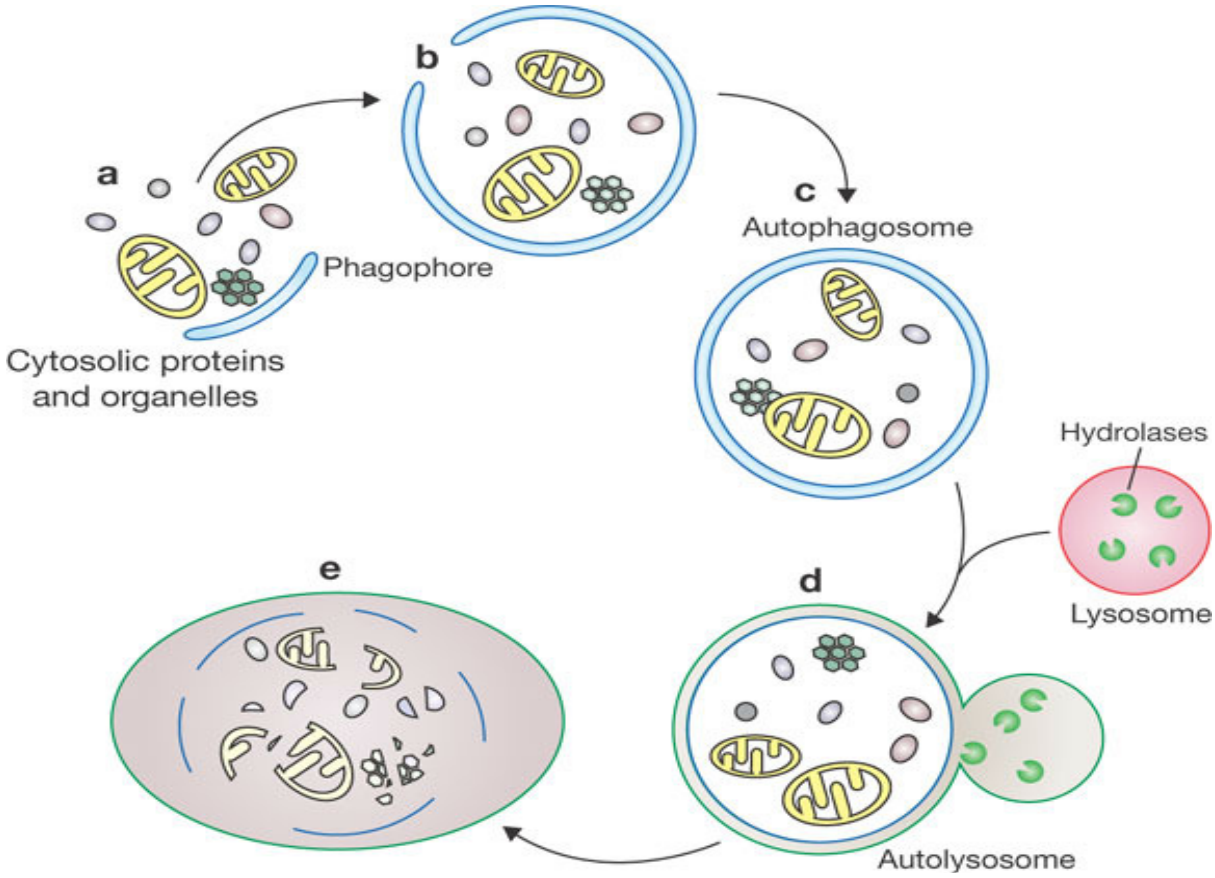

Figur 1.2 Schematic depiction of autophagy in mammalian cells. (a, b) Cytosolic material is sequestered by an expanding membrane sac, the phagophore, **(c)** resulting in the formation of a double-membrane vesicle, an autophagosome; **(d)** the outer membrane of the autophagosome subsequently fuses with a lysosome, exposing the inner single membrane of the autophagosome to lysosomal hydrolases; **(e)** the cargo-containing membrane compartment is then lysed, and the contents are degraded (from Xie and Klionsky 2007).

The basic function of autophagy is to serve as a "household cleaning mechanism", referred to as constitutive autophagy. Organelles are degraded when they become old and accumulate damage from radicals and mutations (Bellu *et al.* 2001, Lemasters 2005). Long-lived and damaged proteins also needs to be removed, else they are prone to form protein aggregates which can accumulate and harm the cell (Rubinsztein 2006).

Autophagy is upregulated in response to various types of stress, like starvation, organelle damage and oxidative stress. Starvation-induced autophagy, as by rapamycin-induced inhibition of the Tor-pathway, allows the cell to rapidly degrade proteins and organelles that are not essential for survival, thus freeing valuable amino acids that can be used for energy or synthesis of new proteins that supports basic cellular functions (Kristensen *et al.* 2008, Kuma *et al.* 2004, Noda and Ohsumi 1998). The connection between the UPS and autophagy is not very well understood, but two independent studies confirm that the two are mechanistically

linked. A very recent paper reports that two heat-shock proteins, Bag1 and Bag3, are regulators of the proteosomal and autophagic pathways. Bag1 is required for effective proteosomal degradation while Bag 3 promotes autophagy, and the flux between these two proteins provides a "switch" between the UPS and autophagy (Gamerdinger *et al.* 2009). When the UPS is impaired in *Drosophila melanogaster*, autophagy acts as a compensatory degradation system in an HDAC6-dependent manner (Pandey *et al.* 2007).

It is also becoming increasingly clear that, like the uibiquitin proteasome system, autophagy deficiency is linked to severe diseases in humans. Whether it prevents or cause disease is sometimes unclear, and the paradox of autophagy is that it can act to promote both cell survival and cell death, depending on the specific conditions of the disease (Levine and Kroemer 2008). Among the first diseases to be associated with defects in the proteolytic machinery were the neurodegenerative diseases Alzheimers, Parkinsons and Huntingtons. Common for these types of disease is the accumulation of autophagic vesicles and protein aggregates in neuronal brain cells, resulting in cell death and loss of brain function (Komatsu *et al.* 2007a). Experiments in mice have shown that a shut-down of constitutive autophagy leads to symptoms of neurodegeneration (Hara *et al.* 2006). As autophagy is closely connected to cell homeostasis it is predictably also involved in cancer (tumorigenesis), and accumulating evidence now points to autophagy as a tumor suppressor pathway (Mizushima *et al.* 2008). The term Xhenophagy have been coined to describe selective autophagic digestion of microbes in response to pathogen invasion (Klionsky, et al. 2007). A good example of this is the autophagic degradation of the Herpex simplex virus (Talloczy *et al.* 2006). On the other hand, pathogens have also evolved strategies to utilize/avoid autophagic degradation (Orvedahl and Levine 2008). Yersinia pestis, the bacteria responsible for the Black death, is sequestered to autophagosomes by xenophagy, but the bacteria then prevents the acidification of the autophagosome, essentially creating a protected environment where it survives and replicates (Pujol *et al.* 2009). Toxoplasma is a mammalian parasite that has been shown to derive nutritional benefits from upregulating host cell autophagy (Wang *et al.* 2009).

Most of our understanding of the molecular mechanism of autophagy comes from experiment with yeast (*Saccharomyces cerevisiae)*. In 1992, Yoshinori Ohsumi's laboratory demonstrated active autophagy in yeast (Takeshige et al. 1992), which sparked the use of yeast as a model species for studies on autophagy. Approximately 30 genes have now been identified that are

involved in the core machinery of autophagy, so-called AuTophaGy genes (ATG) (Klionsky *et al.* 2003), and half of these are associated with the basic task of forming the autophagosome (Xie and Klionsky 2007). After identifying the ATG-genes it became evident that autophagy is directed by a sequential series of post-translational modifications, two of which employs the Ub-like conjugation systems Atg8-phosphatidylethanolamine (Atg8-PE) and Atg12-Atg5 (Mizushima *et al.* 1998). These modifications are ATP-dependent and involves E1 (activating) and E2 (conjugating) enzymes that attach two small proteins, ATG8 and ATG12, to their respective targets, phosphatidylethanolamine (PE) and the ATG5 protein. The two steps are initiated by the same E1 enzyme ATG7. ATG8 is anchored to the isolation membrane of the autophagosome and is conserved among higher eukaryotes (Ohsumi 2001). It has been shown that the size of the autophagosome is directly dependent on the amount of ATG8 (Xie *et al.* 2008), and the theory is that ATG8 helps enlarge the forming autophagosome to wrap around the target substrate. ATG8 has proved particularly useful in studying the autophagic process, as ATG8-fusion proteins can be used without disrupting membrane formation (Kimura *et al.* 2009). In mammals, ATG8 is represented by at least seven related proteins that fall into two subgroups, LC3- and GABARAP-like proteins (He *et al.* 2003, Xin *et al.* 2001).

1.2 The UPS and Autophagy in plants

As mentioned earlier, plants are sessile organisms that have to adapt to changing environmental conditions, and furthermore they undergo several metamorphic changes during their lifecycle, like germination, flowering and senescence. For this to be possible, the plants need a high degree of proteomic plasticity to quickly reorganize cells and tissue. This rapid turnover of cell components is orchestrated by the proteosomal and autophagic pathways.
Consistent with this is the large number of genes coding for components in the proteosomal machinery. Approximately 6% of the genome in *Arabidopsis thaliana* is UPS coding genes (Downes and Vierstra 2005b), and with the notable exception of *Caenorhabditis elegans,* this is more than any other known eukaryotic model organism (Schwechheimer and Schwager 2004). The UPS has been linked to most of the major biological processes in plants, like hormone regulation (Dreher and Callis 2007), circadian rhythm (Han et al. 2004), light signaling (Hoecker 2005, Somers and Fujiwara 2009) and organ initiation and patterning (Imaizumi et al. 2005). The major part of the UPS proteome consists of the Ub conjugating enzymes (E1, E2 and E3). One of the largest known gene superfamilies in *Arabidopsis* is the

700 potential F-box genes (Gagne et al. 2002), which are a part of over 1600 E3 ligases encoded for by the *Arabidopsis* genome (http://plantsubq.genomics.purdue.edu/). The core machinery of the UPS in plants is not much different from that of other eukaryotes. Protein degradation by the UPS in plants is basically the same as presented in figure 1.1.

When discovering the importance of the UPS in plants there was reason to believe that autophagy plays an equally important role, and as a consequence there has been an increase in research on autophagy in plants. Much of this research has been carried out in *Arabidopsis thaliana,* which is a fully sequenced plant model organism that is favored for easy genetic manipulation and short generation time (Meyerowitz 2001). Several other species like tobacco, rice, barley and even mango, are used due to their physical properties or commercial value. We now know that autophagy proceeds in plants much as it does in other eukaryotes. The single biggest difference between plant cells and animal cells is the central vacuole. Whereas animal cells have many small acidic vacuoles (lysosomes), plant cells have one acidified vacuole that fills almost the entire cell, and autophagic substrates wrapped in an autophagosome are sent to the central vacuole to be degraded. Two of the best described autophagic systems in Arabidopsis is micro- and macroautophagy (Bassham *et al.* 2006). Autophagy has been shown to act constitutively in plants during nutrient-rich conditions, presumably as a housekeeping machinery to recycle molecules for biosynthesis and for supplying substrates for respiration (Inoue *et al.* 2006, Slavikova *et al.* 2005, Yano *et al.* 2007). Upon starvation stress, autophagy is upregulated and important for proper nutrient recycling (Doelling *et al.* 2002, Rose *et al.* 2006). Autophagy is also especially important in response to oxidative-stress, which occurs even in nutrient-rich conditions (Xiong *et al.* 2007).

Autophagic degradation of mitochondria and peroxisomes has so far not been shown in plants. A comparative study of ATG genes has shown that the genes involved in the pexophagic pathway of yeast are not found in Arabidopsis (Wiebe *et al.* 2007). Considering this, an interesting recent finding is that the chloroplasts, or pieces of the chloroplast, is degraded by autophagy during starvation stress (Ishida *et al.* 2008, Wada *et al.* 2009).
An analogue of the yeast cytoplasm to vacuole targeting (Cvt9 pathway has been described (Herman and Schmidt 2004), but the alternative autophagic pathways vacuole import and degradation (Vid) and chaperone mediated autophagy (CMA) has not yet been shown to operate in plants.

As with the UPS, autophagic pathways have been shown to function in numerous developmental processes, but the characterization of ATG-genes involved in developmental stages is made difficult by a lack of obvious phenotypes. Autophagy-deficient plants can go through normal lifecycles from germination to seeding, and only careful phenotypic analysis in combination with stress treatment has revealed some differences between wild type and Atg-mutants. Autophagy-deficient plants have shorter root growth and accelerated senescence during stress, strengthening the theory that autophagy is required, but not essential, for proper protein and nutrient recycling. During plant development, autophagy generally coincides with programmed cell death. Plants do not seem to have apoptosis, and it is believed that programmed cell death is largely associated with autophagy (van Doorn and Woltering 2005). Programmed cell death is also used as defense against invasive pathogens, and autophagy has been shown to regulate programmed cell death in the hypersensitive response to pathogen infections (Liu *et al.* 2005).

Due to the high degree of ATG gene conservation, the dissection of autophagy in yeast has also laid foundation for understanding autophagy in plants (Thompson and Vierstra 2005). There is a high overall conservation of ATG-genes between yeast and plants, and several Arabidopsis ATG proteins have been shown to be able to complement the function of their yeast counterparts (Ketelaar *et al.* 2004). A feature of the Arabidopsis ATG-proteins is that some are encoded for by small gene families. For an overview of ATG-homologues in plants, see (Bassham, et al. 2006). The previously described Ub-like conjugation systems Atg8-PE and Atg12-Atg5 are also present and are essential for autophagy in plants (Fujioka *et al.* 2008, Ishida, et al. 2008, Suzuki *et al.* 2005, Thompson *et al.* 2005). ATG8 is present in Arabidopsis as a small family of nine different homologues (AtATG8A-I), and has been visualized in autophagic bodies that are delivered to the central vacuole (Thompson, et al. 2005). In autophagy-deficient Arabidopsis, no AtATG8-containing inclusions could be seen in the vacuole, which proves that the dotted structures are AtATG8 containing autophagic bodies. Fluorescently tagged AtATG8 is now commonly used as a marker protein, which allows nondestructive detection of autophagy induction (Matsuoka 2008). In a comprehensive study of AtATG8 in Arabidopsis seedlings, the expression was found to be highest in the elongating parts of the root, which is thought to be connected to the high degree of damage that new roots suffer when penetrating the soil. Also, the different homologues of AtATG8 showed different expression patterns, indicating differential non-redundant functions of the individual

homologues (Slavikova, et al. 2005). Little is known about the signaling pathways that regulate autophagy in plants, but the target of rapamycin (TOR) signaling pathway has recently been described in plants, and considering the connection between autophagy and TOR in mammalian cells there is reason to believe that TOR have a role in regulating plant autophagy (Bassham 2009).

1.3 p62 and NBR1

The fate of ubiquitinated proteins is not only decided by the length of the Ub-chain. Several proteins have been found to act as Ub-receptors, and these proteins help direct the traffic of ubiquitinated proteins, further establishing the diversity of pathways that ubiquitination can lead to. One of these proteins is the mammalian protein p62/SQSTM1 (sequestosome 1), which was first investigated for interaction with atypical PKC (Park *et al.* 1995, Puls *et al.* 1997, Sanchez *et al.* 1998). p62 is actually a 50kDa protein, but the name was given because the protein migrates like a 62kDa protein SDS polyacrylamide gels. It was found to interact with Ub using the C-terminal region, and then suggested to be partly involved in signal transduction through Ub-mediated protein degradation (Vadlamudi *et al.* 1996). This established p62 as a multifunctional scaffolding protein involved in both transcriptional activation and protein degradation. Later studies demostrated that p62 interacts with itself and other proteins through a N-terminal PB1 domain (Gong *et al.* 1999, Lamark *et al.* 2003, Wilson *et al.* 2003), and an interaction was established between the proteasome and p62, indicating that p62 might work as a shuttling protein for the UPS (Seibenhener et al. 2004).

When studying the fate of these p62-containing protein aggregates, which in many cases are too big to be degraded by the proteasome, the next evidence lead to the lysosome. Protein aggregates containing p62 was found to be delivered to autophagosomes for lysosomal degradation (Bjørkøy *et al.* 2005), thus suggesting a novel role for p62 in protein degradation. It indicated that p62 acts as a shuttling protein in the autophagic machinery, collecting ubiquinated protein aggregates and delivering them for autophagic degradation. This was supported by the identification of a 22-residue LC3 interaction region (LIR) in p62 (Pankiv *et al.* 2007), which allows p62 to bind ATG8. The working theory is that p62 binds ubiquitinated proteins and creates protein inclusions by self-polymerization. The p62-containing inclusions bind to phagophore-associated ATG8 in a forming autophagosome, which then fuses with a lysosome and the content is degraded (Bjørkøy, et al. 2005, Ichimura

et al. 2008, Komatsu *et al.* 2007b, Pankiv, et al. 2007). Recent studies have shown that long-lived cytosolic proteins, peroxisomes, and midbody rings can be targeted for autophagic degradation by ubiquitination, and that p62 is required for targeting of these substrates (Kim *et al.* 2008, Pohl and Jentsch 2009). In addition, p62 has been detected in Ub-containing protein inclusions (protein aggregates) in neurodegenerative and liver diseases (Kuusisto *et al.* 2001, Strnad *et al.* 2008, Utako Nagaoka 2004, Zatloukal *et al.* 2002), which suggest that p62 contributes to their clearance by autophagy.

The ability to interact with other PB1 containing proteins as well as ubiquitinated proteins allows p62 to integrate kinase-activated and Ub-mediated signaling pathways (Moscat *et al.* 2007). Experiments with p62-knockout mice have shown that p62 is required for activation of NF-κB by Ras, and this identified p62 as target of Ras regulation (Duran *et al.* 2008). p62 has been shown to bind other regulatory proteins such as TNF receptor-associated factor 6 (TRAF6) and extracellular regulated kinase (ERK), which are important signaling adaptor proteins. TRAF6 plays an essential role in osteoclastogenesis and bone remodeling, and mutations in the UBA domain of p62 have been linked to Paget's disease of bone, a genetic disorder characterized by aberrant osteoclastic activity (Kurihara *et al.* 2007). A recent study has also reported p62 to be involved in the regulation of hypoxic cancer cell survival responses by activation of the ERK1/2 pathway (Pursiheimo *et al.* 2009).

Another mammalian protein that is now linked to autophagy is NBR1. It has not been as extensively studied as p62, but is known to interact with p62 in the assembly of sarcomeric proteins, and is involved in linking the titin kinase to a signalosome to regulate expression of muscle-specific genes (Lange et al. 2005). Although NBR1 is about twice the size of p62 and the sequence identity is low, the two proteins share an overall domain architecture, with an N-terminal PB1 domain and a C-terminal UBA domain (see figure 1.4). NBR1 has the ability to self-interact through a coiled coil domain and interacts with p62 through the PB1 domain (Lamark, et al. 2003). These factors led to the belief that NBR1 may also be a target of autophagy, and a recent paper confirms this hypothesis. NBR1 interacts with human ATG-8 homologues through a conserved LIR and a secondary interaction surface, and is degraded by autophagy in a similar manner as p62 (Kirkin *et al.* 2009b). Both proteins are found in Ub-positive aggregates upon inhibition of autophagy, indicating that p62 and NBR1 cooperate in bringing ubiquitinated cargo to the forming autophagosome via interaction with membrane-bound ATG8 family proteins (Kirkin *et al.* 2009a, Lamark *et al.* 2009).

1.4 Q9SB64, the plant homologue of NBR1?

In view of the newly discovered importance of p62 and NBR1 in mammalian autophagic systems, and considering the high conservation of genes involved in autophagy, it is reasonable to believe that these proteins are conserved in other eukaryotes. The protein Ref(2)P has been found to colocalize with Ub-containing protein aggregates in the adult brain of *Drosophila melanogaster* (Nezis *et al.* 2008). Ref(2)P also has a similar domain architecture as p62, with an N-terminal PB1 domain, a central ZZ-type zinc finger domain and a C-terminal UBA domain, and is considered a homologue of p62. No homologues to p62 or NBR1 has been described in yeast, but the yeast protein ATG19 have been shown to bind ATG8 in a similar manner as p62 (described later) in an interaction that mediates transport of aminopeptidase I (Ape1) into the vacuole via the Cvt pathway (Scott *et al.* 1997), and although ATG19 is unrelated to p62 in sequence, this pathway is similar to the p62-mediated autophagic degradation of protein aggregates.The field of research on autophagy in plants is quickly expanding, and it is beyond questioning that autophagy plays a crucial role in plant development and in response to stress. Autophagic bodies containing various cytosolic components are known to be delivered to the central vacuole for degradation, but the mechanisms behind the sequestration of autophagic substrates to the autophagosomes have not been described. It would be of great interest to find a protein that serves the same functional role as p62 and NBR1, as these proteins plays a crucial role in selective autophagy in mammalian systems. This would also shed light on the evolutionary development of autophagy.

Out of the 44 PB1 domain containing proteins in *Arabidopsis thaliana*, the uncharacterized protein Q9SB64 (gene At4g24690) shows a distinct structural resemblance to p62 and mammalian NBR1 (see figure 1.3).

Figur 1.3: Predicted domain architecture of Q9SB64. This schematic representation of Q9SB64 was obtained from the SMART database (http://smart.embl-heidelberg.de/)

Q9SB64 is intermediate to p62 and NBR1 in length (704 amino acids), has a predicted N-terminal PB1 domain, a zinc finger, and two C-terminal UBA domains. This is strikingly similar to the domain organization of p62 and NBR1 (see figure 1.4)

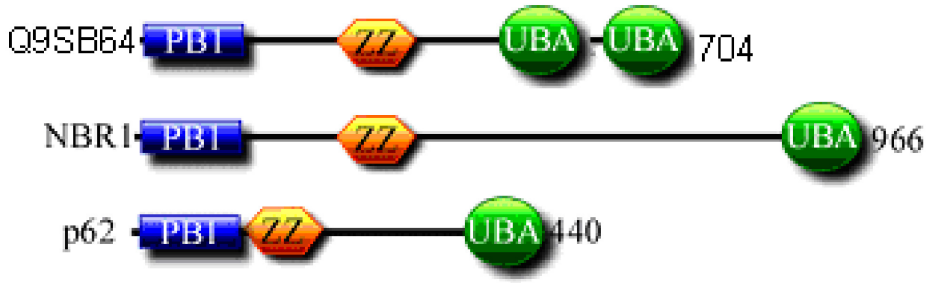

Figur 1.4. The domain architecture of Q9SB64 is similar to that of p62 and NBR1. Schematic illustration of the domain architecture of Q9SB64, p62 and NBR1.

To further establish the function of AtNBR1 it is necessary to review the protein domains. A PB1 domain possibly gives Q9SB64 the ability to interact with other proteins, and perhaps also to self-interact. The UBA domains are the largest group of Ub-receptors, which suggests that Q9SB64 interacts with ubiqiutinated proteins.

1.5 Domain Phox and Bem 1 (PB1)

Through various interactions, proteins are able to self-interact to form polymers. The described proteins p62 and NBR1 both have the ability to self-interact, but while NBR1 has been found to self-interact using a coiled-coil (CC) domain, p62 uses its PB1 domain (Lamark, et al. 2003). Coiled-coil domains are structural motifs in proteins that enables two or more α-helixes to coil up like a twisted rope (Crick 1953). Coiled coil domains are implied in many polymerizing proteins (Beck and Brodsky 1998). PB1 is a conserved protein domain found in animals, plants, amoebae and fungi. The domain is used to mediate protein-protein interactions and was named PB1 (Phox and Bem 1), because it was initially discovered in mammalian p67^{phox} (microbicidal phagocyte NADPH oxidase activator) and the yeast polarity protein Bem1 (T. Ito 2001). Three separate groups of PB1 domains are now recognized (Lamark, et al. 2003, Noda *et al.* 2003, Sosuke *et al.* 2003, Sumimoto *et al.* 2007, Wilson, et al. 2003). Type I contains an OPCA motif of the conserved sequence Asp-X-(Asp/Glu)-Gly-Asp-X8-(Glu/Asp), where X is any amino acid. Type II PB1 does not contain the OPCA motif, but instead a conserved Lys on the first β-strand which is not found in type I. In addition a third type exists, type I/II which contains both the OPCA motif and the conserved Lys (see figure 1.5).

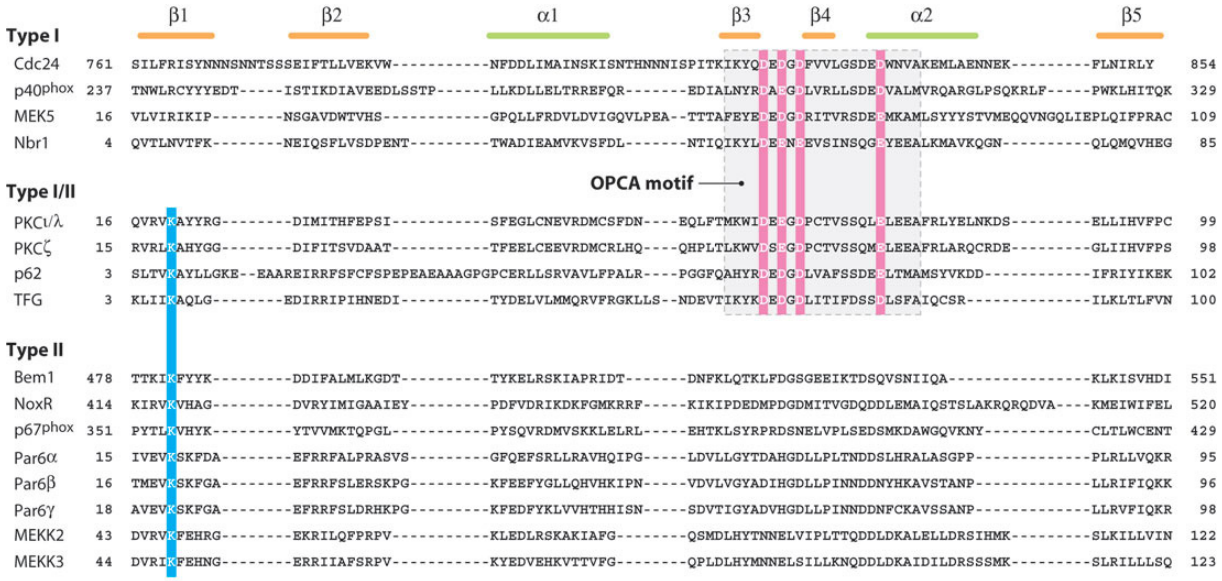

Figure 1.5: Alignment of PB1 protein sequences. Conserved amino acids in the basic (cyan) and acidic (magenta) regions of the PB1 domains are indicated (from Sumimoto, et al. 2007).

All the three types of PB1 domains are structured like a Ub-like β-grasp fold, and consist of two α helices and a mixed five-stranded β sheet (Hirano *et al.* 2004, Hirano *et al.* 2005, Honbou *et al.* 2007, Ito *et al.* 2001, Müller *et al.* 2006, Sosuke, et al. 2003, Wilson, et al. 2003).

Binding between proteins that contain PB1 is due to electrostatic forces between the charged basic cluster and the acidic OPCA motif (see figure 1.6). Heterodimerization is theoretically possible between proteins containing type I and type II PB1 domains, while type I/II can interact with both other types. However, the interaction between PB1 containing proteins is highly specific (Lamark, et al. 2003). Type I/II also have the possibility to homo-oligomerize, but so far only the PB1 domain of p62 have been shown to bind to itself (Lamark, et al. 2003). NBR1 contains a Type I PB1 domain that cannot be used for homo-oligomerization, which is consistent with the knowledge that NBR1 uses a coiled coil-domain to polymerize. p62 can self-interact and form polymers through its type I/II PB1 domain, and mutations that affects the acidic or basic properties of the domain disrupts the ability to polymerize (Lamark, et al. 2003). The PB1 domains also allow p62 and NBR1 to interact and work together.

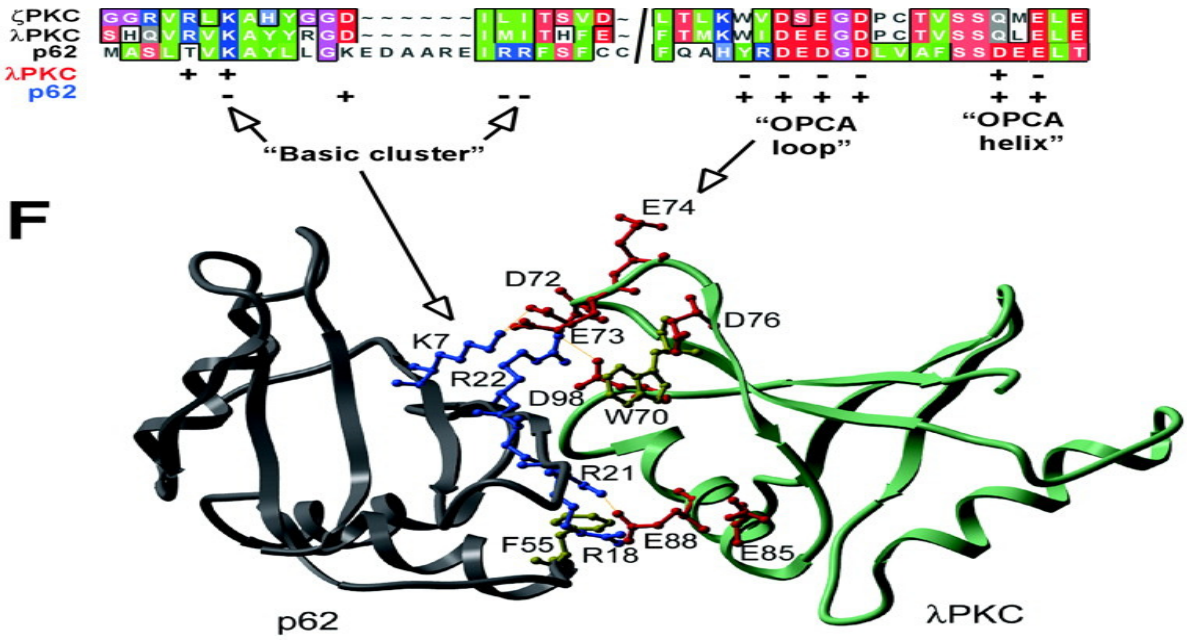

Figur 1.6: Binding between p62 and aPKC through a basic cluster and the acidic OPCA loop and helix in PB1 (from Lamark, et al. 2003)

1.6 Ubiquitin associated domain (UBA)

UBA was the first of the Ub binding domains to be described in a group of domains that now contains at least 16 different Ub binding domains (Hurley J *et al.* 2006). The domain is a compact three helix bundle that binds to Ile^{44} on Ub through a hydrophobic patch (see figure 1.7). Four different classes of UBA domains are now recognized, based on their ability to bind poly-Ub (Raasi *et al.* 2005).

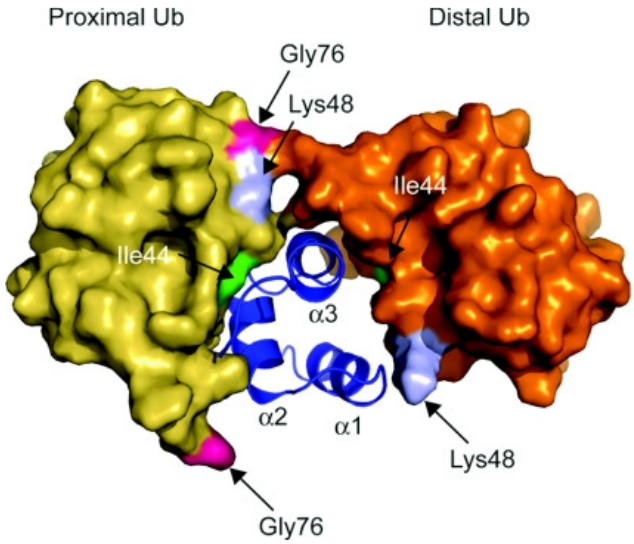

Figure 1.7: Poly-Ub recognition by the human HR23a UBA 2 domain. The Lys48 linked di-Ub (yellow and orange) is bound to UBA (blue) through a hydrophobic interaction. (from Hurley J, et al. 2006)).

p62 and NBR1 have both been shown to bind Ub through a C-terminal UBA domain (Kirkin, et al. 2009b, Vadlamudi, et al. 1996). This enables p62 and NBR1 to bind ubiquitinated proteins and deliver them to the autophagosome. Affinity studies have shown that the isolated UBA domain of NBR1 bound mono- and di-Ubquite well, while the isolated UBA domain of p62 binds to weakly for affinity constants to be determined (Kirkin, et al. 2009b). Experiments with full-length proteins gave the opposite results. Full-length NBR1 had a weak affinity for tetra-Ub (4xUb), and this interaction was further weakened by deletion of the CC1 domain. Polymeric p62 bound 4xUb much more strongly, and this interaction was only slightly weakened when using monomeric p62 (Kirkin, et al. 2009b).

1.7 LC3-interacting region (LIR)

ATG8 is a Ub-like protein that is essential for autophagosome formation (Ohsumi 2001). The typical ATG8 protein is composed of two domains, a C-terminal Ub-fold and two alpha helices made of N-terminal residues (Sugawara *et al.* 2004). Both p62 and NBR1 have been shown to interact with LC3 and GABARAP family proteins, the mammalian orthologues of yeast ATG8, and this interaction is required for autophagic degradation of p62 and NBR1 positive inclusions (Kirkin, et al. 2009b, Pankiv, et al. 2007). A similar motif is found in yeast ATG19, which binds to yeast ATG8 in the selective Cvt pathway. The interaction is mediated by a short region of approximately 10 aa that binds to LC3, hence the name LC3 interaction region (LIR) (Pankiv *et al.* 2007a). Determination of crystal structures have revealed that binding is dependent on a hydrophobic motif (WXXL) that is conserved in p62 and yeast ATG19 (Ichimura, et al. 2008, Kirkin, et al. 2009b, Noda *et al.* 2008). The side chain of the tryptophan is bound to a hydrophobic core between the N-terminal domain and the Ub-like domain, while the side chain of the leucine is bound to the hydrophobic pocket on the Ub-like domain. In addition, the hydrophobic motif is surrounded by acidic residues that contributes to the binding (Pankiv, et al. 2007). NBR1 is found to have a LIR similar to that of p62 and yeast ATG19 (amino acids 727–738), and a second interaction surface has also been identified (LIR2), but this one does not seem to have the same importance as LIR1. (Kirkin, et al. 2009b). Both in p62 and NBR1, LIR is located in the C-terminal part of the protein, upstream of the UBA domain (see figure 1.8).

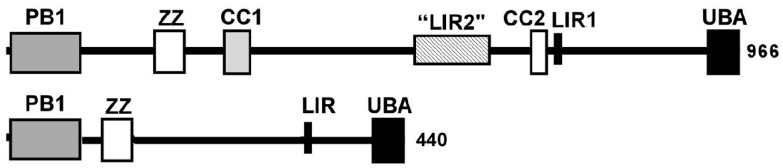

Figur 1.8: LIR is located in the C-terminal region of p62 and NBR1. Schematic illustration of protein domains in p62 and NBR1.

Arabidopsis contains a family of nine ATATG8 (A-I) homologues of yeast ATG8. AtATG8 is present in inclusions that are transported by autophagy to the central vacuole, and is at present used as a model protein for observing autophagy in plants (Matsuoka and Klionsky 2008). A possible interaction between Q9SB64 and AtATG8 is therefore a strong indication of involvement in autophagy. To further investigate this interaction, the identification of an ATG8 interaction surface in Q9SB64 is necessary.

1.8 Aim of study

The overall aim of this study was to investigate whether Q9SB64 is the Arabidopsis homologue of mammalian NBR1 or p62, and to find out if Q9SB64 is a selective autophagy substrate in plants. Determining whether Q9SB64 is involved in autophagy will be a large step towards understanding of autophagy in plants, and from an evolutionary point of view, identifying a plant homologue of p62 and NBR1 is interesting in itself. The first part of the study was dedicated to biochemical experiments with Q9SB64 to determine the function of the protein domains. Similar experiments have previously been performed with p62 and NBR1, and should provide a basis for determining whether Q9SB64 is functionally related to NBR1 or p62.

The following questions were posted for biochemical experiments with Q9SB64;

1. Does Q9SB64 have the ability to self-interact, and if so, is this mediated by the PB1 domain?
2. Does Q9SB64 bind Ub, and if so, do the UBA domains participate in this interaction?
3. Does Q9SB64 bind AtATG8, and if so, what is the minimal sequence required for this interaction?

The second part of the study was dedicated to cell based experiments with Q9SB64, where fluorescent tags were used to study how wild type and mutated Q9SB64 behave in cells. The experiments were performed in Arabidopsis protoplast and human HeLa cells.

The following questions were posted for cell based experiments with Q9SB64;

1. Does Q9SB64form aggregates in cells, and if so, is the aggregation dependent on the PB1 and/or UBA domains?
2. Does Q9SB64 colocalize with AtATG8 in cells and is AtNBR1 sequestered to acidified compartments in plant or mammalian cells?

In addition, transformation of whole plant Arabidopsis was carried out with fluorescently tagged Q9SB64. This will provide the basis for experiments with Q9SB64 in transgenic plants.

2.0 Materials and methods

2.1 Materials

Table 2.1: Vectors used in the study

Plasmids used in this study	Description	Reference
	Gateway cloning vectors	
pENTR 1A	Gateway® Entry Vector, Kan^R	Invitrogen
pENTR 2B	Gateway® Entry Vector, Kan^R	Invitrogen
pENTR 3C	Gateway® Entry Vector, Kan^R	Invitrogen
pENTR 2B-end	Gateway® Entry Vector, pENTR 3C, with three stop codons in the last part of the downstream polylinker, Kan^R	T. Lamark
pDONR201	Gateway® DONR vector, DONR201, Kan^R	Invitrogen
pDest-EGFP-C1	Mammalian EGFP fusion expression vector, CMV promoter, Amp^R	Bjørkøy *et al.,* 2005
pDest-myc	Mammalian myc-tag fusion expression vector, CMV & T7 promoters, Amp^R	Lamark *et al.,* 2003
pDest-mCherry-C1	Mammalian mCherry fusion expression vector, backbone as pDestEGFP-C1, Amp^R	Pankiv *et al.,* 2007
pDestHA	Mammalian HA-tag fusion expression vector, CMV and T7 promoters, Amp^R	Lamark *et al.,* 2003
pcDNA-Dest53	Mammalian GFP fusion expression vector CMV and T7 promotors, Amp^R	Invitrogen
pDest15	Mammalian GST fusion expression vector CMV and T7 promotors, Amp^R	Invitrogen
pENTR-AtNBR1	Gateway® PENTR/SD-DTOPO vector with At NBR1	SSP Consortium
pENTR-AtATG8G	Gateway® PENTR/SD-DTOPO vector with Arabidopsis ATG8G	SSP Consortium
pENTR- NBR1	Gateway® Entry Vector with human NBR1	Lamark *et al.,* 2003
pENTR- p62	Gateway® Entry Vector with human p62	Lamark *et al.,* 2003
pENTR- p62Δend	Gateway® Entry Vector with human p62 lacking stop codon	T. Lamark
	pUNI51 cloning vector	
pUNI51	pUNI51 Cloning Vector, Universal cloning vector used for ORF clones	SSP Consortium
	Plant expression vectors	
pEarleygate104	Plant YFP fusion vector, Binary, 35S promotor, Kan^R, Bar	(Keith W. Earley 2006)
pB7FWG2,0	Plant EGFP fusion vector, 35S promotor, Binary, Sm^R, Bar	*(Karimi et al. 2002)*
pB2GW7	Plant overexpression vector, 35S promotor, Binary, Sm^R, Bar	*(Karimi, et al. 2002)*
pB2WG7	Plant anti-sense overexpression vector, 35S promotor, Binary, Sm^R, Bar	*(Karimi, et al. 2002)*

Table 2.1 continued: Vectors used in the study

pUNI51 cloning vectors

pUNI51-ATG8A	pUNI51 Cloning Vector with AtATG8A	SSP Consortium
pUNI51-ATG8B	pUNI51 Cloning Vector with AtATG8B	SSP Consortium
pUNI51-ATG8C	pUNI51 Cloning Vector with AtATG8C	SSP Consortium
pUNI51-ATG8D	pUNI51 Cloning Vector with AtATG8D	SSP Consortium
pUNI51-ATG8F	pUNI51 Cloning Vector with AtATG8F	SSP Consortium
pUNI51-ATG8H	pUNI51 Cloning Vector with AtATG8H	SSP Consortium

Entry clones made by subcloning and/or site-directed mutagenesis

pENTR- AtNBR1 K11A	Gateway® Entry Vector with AtNBR1 point mutant K11A	This study
pENTR- AtNBR1 R19A	Gateway® Entry Vector with AtNBR1 point mutant R19A	This study
pENTR- AtNBR1 D60A	Gateway® Entry Vector with AtNBR1 point mutant D60A	This study
pENTR- AtNBR1 D73A	Gateway® Entry Vector with AtNBR1 point mutant D73A	This study
pENTR- AtNBR1 PB1 (aa 1-100)	Gateway® Entry Vector with AtNBR1 PB1 (aa 1-100)	This study
pENTR- AtNBR1 PB1 K11A	Gateway® Entry Vector with AtNBR1 PB1 K11A	This study
pENTR- AtNBR1 PB1 R19A	Gateway® Entry Vector with AtNBR1 PB1 R19A	This study
pENTR- AtNBR1 PB1 D60A	Gateway® Entry Vector with AtNBR1 PB1 D60A	This study
pENTR- AtNBR1 PB1 D73A	Gateway® Entry Vector with AtNBR1 PB1 D73A	This study
pENTR- AtNBR1ΔUBA1 (617-656)	Gateway® Entry Vector with AtNBR1ΔUBA1	This study
pENTR- AtNBR1ΔUBA2 (656-704)	Gateway® Entry Vector with AtNBR1ΔUBA2	This study
pENTR-AtNBR1ΔUBA1+2 (614-704)	Gateway® Entry Vector with AtNBR1ΔUBA3	This study
pENTR- AtNBR1UBA1 (617-656)	Gateway® Entry Vector with AtNBR1UBA1	This study
pENTR- AtNBR1UBA2 (656-704)	Gateway® Entry Vector with AtNBR1UBA1	This study
pENTR- AtNBR1UBA1+2 (617-704)	Gateway® Entry Vector with AtNBR1UBA1	This study
pENTR- AtNBR1Δ1-142	Gateway® Entry Vector with AtNBR1Δ1-142	This study
pENTR- AtNBR1Δ1-412	Gateway® Entry Vector with AtNBR1Δ1-412	This study
pENTR- AtNBR1Δ142-493	Gateway® Entry Vector with AtNBR1Δ1-493	This study
pENTR- AtNBR1Δ491-617	Gateway® Entry Vector with AtNBR1Δ491-704	This study
pENTR- AtNBR1 (412-491)	Gateway® Entry Vector with AtNBR1 412-491	This study
pENTR-ATG8A	Gateway® Entry Vector with AtATG8A	This study
pENTR-ATG8B	Gateway® Entry Vector with AtATG8B	This study
pENTR-ATG8C	Gateway® Entry Vector with AtATG8C	This study
pENTR-ATG8D	Gateway® Entry Vector with AtATG8D	This study
pENTR-ATG8F	Gateway® Entry Vector with AtATG8F	This study
pENTR-ATG8H	Gateway® Entry Vector with AtATG8H	This study
pENTR- AtNBR1ΔStart	Gateway® Entry Vector with AtNBR1 lacking start codon	This study
pENTR- AtNBR1Δstop	Gateway® Entry Vector with AtNBR1 lacking stop codon	This study
pENTR- Cherry-AtNBR1	Gateway® Entry Vector with AtNBR1 containing an N-terminal cherry-tag	This study
pENTR- ECFP-AtNBR1	Gateway® Entry Vector with AtNBR1 containing an N-terminal ECFP-tag	This study
pENTR- NBR1Δstop	Gateway® Entry Vector with human NBR1 lacking stop codon	This study

Entry clones made by subcloning and BP/LR Gateway

pdestEGFP-AtNBR1Δ202-412	Mammalian EGFP fusion expression vector with AtNBR1Δ202-412	This study
pdestEGFP-AtNBR1Δ412-617	Mammalian EGFP fusion expression vector with AtNBR1Δ202-412	This study
pDONR201-AtNBR1Δ202-412	Gateway® DONR Vector with AtNBR1Δ202-412	This study
pDONR201-AtNBR1Δ412-617	Gateway® DONR Vector with AtNBR1Δ202-412	This study
pENTR-AtNBR1Δ202-412	Gateway® Entry Vector with AtNBR1Δ202-412	This study
pENTR-AtNBR1Δ412-617	Gateway® Entry Vector with AtNBR1Δ202-412	This study

cDNA constructs, Amp^R, made by gateway LR reactions (this study)

pDest-myc-AtNBR1	pcDNA-Dest53-AtNBR1
pDest-HA-AtNBR1	pDestEGFP-C1-AtNBR1
pDest-mCherry-AtNBR1	pDestEGFP-Cherry-AtNBR1
pDestEGFP-C1-AtNBR1 K11A	pDestEGFP-C1-AtNBR1ΔUBA1+2
pDest-myc-AtNBR1 K11A	pDestmyc-AtNBR1 R19A
pDest-myc-AtNBR1 D60A	pDest-myc-AtNBR1 D73A
pcDNA-Dest53-AtNBR1 K11A	pcDNA-Dest53-AtNBR1 R19A
pcDNA-Dest53-AtNBR1 D60A	pcDNA-Dest53-AtNBR1 D73A
pDest-HA-AtNBR1 K11A	pDest-HA-AtNBR1 R19A
pDest-HA-AtNBR1 D60A	pDest-HA-AtNBR1 D73A
pcDNA-Dest53-AtNBR1-PB1	pcDNA-Dest53-AtNBR1-PB1 K11A
pcDNA-Dest53-AtNBR1-PB1 R19A	pcDNA-Dest53-AtNBR1-PB1 D60A
pcDNA-Dest53-AtNBR1-PB1 D73A	pDest15-AtNBR1-PB1
pDest15-AtNBR1-PB1 K11A	pDest15-AtNBR1-PB1 R19A
pDest15-AtNBR1-PB1 D60A	pDest15-AtNBR1-PB1 D73A
pDest-myc- AtNBR1ΔUBA1	pDest-myc- AtNBR1ΔUBA2
pDest-myc- AtNBR1ΔUBA1+2	pcDNA-Dest53-AtNBR1 UBA1
pcDNA-Dest53-AtNBR1 UBA2	pcDNA-Dest53-AtNBR1 UBA1+2
pDest-myc-AtNBR1Δ1-142	pDest-myc-AtNBR1Δ1-412
pDest-myc-AtNBR1Δ142-493	pDest-myc-AtNBR1Δ491-617
pDest-myc-AtNBR1 (412-491)	pDest15-AtATG8A
pDest15-AtATG8B	pDest15-AtATG8C
pDest15-AtATG8D	pDest15-AtATG8F
pDest15-AtATG8G	pDest15-AtATG8H
pDestEarleygate104-AtNBR1	pDestEarleygate104-AtNBR1 D60A
pDestEarleygate104-AtNBR1 ΔUBA1+2	pDestEarleygate104-Cherry-AtNBR1
pDestEarleygate104-ECFP-AtNBR1	pDestEarleygate104-ECFP-AtNBR1ΔUBA1+2
pDestearleygate104-mNBR1	pDestEarleygate104-AtATG8A
pDestEarleygate104-AtATG8B	pB7FWG2-Δend AtNBR1
pB7FWG2-Δend mNBR1	pB7FWG2-Δend p62
pB2GW7-AtNBR1	pB2GW7-AtNBR1 ΔUBA1+2
pB2WG7-AtNBR1	pB2WG7-AtNBR1 ΔUBA1+2
pB2GW7-ECFP-AtNBR1	pB2GW7-ECFP-AtNBR1 ΔUBA1+2

Other cDNA construct

pDest15-Ub	Mammalian GST-fusion expression vector with mono-Ubiquitin	T.Lamark
pDest15-4xUb	Mammalian GST-fusion expression vector with 4x-Ubiquitin	T.Lamark

All plasmid constructs made by traditional subcloning or gateway LR/BP reactions in this study were verified by restriction digestion and/or DNA sequencing.

Table 2.2: Buffers and solutions used in the study

Method	Buffer	Contents
General buffer		
	Phosphate buffered saline (PBS)	0.1 M Natrium phosphate buffer pH 7.2 0.7% NaCl (w/v)
Cloning		
	TE-buffer	10 mM Tris-HCl pH 8.0 1 mM EDTA
	10xTA	330 mM Tris-HCl pH 7.9 660 mM KOAc 100 mM $Mg(OAc)_2$ 5 mM DTT 1 mg/ml BSA
	10xNEB1 (supplied and used as 10x)	1X NEBuffer1: 10 mM Tris-HCl 10 mM $MgCl_2$ 1 mM DTT pH 7.9, 25 °C
	10xNEB2 (supplied and used as 10x)	1X NEBuffer2: 50 mM NaCl 10 mM Tris-HCl 10 mM $MgCl_2$ 1 mM DTT pH 7.9, 25 °C
	10xNEB3 (supplied and used as 10x)	1X NEBuffer3: 100 mM NaCl 50 mM Tris-HCl 10 mM $MgCl_2$ 1 mM DTT pH 7.9, 25 °C
	10xNEB4 (supplied and used as 10x)	1X NEBuffer4: 50 mM potassiummacetate 20 mM Tris-acetate 10 mM MagnesiumAcetate 1 mM Dithiothreitol pH 7.9, 25°C
	100x BSA (supplied as 100x, used as 10x)	100xBSA diluted to 10xBSA
	6xT	0.25% Bromophenol Blue (w/v) 60 mM Na_2 EDTA pH 8.0 0,6 % SDS (w/v) 40 % sucrose in H_2O (w/v)
	5x sequencing buffer	400 mM Tris-HCl pH 9.0 10 mM $MgCl_2$
	5 x ligation buffer	1 M Tris pH 7.6 1 M $MgCl_2$ 0.1 M ATP 1 M DTT 40 % PEG (8000) (v/v) 10 µg/µl BSA

Table 2.2 continued: Buffers and solutions used in the study

Agarose Gel electrophoresis		
	20x minigelbuffer	193.76 g Tris-HCl 27.22 g NaOAc 14.9 g EDTA dH_2O to 2 litres pH adjusted to 8.0 with acetic acid
	Ethidium bromide	0.1 g ethidium bromide (Sigma) 100 ml dH_20
SDS-PAGE gel		
	4x separating gel buffer	181.65 g Tris-base 4 g SDS dH_2O to 1 litre pH adjusted to 8.8 with HCl
	4x concentrating gel buffer	60.55 g Tris-base 4 g SDS dH_2O to 1 litre pH adjusted to 6.8 with HCl
	Electrophoreis buffer	15 g Tris-base 75 g glycine 5 g SDS dH_2O to 5 litres
	2x SDS gel loading buffer	100 mM Tris-HCl pH 6.8 200 mM DTT (added fresh) 4 % SDS (w/v) 0,2 % Bromophenol Blue (w/v) 20% glycerol (w/v)
Coomassie staining		
	Fix solution	400 ml MeOH 100 ml Acetic acid 500 ml dH_2O
	Stain stock	2 g Coomassie Brilliant Blue R250 dH_2O to 200 ml
	Staining solution	62.5 ml stain stock 250 ml MeOH 50 ml acetic acid dH_2O to 500 ml
	Destain I	500 ml MeOH 100 ml Acetic acid dH_2O to 1 litre
	Destain II	50 ml MeOH 70 ml Acetic acid dH_2O to 1 litre

Table 2.2 continued: Buffers and solutions used in the study

Protein production and purification		
	Lysis buffer (GST proteins)	50 mM Tris-HCl pH 8.0 250 mM NaCl 1 mM EDTA (optional for proteins lacking a zinc finger) 1 mM DTT (add fresh) 0.35 mg/ml lysozyme (added fresh)
	PBS with inhibitors	10 ml PBS 1 protease inhibitor cocktail mini tablet (Roche)
	NETN buffer	43.7 ml H2O 1 ml Tris-HCl pH 8.0 2.5 ml 2 M NaCl 2.5 ml 10% Np-40 600 µl 0.5 M EDTA 600 µl 0.5 M EGTA (for strong interactions)
	NETN buffer with inhibitors	10 ml NETN buffer 1 protease inhibitor cocktail mini tablet (Roche)
Confocal microscopy		
	Fix solution	0.16 g paraformaldehyde (PFA) 1.7 ml autoclaved H_2O 50 µl 2M NaOH 200 µl sterile 10x PBS Adjust pH to ≈ 7 with 3M HCl
Protoplastation		
	MS- 0,34 M Glucose Mannitol	4,3 g MS-powder (Duchefa) 30,5 g Glucose 30,5 g Mannitol Water up to 1 liter
	Enzyme solution	1 % cellulase (Rio Yakult) 0,2% Macroenzyme (Rio Yakult) In MS-0,34 M GM
	MS-0,28M Sucrose	4,3 g MS-powder (Duchefa) 96 g Sucrose Water up to 1 liter
	PEG	25% Peg 6000 0,45 M Mannitol O,1 M $Ca(NO_3)_2$
	$Ca(NO_3)_2$	64,94 g $Ca(NO_3)_2$ Water up to 1 liter
Agrobacterium transformation		
	5% Sucrose	50 g sucrose Water up to 1 liter

Table 2.2 continued: Buffers and solutions used in the study

Western blot		
	Protein extraction buffer (PEB)	62,5 mM Tris pH 6,8 10% (v/v) Glyzerin 1% (w/v) SDS 1mM DTT 1mM PMSF 3mM EDTA
	TBST buffer	75 ml 2 M NaCl 10 ml 1M Tris-HCl pH 7.5 1 ml Tween 20 914 ml dH2O

NB: All buffers are made in dH_2O if nothing else is mentioned.
pH values are for room temperature.

Table 2.3: Growth media for bacteria

Luria Bertani (LB) medium	LA plates	2 x TY	SOC
10 g Bacto trypton 5 g Bacto yeast extract 10 g NaCl dH_2O to 1 litre pH adjusted to 7.0 with NaOH Supplemented with appropriate antibiotics	18 g agar 10 g Bacto trypton 5 g Bacto yeast extract 10 g NaCl dH_2O to 1 litre pH adjusted to 7.5 with NaOH Supplemented with appropriate antibiotics	16 g Bacto trypton 5 g Bacto yeast extract 5 g NaCl dH_2O to 1 litre pH adjusted to 7.0 with NaOH 20 mM glucose Supplemented with appropriate antibiotics	20 g Bacto trypton 5 g Bacto yeast extract 5 g NaCl 10 ml 250 mM KCl dH_2O to 1 litre pH adjusted to 7.0 with NaOH Supplemented prior to use with $MgCl_2$

Table 2.4: Growth media for mammalian cells

Cells	Growth media	Antibiotics
HeLa	Minimum Essential Medium (MEM) 10% (vol/vol) Fetal bovine serum (Biochrom AG)	100 U/ml Penicillin 100 µg/ml Steptomycin

Table 2.5: Bacterial strains used in this study

Strain	Reference
DH5α	Bethesda research laboratories
BL21(DE3)	Novagene
Agrobacterium tumerifaciens pMP90 strain GW3101	(Koncz and Schell 1986)

Table 2.6: Concentration of antibiotics in bacterial growth medium

Antibiotic	Concentration (µg/ml)
Ampicillin (amp)	100 µg/ml
Kanamycin (kan)	50 µg/ml
Spectionomycin	50 µg/ml
Rifampicin	50 µg/ml
Gentamycin	10 µg/ml

Table 2.7: Oligonucleotides and corresponding cDNA clones used in this study

cDNA clones	Oligo name	Sequence 5' to 3'
AtNBR1 K11A	K11A.5pr	CTAACGCACTCGTCGTCGCGGTGAGCTATGGAGGTGTG
	K11A.3nt	CACACCTCCATAGCTCACCGCGACGACGAGTGCGTTAG
AtNBR1 R19A	R19A.5pr	GAGCTATGGAGGTGTGCTTGCGCGTTTCAGGGTGCCTG
	R19A.3nt	CAGGCACCCTGAAACGCGCAAGCACACCTCCATAGCTC
AtNBR1 D60A	D60A.5pr	GCTGAATTGAGTCTGACTTACTCTGCGGAGGATGGGGATGTGG
	D60A.3nt	CCACATCCCCATCCTCCGCAGAGTAAGTCAGACTCAATTCAGC
AtNBR1 D73A	D73A.5pr	CTTGTTGATGACAACGCGCTCTTTGATGTTACTAATCAGC
	D73A.3nt	GCTGATTAGTAACATCAAAGAGCGCGTTGTCATCAACAAG
DstartAtNBR1	DstartAtNBR1.5pr	GGAGCCCTCCACCTTGGAGTCTACTGCTAACGC
	DstartAtNBR1.3nt	GCGTTAGCAGTAGACTCCAAGGTGAAGGGCTCC
AtNBR1UBA1	UBA1.5pr	TTTGATATCGTCTGGTGGTTCTTCATCTACTAC
	UBA1.3nt	TTTTCTAGATCAGCTAACTCCACAAAGAGC
AtNBR1UBA2	UBA2.5pr	TTTGATATTGTGGAGTTAGCGAGTGG
	UBA2.3nt	TTTTCTAGATCATCAAGCCTCCTTCTCC
AtNBR1ΔUBA1(FspI)	ΔUBA1FspI.5pr	GTTGATGCTCTTTGTTGCGCAGGAGTTAGCGAGTGGGATC
	ΔUBA1FspI.3nt	GATCCCACTCGCTAACTCCTGCGCAACAAAGAGCATCAAC
AtNBR1ΔUBA1(SfoI)	ΔUBA1SfoI.5pr	GGAGGATATAGAAAAGAATGGCGCCGAGATAACCATGCTCAAGG
	ΔUBA1SfoI.3nt	CCTTGAGCATGGTTATCTCGGCGCCATTCTTTTCTATATCCTCC
AtNBR1ΔUBA2(stop)	ΔUBA2stop.5pr	GTCTGTTGATGCTCTTTGTTGAGTTAGCGAGTGGGATC
	ΔUBA2stop.3nt	GATCCCACTCGCTAACTCAACAAAGAGCATCAACAGAC
AtNBR1ΔUBA1+2(stop)	ΔUBA1+2stop.5pr	CT CTTCAGGAGGATATAGAATAGAATGACGTGGAGATAACC
	ΔUBA1+2stop.3nt	GGTTATCTCCACGTCATTCTATTCTATATCCTCCTGAAGAG
AtNBR1ΔPB1(XhoI)	DPB1XhoI.5pr	CTAACTCTGCTGCTCGAGAGAGTAGTGGGAG
	DPB1XhoI.3nt	CTCCCACTACTCTCTCGAGCAGCAGAGTTAG
AtNBR1HindIII(ECFP)	HindIIIECFP.5pr	GCAGGCTCCGCGGAAGCTTTGTTTAACTTTAAGAAGGAGCCC
	HindIIIECFP.3NT	GGGCTCCTTCTTAAAGTTAAACAAAGCTTCCGCGGAGCCTGC
mNBR1Δstop	mNBR1_pET 161-f	CACCATGGACCACAGGTTACTCTAAATG
	mNBR1_rev	ATAGCGTTGGCTGTACCAG
AtNBR1Δstop	pNBR1_pET 161-f	CACCATGGAGTCTACTGCTAACG
	pNBR1_rev	AGCCTCCTTCTCCCCTGTG
Sequencing (myc)	T7 primer	TAATACGACTCACTATAGGG
Sequencing (myc)	SP6	CATACGATTTAGGTGACACTATAG

All primers used in this study were from Operon Biotechnologies

Table 2.8: Antibodies used in this study

Antibody	Manufacturer
αGFP	Custom made (Clontech Europe)
αHA	Roche
αRabbit IgG HRP-conjugated	Calbiochem

Table 2.9: Microscopes and software

Microscope	Confocal system	Software
Zeiss Axio Observer.Z1	NA	Axiovision
Zeiss Axiovert 200	LSM-510	LSM-510
Leica DMI 6000	TSC SP5	LAS AF

Table 2.10: Filter cubes and lasers

Microscope (confocal system)	Filter cubes (manufacturer)	Lasers
Zeiss Axio Observer.Z1 (not confocal)	38HE-GFP(Zeiss)	NA
	31017-Chlorophyll (Chroma)	NA
Zeiss Axiovert 200 (LSM-510)	Ch3-1: LP560	Argon/2 (458,477,488,514)
	Ch2-2 : BP500-550IR	HeNe1 (543)
Leica DMI 6000 (TSC SP5)		Argon

Table 2.11: Settings for Zeiss Axiovert 200 (LSM-510)

	GFP/YFP	Cherry
Laser	488 nm 22%	543 nm 89%
Beam splitter	MBS: HFT UV/488/543/633	MBS: HFT UV/488/543/633
	DBS1: NFT 635 VIS	DBS1: NFT 635 VIS
	DBS2: NFT 545	DBS2: NFT 545
	DBS3:Plate	DBS3:Plate

Table 2.12: Settings for Leica DMI 6000 (TSC SP5)

	GFP/YFP	ECFP	BF
Laser	Argon 30%	Argon 30%	
AOTF	514 (33%)	458 (33%)	
AOBF	514	458	
Emmision	525-600 nm	465-600 nm	
Output	800-1000 V	800-1000 V	Approx.250 V

2.2 Methods

2.2.1 Cloning using Gateway® technology

Gateway® is a cloning system created by Invitrogen for shuttling genes of interest between different plasmid vectors. It utilizes the site-specific recombination properties of bacteriophage Lambda in a universal platform that enables fast and in-frame cloning. Vectors are divided in three categories; Entry, destination and donor. From the Entry vector, the gene can be transferred by recombination to any Destination vector. Destination vectors have been designed to enable functional analysis of the protein, e.g. in the form of fusion proteins or protein expression in different organisms. Donor vectors are used to shuttle genes between Destination vectors. The procedure starts with an Entry vector that contains the gene of interest. Recombination takes place between Entry and Destination vector AttLR recombination sites by adding a ready-made LR Clonase mix, and after recombination the plasmid is transformed into a bacterial host. The gene of interest replaces a toxic *ccdB* gene in the Destination vector, and together with the antibiotic resistance marker in the destination vector, this ensures selective growth of transformants that contains the recombinant destination vector. (www.invitrogen.com). Shuttling between Destination and donor vectors utilizes AttBP recombination sites, using a BP Clonase mix.

Procedure:
The following were mixed (on ice)
100 ng Entry vector
150 ng Destination vector
→9 µl TE-buffer
1 µl LRII/BPII

Incubated for 1h at 25 °C water bath
1 ul Proteinase K was added
Incubated for 10 minutes at 37°C water bath
3 ul was used for transformation of E.*coli* dH5α

2.2.2 Transformation of bacterial cells

Transformation is the genetic manipulation of a bacterial cell resulting from uptake and expression of foreign DNA. The term transformation was first proposed in 1944, which was incidentally also the first mention of DNA as the material of inheritance (Avery *et al.* 1944). Bacteria that are naturally competent will take up DNA from its environment, but this process can also be provoked by chemical or mechanical treatment. Two commonly used methods are

electroporation and heat shock, which both enlarge the pores in the plasma membrane to allow passage of DNA. Transformed bacteria are placed on a selective medium, and if the transformation rate is not too high, discernible colonies will form. These colonies can be selected for liquid growth, and from these cultures the plasmid is isolated.

Transformation using heat-shock:
The following were mixed in 15 ml falcon tubes and left on ice for 30 minutes:
30 µl dH_2O
1-5 ul DNA (should contain approximately 25 ng DNA)
100 µl competent bacteria

The tubes were gently moved to 37°C water bath for 2 minutes
500 µl SOC was added
The tubes were then incubated at 37°C for 45 minutes (shaking)
150 µl transformation mix was plated out and plates were incubated at 37°C for 8-13 hours.

Two individual colonies were transferred to liquid media and incubated at 37°C for approximately 13 hours.

2.2.3Plasmid purification using the Miniprep system

The QIAprep® Miniprep kit is used to purify plasmids from bacterial cells. The method is based on alkaline lysis of bacteria followed by adsorbtion of DNA to silica in high-salt concentration (Bimboim and Doly 1979, Vogelstein and Gillespie 1979). After lysate clearing, a spin column featuring a silica based membrane is used to purify the plasmid. The miniprep is more costly than doing a standard precipitation, but it is also faster and gives a higher degree of purification. Higher throughput kits like the Midi- and Maxiprep® are also available for plasmid purification from larger cell cultures.

Procedure:
Miniprep:
1.5 ml log phase bacterial culture was transferred to a 1.5 ml eppendorf tube.
Centrifuged at 6000 rpm for minimum 2 minutes
Supernatant was removed and 250 µl buffer P1(w/ethanol) was added
Pellet was vortexed until it was completely dissolved
250 µl buffer P2 was added, and the tube gently turned up and down until the blue color was homogenous
Incubated for maximum 5 minutes at room temperature
350 µl buffer N3 was added and the tube gently turned up and down until all the blue color was gone and a white precipitate had formed.
Centrifuged at 13000 rpm for 10 min
Supernatant was transferred to a QIAprep column and centrifuged for 1 minute at 13000 rpm

Flow-through was discarded and 500 µl Buffer PB1was added
Centrifuged for 1 minute at 13000 rpm
Flow-through was discarded and 750 µl Buffer PE was added
Centrifuged for 1 minute at 13000 rpm, flow-through discarded, and centrifugation repeated

The spin column was transferred to a clean eppendorf tube, and then 50 µl Buffer EB was added to the column.
The column was incubated for 1 minute and then centrifuged for 1 minute at 13000 rpm
Concentration of the eluted plasmid was measured using a Nanodrop® ND-1000 Spectrophotometer

Midiprep:
50-100 ml log phase bacterial culture was transferred to an ultracentrifuge container.
Centrifuged at 6000 rpm for 10 minutes
Supernatant was removed and 4ml cold buffer P1 (w/ethanol) was added to the pellet
The pellet was vortexed until completely dissolved
4 ml buffer P2 was added, and the container gently shaken until the blue color was homogenous
Incubated for 5 minutes at room temperature
4ml chilled buffer N3 was added and the container gently shaken until all the blue color was gone and a white precipitate had formed.
Incubated 15-20 minutes on ice
Centrifuged at 13000 rpm for 15 min
Qiagen-tip 100 was prepared by adding 10 ml Equilibration buffer QBT
The supernatant was transferred to the Qiagen-tip, and then left enter the resin by gravity flow
Qiagen-tip was then washed two times with 10 ml wash buffer QC
DNA was eluted to ultracentrifuge glass-tube by adding 4 ml Elution buffer QF
Precipitation by adding 3.5 ml room temperature isopropanol
Centrifugation at 9500 rpm for 30 minutes at 4ºC
Supernatant was removed and the pellet was washed with 2 ml 70% ethanol
Centrifugation at 9500 rpm for 15 minutes at 4ºC
The ethanol was removed and the pellet was dried for 10 minutes at room temperature
The pellet was then dissolved in an appropriate amount of Elution buffer (EB)
Concentration of the eluted plasmid was measured using a Nanodrop® ND-1000 Spectrophotometer

2.2.4 Cutting DNA with restriction enzymes

Restriction enzymes (also called restriction endonucleases) are bacterial enzymes first identified and isolated during the 60's (Meselson and Yuan 1968). In molecular biology, restriction enzymes are used to cleave DNA at specific cut sites, and most restriction enzymes recognizes unique palindromic sequences of 4-8 basepairs and make overhang cuts in which one of the strands is slightly protruding, while the remaining enzymes make blunt end cuts with no overhangs. The restriction enzymes all have different properties when it comes to efficiency of cutting, buffer requirements and sensitivity to methylation. Most enzymes will only cut at its unique cut site, but some enzymes are prone to STAR-activity (unspecific cutting).

Procedure (for restriction enzymes from New England Biolabs);
The following were mixed in an eppendorf tube on ice
Desired amount of template (0, 1-1 µg)
1 µl 10x NEB buffer
2 µl 10x BSA (if required)
1 µl of each restriction enzyme
$H_2O \rightarrow 20$ µl
Incubated for 1-3 hours (1 hour for test cutting, 3 hours for cloning) in 37 °C water bath

2.2.5 Polymerase Chain Reaction (PCR)

PCR is used to amplify a segment of DNA from a template sample. The theory behind the method was described almost 40 years ago (Kleppe *et al.* 1971), but due to experimental limitations it was not developed fully until the 80's (Mullis and Faloona 1987, Saiki *et al.* 1988). The template can be anything from a short oligomer to a whole genome. The amplification is performed by some kind of heat stable polymerase (Kaledin *et al.* 1980), and it requires a set of single stranded oligonucleotides to prime the reaction. Knowledge of the template is needed to synthesize primers that will bind to the desired sequence.

Below follows some important steps in primer design.
- The primer should be between 20 to 40 bp in length (depending on the type of PCR)
- Total GC content should be above 40%
- Melting temperature should at least be above 50 °C and the primer pair should not differ more than 5 °C in melting temperature.
- Primer pairs should not form dimers or hairpin loops

First the sample is heated to denature the template DNA and then cooled to a temperature that allows the primers to anneal. Then the temperature is taken up again to the optimal working range of the polymerase, and complementary strands are synthesized, resulting in twice the amount of template DNA. When this cycle is repeated over and over the concentration of template will increase exponentially.

Formula for calculating the melting temperature (Tm) of primers;

Tm = 64.9°C + 41°C x (number of G's and C's in the primer – 16.4)/N
Where N is the total length of the primer

Basic PCR reaction;
The following were mixed in PCR tubes on ice
50 ng template DNA
10 µM forward primer
10 µM reverse primer
10 µM dNTP mix
1 µl heat stable polymerase
5 µl 10x PCR buffer
H2O → 50 µl

The main variables of the program are based on annealing temperature of the primers and of the length of the product. A standard annealing temperature would be between 50 and 60 °C, and the elongation time was set to 2 minutes per kb product.

Standard PCR program:
Initial denaturing cycle 94 °C, 1 minute

Denaturation, 94 °C 30 seconds
Annealing, 56 °C 1minute 30-35 cycles
Elongation, 68 °C, 2 minutes pr kb

End cycle, 72 °C 7 minutes
Storage, 4 °C ∞

2.2.6 Purification of PCR products

QIAquick® PCR Purification Kit (QIAGEN) was used for purification of PCR products. This is necessary to remove primers, nucleotides, salts and polymerase that would interfere with subsequent cloning procedures. The QIAprep column will retain single and double stranded PCR products ranging from 100 bp to 10 kb.

Procedure:

5 volumes of buffer P1 was added to the PCR product
The mix was transferred to a QIAprep column
Centrifugation at 13000 rpm for 1 minute
Flow-through was discarded, and 750 µl buffer PE was added
Centrifugation for 1 minute at 13000 rpm, flow-through discarded, and then centrifugation for another minute.
The QIAprep column was transferred to a clean 1.5 ml eppendorf tube
30-50 µl buffer EB was added
Centrifugation for 1 minute at 13000 rpm
Concentration of eluted PCR-product was measured by agarose gel electrophoresis

2.2.7 Introducing mutations by site directed mutagenesis

One way to introduce point mutations to DNA is to synthesize the DNA with oligonucleotides that contains the desired mutation (Hutchison *et al.* 1978). Combining this technique with PCR provides a fast and accurate method of producing site-mutated DNA (Higuchi *et al.* 1988). One popular method for PCR mutagenesis used today is the QuickChange (Wang 1999). As in a normal PCR, the critical step lies in primer design, and the QuickChange® mutagenesis kit (Stratagene) gives these instructions for designing a mutagenesis primer;

- The primer should be between 30-45 bp in length.
- The mutation is placed in the center of the primer, and the number of GC's is

approximately equal on both sides of the mutation.

- Total GC content should be above 40%
- The melting temperature should be above 78 °C.

Formula for calculating the melting temperature of mutagenesis primers;

Tm = 81.5 + 0.41(%GC)) - 675/N - %mismatch
N is the total length of the primer

Basic Mutagenesis reaction;
The following were mixed in PCR tubes on ice
10 ng template DNA
10 µM mutated forward primer
10 µM mutated reverse primer
10 µM dNTP mix
1 µl Pfu TURBO polymerase (2500 U/ml, Stratagene)
5 µl 10x Cloned Pfu Reaction buffer (Stratagene)
H2O → 50 µl
Mutagenesis program;
Initial denaturing cycle 94 °C, 1 minute

Denaturation, 94 °C 30 seconds
Annealing, 56 °C 1minute 30-35 cycles
Elongation, 68 °C, 2 minutes pr kb

End cycle, 72 °C 7 minutes
Storage, 4 °C ∞

After the PCR was completed, 1 µl of restriction enzyme DpnI was added and the mix was incubated at 37ºC for 1hour. 5 µl of the digested product was then used for bacterial transformation.

2.2.9 Separation of DNA fragments by agarose gel electrophoresis

Agarose is a polysaccharide extracted from algae that can polymerize to form a porous gel. It was first taken into use in microbiology as a substance for solid growth media, and during the 50's it was combined with electrophoresis to separate proteins (Crowle 1956). Ten years later it was reported in use for separating DNA molecules (Thorne 1966).

Today the agarose gel is mainly used to separate pieces of DNA. An electrical current separates the DNA fragments mainly according to difference in size, but the conformation of the DNA-molecule also affects migration. A supercoiled strand will typically migrate faster than linearized DNA. A ladder is used to establish the size of the migrated fragments and a

DNA intercalating fluorophore is added to visualize the fragments. A commonly used fluorophore is Ethidium Bromide.

Procedure:
0, 7 % agarose gel;
The following were mixed in a 250 ml Erlenmeyer flask
0, 7 g agarose
5 ml 20x minigel buffer
95 ml dH_2O
The mix was heated for 2 minutes in a microwave oven
The mix was then cooled down to approximately 60 °C.
Appropriate amount of agarose gel was then applied to a casting frame with a comb.
The gel was left to solidify for 20 minutes

The comb was removed, and the gel was transferred to an electrophoresis chamber which was filled with minigel buffer
6xT loading buffer was added to DNA samples
Samples and ladder was loaded into the wells of the gel

The gel was run for 50-60 minutes in a 90 V electric field.
The gel was incubated ncubate gel in Ethidium Bromide for 10-20 minutes

Gels were documented by exposure in UV-light, and pictures were taking using a Gel-Doc imaging system.

2.2.8 Traditional cloning

Traditional cloning is based on the use of restriction enzymes and DNA ligase to cut and religate pieces of DNA. Cutting two pieces of DNA with the same "sticky-end" restriction enzyme will create identical ends that can be ligated back together. Blunt end cuts can be religated independent of the restriction enzyme used.
Traditional cloning has been, and still is, an important method to insert a gene of interest into a self replicating bacterial plasmid, allowing production of the gene for use in analytical studies. The method can also be used to delete pieces of a gene simply by cutting and religating. When cloning PCR-products the primers have added cut-sequences in the ends, and the PCR-products can then be ligated into a pre-cut plasmid.

Procedure:
About 700 ng of insert and vector was cut with the appropriate restriction enzymes (3h)
6xT was added and the mix was loaded onto an agarose gel
The gel was run for 50-60 minutes in a 90 V electric field
The gel was then incubated for 5 minutes in Ethidium bromide
The gel was movedl to a Dual Intensity Transilluminator of very low light intensity
Bands of sized corresponding to the desired fragments was cut out of the gel and added to "gel towers" (speed was required, as the DNA is degraded in UV-light)

The gel towers were centriguged for 10 minutes at 13000 rpm
Optional; if the concentration of DNA was too low:
DNA was precipitated using 2 volumes of 96% ethanol and 0.2 volumes of 3 M NaOAc
Vortexing for 10 seconds
Incubated at -20 °C for at least 1h (overnight was recommended)
Centrifugation for 30 min at 13000 rpm (4°C)
Supernatant was removed and 2 volumes of 70% ethanol was added carefully
Centrifugation for 15 minutes at 13000 rpm (4°C)
Supernatant was removed and the pellet was dried in vacuum for 10 minutes
The pellet was dissolved in 10 µl TrisHcl pH=8.0
Concentration of eluted DNA was measured by agarose gel electrophoresis

For cloning, approximately 100 ng of vector and a five fold concentration of vector (assuming the vector and insert are the same size) was used
The following were mixed on ice:
Vector and insert
5µl 4x ligase buffer (should net be re-used once thawed)
1 µl T4 DNA ligase
→20 µl H_2O

The ligation mix was vortexed and incubated at 25°C for 1h (or more)
4µl was used in the transformation of *E.coli*

Making towers;
Two 0.5 ml Eppendorf tubes were needed for each gel piece.
A needle was used to make four holes in the bottom of one tube and one hole in the bottom of the second tube
A piece (0.5x0.5cm) of glasmicrofibre filter (Whatman) was put in the bottom of the tube with one hole.
The tube with four holes was put in the tube with one hole, and these were put in a 1.5 ml eppendorf tube.
The lids of all tubes were cut of
A centrifuge was used that could accommodate the towers

2.2.10 Sequencing

Two independent methods of sequencing were described during the 70's (Maxam and Gilbert 1977, Sanger and Coulson 1975). Maxam and Gilberts method was based on cutting DNA at the specific bases and radioactive labeling. It was initially more successful than Sangers method, since purified DNA could be directly sequenced, but it gradually fell out of use due to its technical complexity and use of hazardous materials. Sanger used a chain-terminator method with fluorescently labeled 2`, 3`-didedoxynucleotide triphosphates (ddNTP). These bases terminate chain elongation, creating fragments of a unique length for each bp in the fragment. Another advance in sequencing technology came with the introduction of Dye-primer sequencing combined with computer-based optical reading of differently colored fluorescent fragments, which set a new standard for high-throughput sequencing (Smith *et al.* 1986). Todays technology is based on a Dye-terminator method, where ddNTP's are labeled with different fluorescent dyes used in a standard PCR reaction. The labeled fragments are

analyzed in a DNA sequencer, which separates the fragments by capillary electrophoresis and creates fluorescent peak trace chromatograms.

Sequencing in Entry vectors is disturbed by the Att1 site, and it is therefore recommended to use Destination vectors for sequencing inserted genes.

Procedure:
The following were mixed in PCR tubes on ice:
200-300 ng plasmid template
2 µl Big-Dye v3.1
1 µl primer
4 µl Sequencing buffer
Water to 20 µl

PCR program:
Initial denaturing cycle 96 °C, 5 minute

Denaturation, 96 °C 10 seconds
Annealing, 50 °C 10 seconds 25 cycles
Elongation, 60 °C, 4 minutes
Hold, 4 °C ∞

2.2.11 Analyzing protein interactions by immunoprecipitation (IP)

The principle of IP is to purify a protein from a solution by using an antibody. The protein is first expressed *in vitro* or *in vivo* with an antigen-tag that is recognized by the antibody. After the antibody has bound the protein, the complex is pulled out from the solution. This is traditionally done by using protein A, G or L-coated agarose or sepharose beads, which recognizes and binds a wide variety of antibodies. To test if two proteins interact, both proteins are translated in vivo, but only one is tagged with an antigen that the antibody can recognize. If the two proteins interact, the untagged protein precipitates together with the tagged protein. This is called co-immunoprecipitation. To visualize the precipitated protein(s), they are first separated from the beads by boiling and then run through SDS PAGE. The protein bands can then be visualized in several different ways, eg. by western blot or autoradiography (if radiolabeled).

Procedure for In-vitro Co-immunoprecipitation:
In vitro translation:
Assay buffer (N=numer of translation assays)
N x 12.5 µl Reticulocyte lysate
N x 1.0 µl TNT buffer
N x 0.5 µl aa mix without Met

N x 0.5 µl ^{35}S-Met (37 MBq/100µl)
N x 0.5 µl Met
N x 0.5 µl TNT T7 polymerase
N x 0.5 µl Cloned RNasin Inhibitor

In vitro translation assay:
The following were mixed in eppendorf tubes on ice;
Controls (one plasmid)
0.25 µg of each plasmid
H_2O → 4.5 µl
8.0 µl assay buffer

Co-immunoprecipitation (two plasmids)
0.5 µg of each plasmid
H_2O → 9 µl
16.0 µl assay buffer

In-vitro assay translation mix was incubated at 30 °C for 90 minutes
After incubation, 3 µl of the vitro translated mix was taken to use as input
15 µl 2x SDS gel loading buffer and 200 mM DTT was added to the inputs
The input were boiled for 5 minutes and stored at -20°C

Preparation of Protein A Sepharose or agarose beads.
NB - cut pipette tips were always used when pipetting beads.
30 µl beads solution were used per assay
Beads were washed three times in chilled NETN buffer
Half the beads were saturated with 2%BSA (in PBS) at room temperature for 30 minutes, and then washd three times with chilled NETN buffer.

22 µl in-vitro translated protein was mixed with 200 µl NETN buffer with protease inhibitor and 15 µl BSA-saturated Protein A-Sepharose beads
Incubation at 4 °C for 10 minutes
Centrifugation at 4 °C, 25 seconds at 13000 (sepharose)/2500 (agarose) rpm
Supernatant was transferred to a new tube and 1 µl antibody was added
Incubation at 4 °C for 45 minutes
15 µl BSA-saturated Protein A-sepharose beads was added to the mix
Incubation at 4 °C for 20 minutes
The mix was washed five times in chilled NETN buffer without inhibitor
After the last wash the supernatant was completely removed
15 µl 2xSDS gel loading buffer with 200 mM DTT was added to the mix
The IP was then boiled for 5 minutes and store at -20 °C

2.2.12 Recombinant protein production

Proteins used for GST-pulldowns in this study were produced using a T7 late promoter system in *E.coli* BL21(DE3). This strain contains a copy of the T7 gene 1 that is under control of a *lac* promoter. Induction of isopropyl-beta-D-thiogalactopyranoside (IPTG) will promote the synthesis of T7 RNA polymerase which will bind to the T7 promoter in the pDest expression vector and drive the expression of the target cDNA.

Procedure:
To create a GST-fusion protein, the gene must first be inserted in a pDest15 vector.
This vector is then transformed into bacterial strain BL(21)DE3 which contains T7 polymerase
A single colony was inoculated in 5 ml LB media and set for shaking at 37°C overnight.
The 5ml overnight culture was added to 100 ml prewarmed 2xTY with Amp
Grown at 37 °C to OD_{600}=0,5-0,9
50 µl IPTG was added and bottle was transferred to gentle shaking at room temperature.
(For proteins with zinc-finger, add Zn-sulphate (100 µl 0.1 M to 100 ml))
Grown for 3-4 hours at room temperature
The culture was Transferred to 250 ml ultracentrifuge containers and kept on ice for some minutes
Centrifugation, 10 min 5000 rpm, 4 °C
The supernatant was removed and the pellet was dissolved in 4 ml ice-cold lysis buffer added lysozyme and DTT
While kept on ice for 20 minutes, each culture were transferred to 3 Nunc-tubes
10% triton-X100 (150 µl to 1,5 ml) was added and tubed were inverted to mix
Frozen at -70 °C
Proteins that were going to be purified were first thawed on ice
Proteins were sonicated for 3x10 seconds on ice
Sonicated lysates were transferred to two eppendorf tubes and centrifuged at 13000 rpm for 10 min, 4 °C
GST beads were prepared by washing three times in cold PBS-buffer. Final conc. was 50%.
Two eppendorf tubes were filled with 100 µl washed GST-beads
Supernatant from centrifuged lysates were added and then incubated for 1 hour at rotating wheel, 4 °C
Beads were washed three times with cold PBS, the last washing step was done with PBS+Inhibitors
10 µl beads were prepared for SDS-PAGE to check protein concentration
Beads were used within one week

2.2.13 Analyzing protein interactions by GST-Pulldown

The GST-pulldown assay is used to an analyze protein interactions (quantitative or qualitative) between a glutathione-S-transferase (GST) fusion protein and potential interactants in a solution (Kaelin *et al.* 1991). The probing protein is produced as a GST-fusion protein and purified using glutathione sepharose beads. The protein-bead complex can then be used to pull target protein(s) from cell lysates out of solution. Potential target protein(s) can also be in-vitro translated with $^{[35]}$S-Met and then incubated with the probing protein. Washing steps with a detergent buffer removes unspecific interactions. Proteins interacting with the probing protein are separated by boiling and run on SDS-PAGE. The gel

is then stained to examine the amount of GST-protein and finally developed to visualize radiolabeled proteins. As a negative control, the target proteins are tested for interaction against GST.

GST-fusion proteins that have been attached to glutathione sepharose beads should be used within a week, as the interaction weakens over time.

Procedure:
Proteins were produced and purified as described in section 2.2.12. Purified GST-fusion proteins were run on SDS-PAGE and stained with Coomassie Brilliant Blue to measure the amount of protein.
NB - cut pipette tips were always used when pipetting beads.

In vitro translation:
Assay buffer (N=numer of translation assays, one translation assay is enough for two pulldowns)
N x 12.5 µl Reticulocyte lysate
N x 1.0 µl TNT buffer
N x 0.5 µl aa mix without Met
N x 0.5 µl ^{35}S-Met (37 MBq/100µl)
N x 0.5 µl Met
N x 0.5 µl TNT T7 polymerase
N x 0.5 µl Cloned RNasin Inhibitor

In vitro translation assay:
The following were mixed in eppendorf tubes on ice:
0.5 µg plasmid
$H_2O \rightarrow$ 9 µl
16.0 µl assay buffer
Iin-vitro assay translation mix was incubated for 90 min at 30°C
3 µl in-vitro assay translation mix was taken out for input and stored on ice.
Empty GST-beads were washed two times in cold NETN buffer
The remaining 22 µl in-vitro assay translation mix was cleared for unspecific binding with 10 µl 50% GST-proteins on glutathione-agarose beads and 100 µl NETN buffer with protease inhibitor.
Incubation on rotating wheel for 30 min at 4ºC.
Centrifugation at 13000 rpm 4°C. Supernatant was transferred to new tube
GST-protein on beads was washed 2x in NETN buffer
5-15 µl GST-protein was added to each pre-cleared in vitro translate. Empty GST-beads were used to increase the amount of beads to 25 µl. Also NETN buffer with inhibitors was added if the volume was low (<100µl)
Incubation on rotating wheel for 60 minutes, 4 °C
Mix was washed five times with cold NETN buffer without protease inhibitors
After the last wash the supernatant was completely removed
20 µl loading buffer was added to each sample and input
GST-pulldown samples and inputs were boiled for 5 minutes
Centrifugation at 13000 rpm for 1 minute
The samples were then frozen at -20 C or run with SDS-PAGE
After SDS-PAGE, were stained with Coomassie and developed in autoradiograph

2.2.14 Separating proteins by SDS - Polyacrylamide gel electrophoresis (SDS-PAGE)

The first publications on the use of acrylamide gels to separate proteins came in 1959 (Raymond and Weintraub 1959). The proteins are separated based on size and charge when being transported through the gel by an electrical current. Varying the concentration of polyacrylamide will change the size of the pores, and this will influence the migration of the proteins. Prior to loading the gel, the proteins are boiled with DTT and SDS, which denatures the proteins and gives them a net negative charge. A low concentration stacking gel is used to concentrate the proteins at the top of the separating gel. The separating gel is longer and has an optimal acrylamide concentration for separating the proteins according to size. 100 kDa proteins can be separated using 6-10% gels, while 10 kDa proteins are best separated on 16% gels.

Procedure:
The following was mixed:

8% separating gel	4% stacking gel
9.8 ml H_20	6.4 ml H_20
5 ml separating gel buffer	2.5 ml concentrating gel buffer
5 ml acrylamide	1 ml acrylamide
200 µl APS	100 µl APS
20 µl TEMED	10 µl TEMED

NB: The stacking gel should not be made until the separating gel is complete and has polymerized
Separating gel was added to a gel casting system.
Gel was left to polymerize for 20 minutes
Comb was inserted and concentrating gel was added
After polymerization, The gel was transferred to an electrophoresis system and add electrophoresis buffer was added.Thick gels (2mm) were run at 20-30 mA until the blue line (gel loading buffer) reached the bottom of the gel
Gels were transferred to two sheets of paper and dried for 2 hours in a Gel Dryer
Gels with radiolabeled proteins were transferred to an imaging plate for approximately 12 hours. The developing time depended on the strength of the signal.
The imaging plates were then scanned using an autoradiograph

2.2.15 Agrobacterium mediated transformation of Arabidopsis thaliana

Agrobacterium tumerifaciens was first identified 100 years ago as the causing agent of crown gall disease (Smith and Townsend 1907). During the seventies it was discovered that the bacteria contains a tumor inducing plasmid (Ti) that is transferred and stably integrated into the plant host genome. Removing the tumor inducing parts of the Ti plasmid while keeping the parts required for gene transfer enabled the use of Agrobacterium as a plant

transformation vector (P. Zambryski 1983). The method is still in use today and is probably the most cost-effective way to achieve stable plant transformation. Agrobacterium can be used to transfect a wide range of plants, but it also targets other eukaryotic cells and has been explored as a transfection vector for yeast and fungi (Bundock *et al.* 1995, de Groot *et al.* 1998). Ideally, the gene of interest is first knocked out and then complemented by introducing the same gene fused to a marker protein. When knockout mutants are not available, the transformation is done with wild type plants. Most commonly the gene is controlled by a cauliflower mosaic virus 35S promoter which ensures that the gene will be constitutively expressed throughout the plant.

The Agrobacterium strain used in this study has a helper plasmid that contains the T-DNA transfer genes as well as Rif^R, $Gent^R$ and $glufosinate^R$. All expression vectors used in plant transformation contains a 35S constitutively active promoter.

Chemically competent agrobacterium was made using an overnight liquid culture grown in Rif+Gent YEB. The culture was at OD_{600}=0.5-0.6. The cells were centrifuged at and the pellet was dissolved in ….100µl batches is transeferred to eppendorf tubes and immediately frozen in liquid nitrogen or dry ice. Cells are then kept at -80°C. One batch of 100ul is used for one transformation. The competent Agrobacterium was thawed on ice and then mixed with 300-500ng of plasmid, immediately frozen in liquid nitrogen, thawed, and then transferred to a 37°C waterbath for 2 minutes (heatshock).

Each batch is then transferred to 2ml prewarmed SOC media and set for shaking (300rpm) at 27-30°C for 2hours. After incubation, 150 ul of each batch were plated on selective (Rif+plasmid encoded antibiotic resistance) LB plates. The plates were incubated at 27-30°C.

When colonies have started forming, usually after three days, individual colonies can be picked for liquid cultures in 10 ml LB media with the same antibiotic mix as the plates. These are then grown overnight before performing PCR to verify that the desired plasmid is present.

When the cultures have been verified to contain the desired plasmid they are grown until the density is high enough for transformation (OD_{600}~1). The cells are spun down and resuspended in 2ml 5% sucrose.

Transformation of Arabidopsis is performed on plants where floral buds had developed but where the flowers were not yet open. The plants are grown for a period at 12°C to make big rosettes without flowers, and then transferred to 20°C for budding. Open flowers cannot be transformed and should be cut away to increase the relative amount of transformed seeds. This removal of open flowers also induces formation of new buds.

For each transformation (each constructs) it is advised to use more than one plant, preferably 3-6 individuals. The 2 ml sucrose suspension with agrobacterium was supplemented with 1µl Silwet L-77 just before starting the transformation.

The method used for transformation is floral-dip. Small drops of agrobacterium suspension were pipetted onto the buds with a Pasteur pipette. About half of the suspension can be kept overnight to repeat the floral-dip the next day, which increases the rate of transformation. This generation of transformed plants is now called T0.

After the floral-dip, plants were put into optimal light and temperature conditions for seeding.

Seeds from the T0generation are sowed in a very dense carpet in large surface area pots, and then stratified for three days. When the seedlings of the T1 generation were about 1 week old they were sprayed with an aqueous 1mM glufosinate ammonium solution (Finale), which interferes with the biosynthetic pathway of glutamate and detoxification of ammonium, killing the untransformed seedlings The plants were given one treatment every second day, three treatments in total. About 40 (minimum 20) of the surviving plants were replanted and left to grow rosettes. These plants are then checked for expression of the protein of interest by western blot. Good

candidates are replanted and left to seed, producing the T2generation. Seeds from the T2 generation can be used as the basis of plants in experiments.

In this study, a total of 17 different constructs were created to be used in protoplast and whole plant transformations. The following table describes each construct:

Table 2.13: Constructs used for in Agrobacterium-mediated transformation of *Arabidopsis thaliana*.

Construct	Description
AtNBR1 pB2GW7	AtNBR1 in an overexpression vector
AtNBR1 pB2WG7	AtNBR1 in an antisense overexpression vector
AtNBR1 ΔUBA1+2 pB2GW7	AtNBR1 ΔUBA3 in an overexpression vector
AtNBR1 ΔUBA1+2 pB2WG7	AtNBR1 ΔUBA3 in an antisense overexpression vector
AtNBR1 pEarleygate104	AtNBR1 with a N-terminal YFP-tag
AtNBR1 ΔUBA1+2 pEarleygate 104	AtNBR1 ΔUBA3 with a N-terminal YFP-tag
AtNBR1 D60A pEarleygate 104	AtNBR1 D60A with a N-terminal YFP-tag
Cherry-AtNBR1 pEarleygate 104	AtNBR1 with a N-terminal double tag, YFP and Cherry
ECFP-AtNBR1 pEarleygate 104	AtNBR1 with a N-terminal double tag, YFP and ECFP
ECFP-AtNBR1 ΔUBA1+2 pEarleygate 104	AtNBR1 ΔUBA3 with a N-terminal double tag, YFP and ECFP
ECFP-AtNBR1 pB2GW7	AtNBR1 with and N-terminal ECFP-tag
ECFP-AtNBR1 ΔUBA1+2 pB2GW7	AtNBR1 ΔUBA3 with a N-terminal double tag , YFP and ECFP
Δend-AtNBR1 pB7FWG2,0	Δend AtNBR1 with a C-terminal EGFP tag
Δend-NBR1 pB7FWG2,0	Δend NBR1 with a C-terminal EGFP tag
Δend-p62 pB7FWG2,0	Δend p62 with a C-terminal EGFP tag
NBR1 pEarleygate104	NBR1 with an N-terminal YFP-tag
p62 pEarleygate104	P62 with an N-terminal YFP-tag

2.2.15 Analyzing protein expression by Western blot

Western blotting is a useful method for the identification and quantification of specific proteins. The proteins are transferred to a membrane (typically nitrocellulose or polyvinylidene Fluoride -PVDF), either by directly loading a protein sample on the membrane or by transferring proteins from SDS-PAGE. Specific antibodies can then be used to detect proteins of interest. The method was first described in the late 70's as the protein counterpart of DNA southern blot (Burnette 1981, Towbin *et al.* 1979) The Dot Blot is a useful way of blotting many protein samples onto a membrane. The apparatus typically consists of a 96- or 150 well loading plate, which is then coupled to a vacuum chamber. The membrane is placed between and retains the proteins from the solution that passes through.

100 mg leaf samples of transformed Arabidopsis (T1 generation) were collected and frozen at -80°C. The samples were then homogenized in a Quiagen tissuelyser using 3mm tungsten beads. Wild type (Col) Arabidopsis was used as negative control, and a transgenic Arabidopsis line containing a chloroplast-targeted GFP (Marques *et al.* 2004) was used as positive control. This line was kindly provided by Dr. J.P. Marques (MLU Halle-Wittenberg). 400 µl PEB(+1 mM DTT) was added to each sample, vortexed, and then boiled for 5

minutes. After boiling, samples were cooled for 30 seconds on ice, then centrifuged for 15 minutes at 14000rpm. 100 µl of the supernatant was diluted in 400 µl water.
A dot-blot apparatus was used to blot the protein sample onto a 45µ PVDF membrane. ThePVDF membrane was first wetted in 100% methanol and then washed in water before being placed in the Dot Blot. Vacuum was applied using water suction. 400 µl of the diluted protein extract was blotted to a membrane used for antibody detection, while 50 µl diluted protein extract was added to a second membrane used for commassie staining. The wells were then washed with 400 µl water.
The membranes used for antibody detection were first blocked in a 4% dry-milk TBST solution overnight (4°C). After washing in TBST the membranes were incubated in 1:500 αGFP antibody in TBST for one hour at room temperature. Membranes were washed again and incubated in a 1:1000 α-Rabbit HRP-conjugated antibody TBST solution for one hour at room temperature. The membranes were then thoroughly washed. All incubating and washing steps were done with gentle shaking.The chemiluminescent signal was developed in a Pierce SuperSignal® for 5-10 minutes (depending on the strength of the signal).
The membrane used for Coomassie staining was washed in 50% methanol after blotting to remove some of the chlorophyll, then incubated for 10 minutes in a Coomassie solution. The membrane was then washed in Destain I and Destain II, to remove excess color. Pictures were taken using a Gel-doc and Fluor-S MAX from BioRad.

2.2.16 PEG-mediated transformation of Arabidopsis protoplast cells

In plant science, protoplasts are defined as plant cells lacking the cell wall. The word is derived from greek meaning to mould or plastic, referring to the first organized body of a species. This is descriptive of plant protoplasts, since the fluid mosaic characteristics of the plant membrane makes the cell more susceptible to manipulation. The isolation of plant protoplasts was first described in 1892 (Klercker 1892) and has since then been widely used in plant research. Protoplasts have the ability to take up DNA from their surroundings, which can be induced either chemically or by electroporation. This provides a relatively fast way of transforming plant cells to look at in vivo expression of tagged proteins. However, when experimenting with protoplasts it should always be taken into consideration that the cells are under stress and may therefore not exhibit natural characteristics. Gene expression has been shown to change during protoplastation (Kalbin *et al.* 1999). All expression vectors used in protoplast transformation contains a 35S constitutively active promoter.

Procedure:
NB – all work was done under sterile conditions and pipetting of protoplasts were done with cut tips

One week old Arabidopsis cell culture was collected in 50 ml falcon tubes
Centrifugation for 5 minutes at 1500 rpm
Supernatant was discarded, 25 ml Enzyme solution was added and filled to 50 ml with MS-0,34M GM. The pellet was dissolved by inerting the tube gently
Suspension was carefully transferred to two large petridishes and set for gentle shaking in dark.
The speed should was set to form one continuous wave going around the petridish.

After 1 hour the rate of protoplastation in light microscope. Protoplasts should be round and not clumped together. If needed, the cells were left for digestion longer.
5 ml cut pipette tip was used to transfer the protoplast to two 50 ml falcon tubes
Centrifugation at 800 rpm for 5 minutes, without brakes
Supernatant was carefully discarded and pellet dissolved in 25 ml MS-0,34 M GM
Centrifugation at 800 rpm for 5 minutes, without brakes
Supernatant was carefully discarded and pellet dissolved in 5 ml MS-0,28 M sucrose
Pellets were combined in a 12 ml falcon tube and centrifuged for 5 minutes at 800 rpm, without brakes
Three separate layers formed, and the top layer was healthy protoplasts
Protoplasts were transferred to eppendorf tubes with cut pipette tip.
50 µl protoplasts were transferred to 2ml flat bottomed eppendorf tube (one transformation)
5-15 µg DNA was added. The concentration was above 1µg/µl. Purer DNA = better transformation
150 µl PEG was immediately added, and the suspension was mixed carefully by ticking against the tube
Incubation 15-30 minutes in dark
Protoplasts were washed by adding 500 µl 0,275 M $Ca(NO_3)_2$, waiting for 1 minute then adding 500 µl more
Centrifugation at 800 rpm for seven minutes
Solution was removed with pipette and protoplast pellet was dissolved in 500 µl MS-0,34 M GM
Eppendorf was left on the side and in darkness for 12-48 hours
Microscopy was performed 24-48 hours after transformation
After 72 h most protoplast had died

2.2.17 Transformation of onion epidermal cells using Gene gun

This method of transformation was developed during the 80's as a rather unsophisticated method of introducing DNA into a cell. The basic principle is to coat heavy metal particles (usually 1µm gold beads) with plasmid DNA, then shooting the particles at a cell preparative. Some of the beads will enter the nucleus, and in some cells this will cause a transient transformation. By using DNA that can integrate with the genome it is also possible to create stably transformed cells. It provides a fast way of transforming almost any type of cell, and for these reasons it remains in use today. The obvious downside is that the blast causes damage to the tissue, and many of the cells die. The transformation rate is low, and a transformed cell is perforated with hundreds of metal particles, which possibly induces changes in gene expression. When used for live cell imaging, this method should therefore be an indicative approach for further experiments or to complement results from other experiments. All expression vectors used in ballistic plant transformation contains a 35S constitutively active promoter.

Procedure:
Onion epidermis was cut into 2x2 cm large squares and placed on ½ MS (-sucrose) plates
Preparation of gold particles:
Gold particles was washed with 100% EtOH and centrifuged at 2000 rpm for 90 seconds
EtOH was discarded and gold particles were left to dry
Gold particle concentration was adjusted with dH_2O to 2 mg gold per 50 µl
50 µl was used for one batch of DNA

Covering gold particles with DNA:
5-10 µg plasmid DNA was mixed with a 50 µl gold particle aliquot
20 µl spermidin and 50 µl $CaCl_2$ were put into the lid of the cap
The lid of the eppendorf was closed, and then the eppendorf was tapped against the table so that the solutions were mixed and the solution was immediately vortexed for two minutes
Centrifugation at 2000 rpm for 2 minutes
Supernatant was discarded and the DNA-covered particles was washed with 250 µl 100% EtOH,
The EtOH was removed and 50 µl 100% EtOH was added. Resuspended by pipetting.
Before using the particle gun:
Select/adjust bombardment parameters for gap distance between rupture disk retaining cap and microcarrier launch assembly. Placement of stopping screen support in proper position inside fixed nest of microcarrier launch assembly.
Check helium supply (200 psi excess of desired rupture pressure)

Equipment was cleaned: rupture disk, retaining cap, microcarrier launch assembly
Microcarriers were washed in 100% EtOH and dried completely
Microcarriers were coated with DNA and loaded onto sterile microcarriers, then left to dry
One aliquot of gold particles was enough to cover four microcarriers,
Vacuum chamber was sterilized with 70% EtOH
The sterilized rupture disk was loaded into sterile retaining cap
The retaining cap was secured to the end of the gas acceleration tube and then tightened with atorque wrench
Macrocarrier and stopping screen was inserted into microcarrier launch assembly
Microcarrier, launch assembly and target cells were placed in chamber and close door
Vacuum was set to desired level and fire button was pressed until pressure was high enough to burst the rupture disk.
Plates containing transformed cells were kept in darkness for 12-48 hours.

2.2.18 Transfection of mammalian HeLa-cells

Transient transfection of HeLa cells was carried out using METAFECTENE® from Biontex. METAFECTENE® is a polycationic reagent based on liposome technology. The method is based on capturing condensed DNA/RNA in a lipid membrane, which then fuses to the plasma membrane of the cell and delivers the DNA/RNA. After Transfection, the cells are grown for 24-48 hours and then fixed, stopping all processes in and around the cell and preserving the cells for microscopy. The fixation is also necessary for subsequent staining procedures that are too toxic to be done on live cells. All expression vectors used in transfection of HeLa cells contains the human CMV promoter.

Procedure:
30 µl MEM (no antibiotics) was mixed with 0,1µg DNA in an eppendorf tube. For co-transfections, 0,1 µg of each DNA was added.
30 µl MEM (no serum or antibiotics) was mixed with 0,5 µl Metafectene in a separate eppendorf tube
The DNA containing MEM was added to the Metafectene containing MEM and incubated for 15 minutes. This is then added to a single well of HeLa cells along with 140 µl MEM with antibiotics.

2.2.19 Fluorescence and confocal microscopy

Fluorescence microscopy:

A fluorescence microscope is used to study a sample that contains fluorescent molecules. A standard fluorescence microscope is basically a light microscope with the added property of fluorescence detection. This consists of a source of excitation light, and filters to separate the weak emitted light from the strong excitation light. Fluorescence microscopy is much used in biological sciences, where fluorescent tags such as the GFP makes it possible to visualize cells and cellular components.

Confocal laser scanning microscopy (CLSM):

In a confocal microscope the light is focused at a desired focal plane, which gives a higher degree of lateral and axial resolution than traditional light microscopy. When used in fluorescence microscopy, the confocal microscope excludes “out of focus” florescent signal, thus providing a sharper image. The Confocal laser scanning microscope is most widely used today, and employs lasers to scan the specimen. Images are acquired point-by-point and reconstructed with a computer.

Procedure:
See table 2.9-2.12 for descriptions of microscopes and settings.
Protoplasts were imaged on standard objective glass with cover slip.
Images of mammalian HeLa cells were taken directly in 8-well growing chambers.

2.2.20 The green fluorescent protein - GFP

The green fluorescent protein was first isolated 50 years ago from the jellyfish Aequorea Victoria by Shimomura and coworkers (Shimomura *et al.* 1962), but it was not until the 90's, when the primary structure was solved, that scientists started using the GFP as a tool in molecular biology (Chalfie *et al.* 1994, Inouye and Tsuji 1994, Prasher *et al.* 1992). Since then, GFP has become one of the most important tools for illuminating cellular structures as well as tissues and organs of multicellular organisms (eg. C.*elegans* and *D. rerio*.) By manipulating the structure of GFP through point mutations, different kinds of fluorescent proteins has been developed that have enhanced luminescence and/or different absorbtion/emission spectra, work which has been pioneered by Roger Tsien and coworkers (Heim *et al.* 1995). Today, scientists can choose between fluorescent proteins of practically any color, with excitations wavelengths ranging from 380-600 nm (EBFP-Far red)

3.0 Results

A protein sequence alignment shows that the *Arabidopsis thaliana* protein sequence Q9SB64 shares sequence similarity with NBR1 (see figure 3.1).

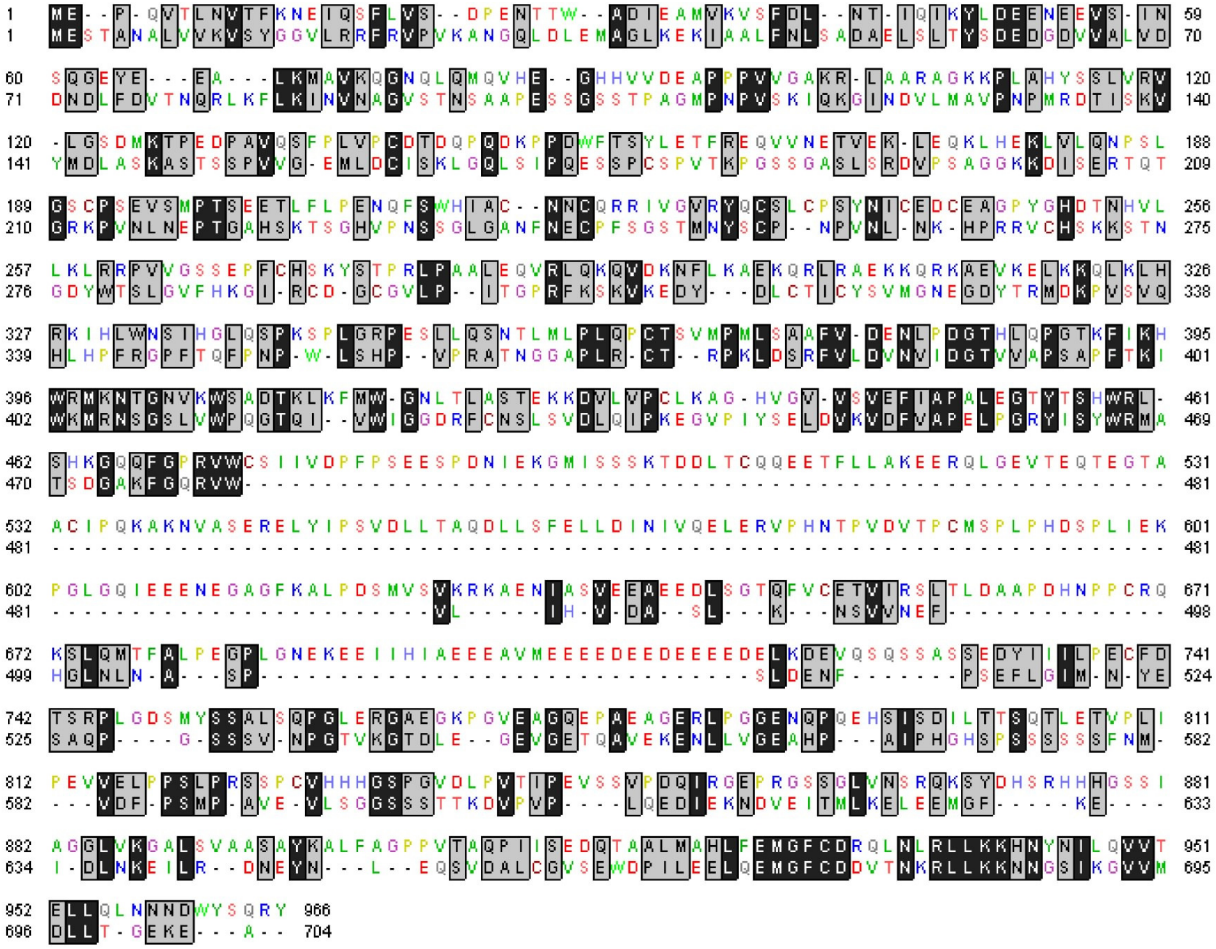

Figure 3.1: Alignment of protein sequences from Q9SB64 and NBR1. Top row: Human NBR1. Bottom row: Arabidopsis Q9SB64. Black boxes indicate sequence identity while gray boxes indicate sequence similarity.

These findings suggest that the uncharacterized protein Q9SB64 (hereafter referred to as AtNBR1) may be the *Arabidopsis* homologue to mammalian NBR1. A multiple sequence alignment of nine homologues of AtNBR1 from different plant species shows that all nine proteins contain four conserved regions (see appendix, figure 6.2); An N-terminal PB1 domain, a zinc-finger domain, two C-terminal UBA domains and a conserved region that constitutes a globular domain (figure 3.2). This suggests that AtNBR1 is conserved throughout the plant kingdom, and further strengthens the identification of the protein domains of AtNBR1.

Figur 3.2: Regions of high sequence similarity in orthologues of AtNBR1 from nine different plant species. Illustration based on multiple sequence alignment of nine homologues of AtNBR1 (see appendix, figure 6.5). Red regions are conserved in all nine homologues, and a putative identification of domains is indicated.

3.1 AtNBR1 self-interacts via its N-terminal PB1 domain

The COILS computer program can be used to test whether a protein contains putative CCs, creating a prediction based on a similarity score to other well known CCs (Lupas *et al.* 1991).When analyzing NBR1 and p62 we find that NBR1 contains two possible CCs, none is found in p62 and a weak prediction is made in the N-terminal region of AtNBR1(see figure 3.3).

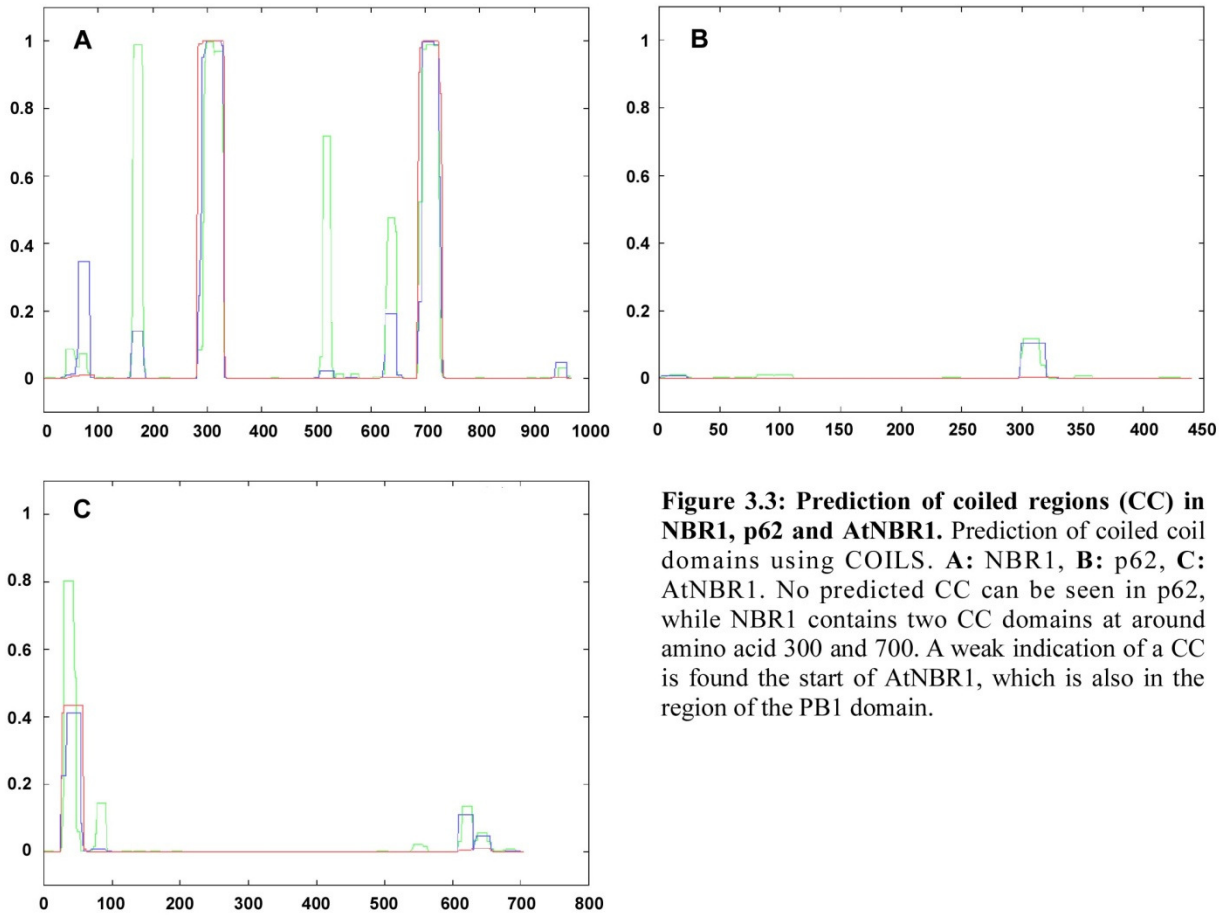

Figure 3.3: Prediction of coiled regions (CC) in NBR1, p62 and AtNBR1. Prediction of coiled coil domains using COILS. **A:** NBR1, **B:** p62, **C:** AtNBR1. No predicted CC can be seen in p62, while NBR1 contains two CC domains at around amino acid 300 and 700. A weak indication of a CC is found the start of AtNBR1, which is also in the region of the PB1 domain.

Mammalian NBR1 has a Type I PB1 domain that contains only the OPCA motif, while p62 contains a Type I/II PB1 domain. When looking at the PB1 domain of AtNBR1, we find that it contains the OPCA motif and the conserved Lys, placing it in the Type I/II group together with p62 (see figure 3.4). In addition, it contains two arginines in the second β-sheet that has

been shown to be important in p62 binding to λPKC and in p62 self-interaction (Lamark, et al. 2003).

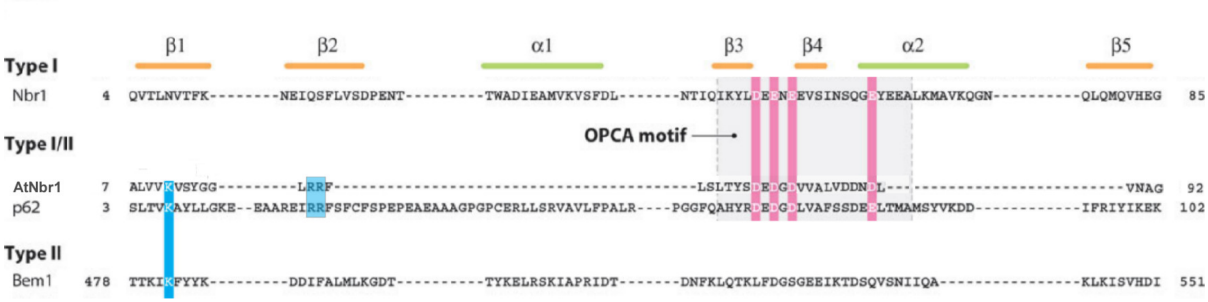

Figur 3.4: Alignment of PB1 protein sequences. Conserved amino acids in the basic (blue) and acidic (red) regions of the PB1 Domain. P62 and AtNBR1 is both in the typeI/II category, with a conserved Lys and OPCA motif (figure modified from (Sumimoto, et al. 2007). Also shown is a basic cluster of two arginines in the second β-sheet (blue box) which in known to be important in p62 PB1 interactions (Lamark, et al. 2003).

The electrostatic surface potential of PB1 in AtNBR1 shows that the positively and negatively charged interaction surfaces are located on opposite sides (see figure 3.5). This suggests that AtNBR1 may be able to form homo-oligomers, as each protein has the potential to interact with two other proteins. A similar distribution of positive and negative charge was reported for the PB1 domain of p62, and is required for the polymeric head-to-tail interaction of p62 (Lamark, et al. 2003).

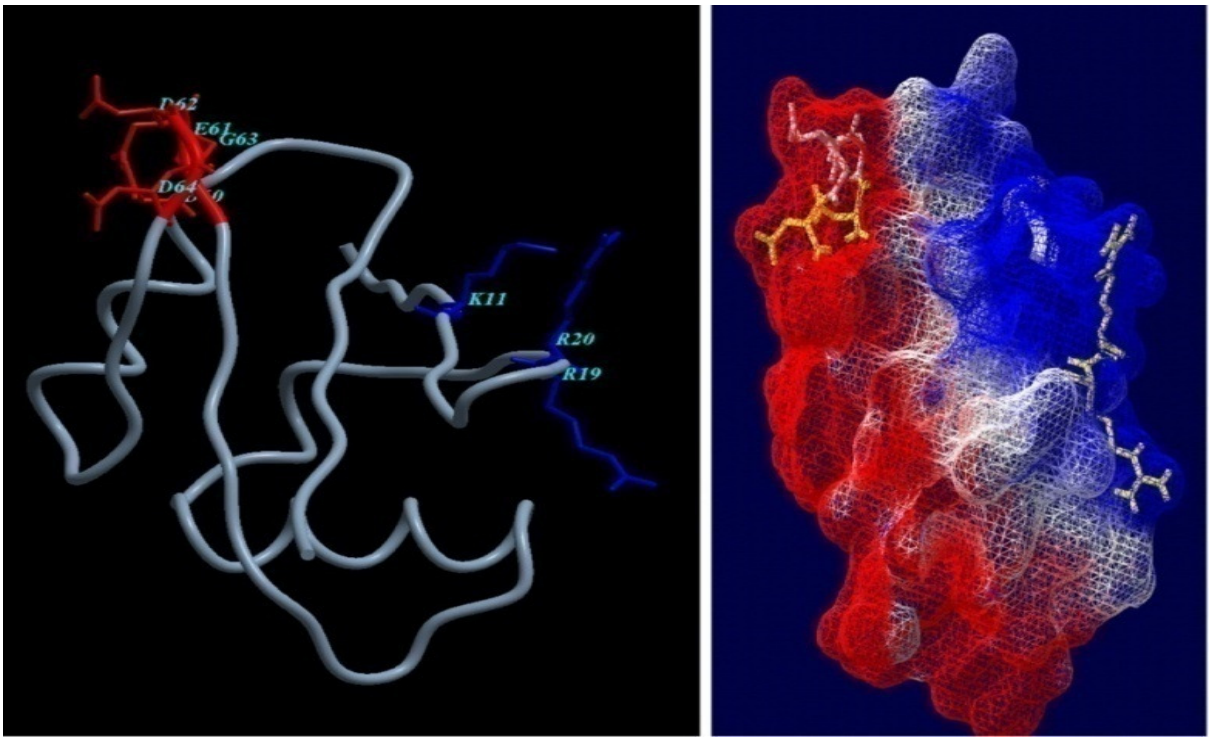

Figure 3.5: Computer generated model of the PB1 domain of AtNBR1. Left: Simplified ribbon diagram of the structure of PB1 in Q9SB64 with acidic amino acids highlighted in red and basic amino acids highlighted in blue. Acidic amino acids; D60, E61, D62, G63 and D64. Basic amino acids; K11, R19 and R20. Created in ICM-Browser. **Right:** Electrostatic surface potential of the AtNBR1 PB1 domain, as predicted by homology to the PB1 domain of pkciota. The model is based on web homology modeling (http://tardis.nibio.go.jp/fugue/) and viewed in Swiss PDB viewer (http://spdbv.vital-it.ch/).

The N-terminal type I/II PB1 domain is responsible for the self-polymerization of p62, and the acidic and basic residues that are essential for the self-interaction of p62 have been characterized (Lamark, et al. 2003). Having established that AtNBR1 also contains a type I/II PB1 domain, AtNBR1 may also be able to self-interact through interaction of PB1. Based on the sequence alignment in figure 3.4, four point mutations in AtNBR1 were chosen and expected to have a negative effect on AtNBR1 PB1-interaction. The residues mutated in AtNBR1 correspond to the residues that are most important in p62 self-interaction. Two positively charged amino acids within the basic cluster, K11 and R19, and two negatively charged amino acids within the acidic OPCA-motif, D60 and D73, were mutated to the neutrally charged alanine by site-specific mutagenesis.

To test if ATNBR1 self-interacts, two series of co-immunoprecipitation experiments were performed. In the first series of experiments (figure 3.6 B), myc- and GFP-tagged AtNBR1 were co-translated using the TNT-T7 Rabbit reticulate lycate system (Promega). GFP-AtNBR1 was precipitated with α-GFP antibodies and self-interaction indicated by the co-

precipitation of myc-AtNBR1. In the second series of experiments (figure 3.6 C), HA-AtNBR1 was co-translated with untagged AtNBR1 (resulting from the use of two native start codons present in the same plasmid). HA-AtNBR1 was precipitated with α-HA antibodies and self-interaction indicated by the co-precipitation of AtNBR1. The results presented in figure 3.6 shows that AtNBR1 is able to interact with itself. To test if the PB1 domain of AtNBR1 is responsible for self-interaction, the experiments were performed with AtNBR1 point mutants (see figure 3.6 B and C).

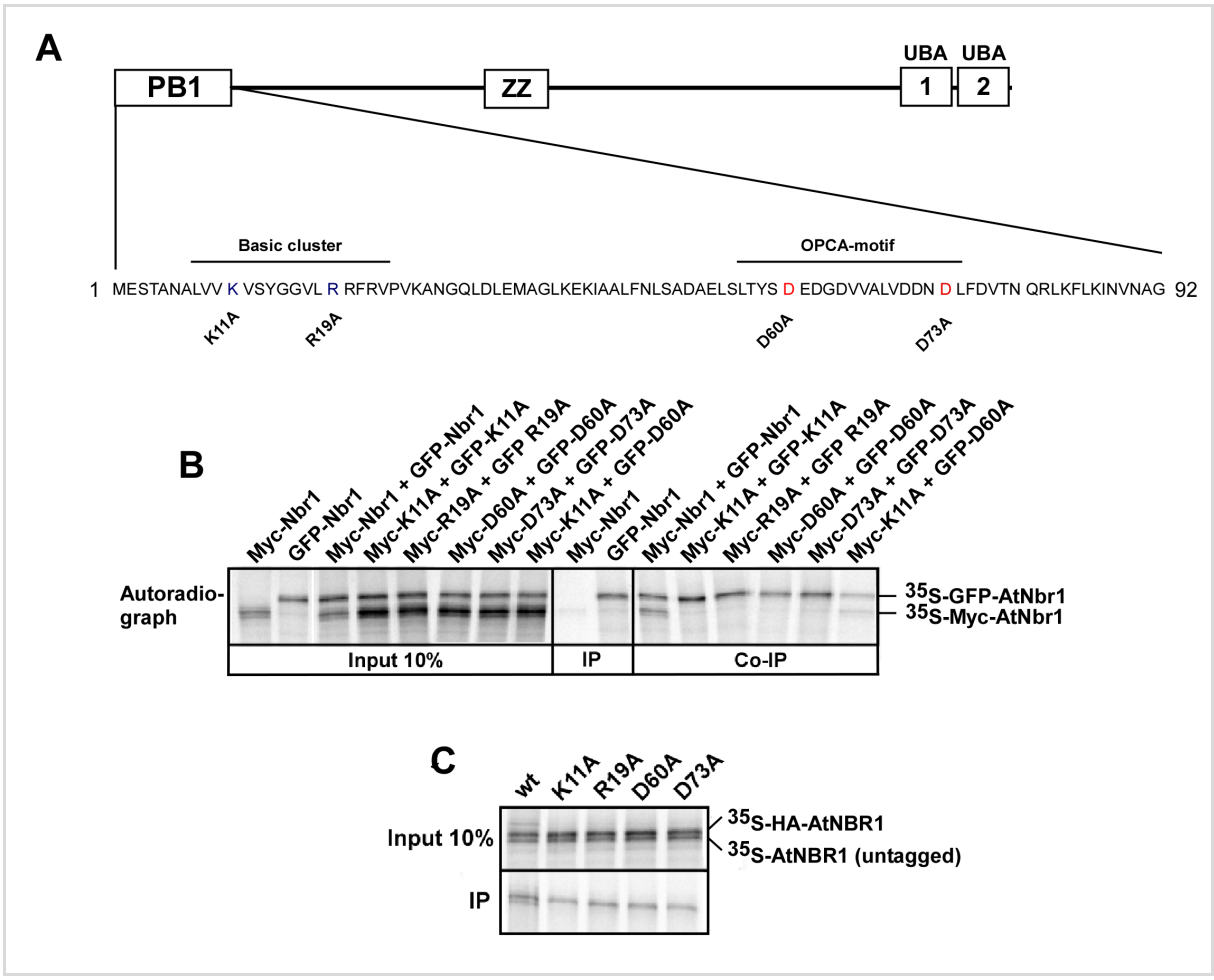

Figure 3.6: The PB1 domain of AtNBR1 is responsible for self interaction of the protein. A: Scehamtic drawing of the domain organization of AtNBR1 and sequence of the PB1 domain with the relevant point mutants indicated. **B:** Co-immunoprecipitation with full-length AtNBR1, wt and point mutants. Myc-tagged AtNBR1 (wt or the indicated mutants) was *in vitro* co-translated together with GFP-tagged AtNBR1 (wt or the indicated mutants) in the presence of $^{[35]}$Smethionine, and precipitated using an αGFP antibody. Immunoprecipitated and co-precipitated proteins as well as in vitro translated proteins corresponding to 10% of the input were resolved by SDS-PAGE and detected by autoradiography. Negativ control: immunoprecipitation, myc-AtNBR1, Positive control; immunoprecipitation, GFP-AtNBR1. **C:** Co-immunoprecipitation with full-length AtNBR1, wt and point mutants. HA-tagged AtNBR1 (wt or the indicated mutants) was in vitro translated in the presence of $^{[35]}$S-methionine, and precipitated using an αHA antibody. Immunoprecipitated and co-precipitated proteins as well as in vitro translated proteins corresponding to 10% of the input were resolved by SDS-PAGE and detected by autoradiography.

The results presented in figure 3.6 shows that self-interaction of AtNBR1 requires a functional PB1 domain. All four PB1 point mutants lose the ability to self-interact (figure 3.6 B and C), while an interaction was observed between a basic motif mutant and an acidic OPCA mutant (figure 3.6 B, last lane). This means that a basic point mutant is able to interact with an acidic point mutant. An additional interaction experiment was carried out using the isolated PB1 domain of AtNBR1 (amino acid 1-100). The PB1 domain was isolated by traditional cloning and point mutants were created as in the full-length protein. The wt PB1 and all four point mutants were then expressed as GST-fusion proteins and used in a GST-pulldown assay with in-vitro translated PB1 domains (figure 3.7).

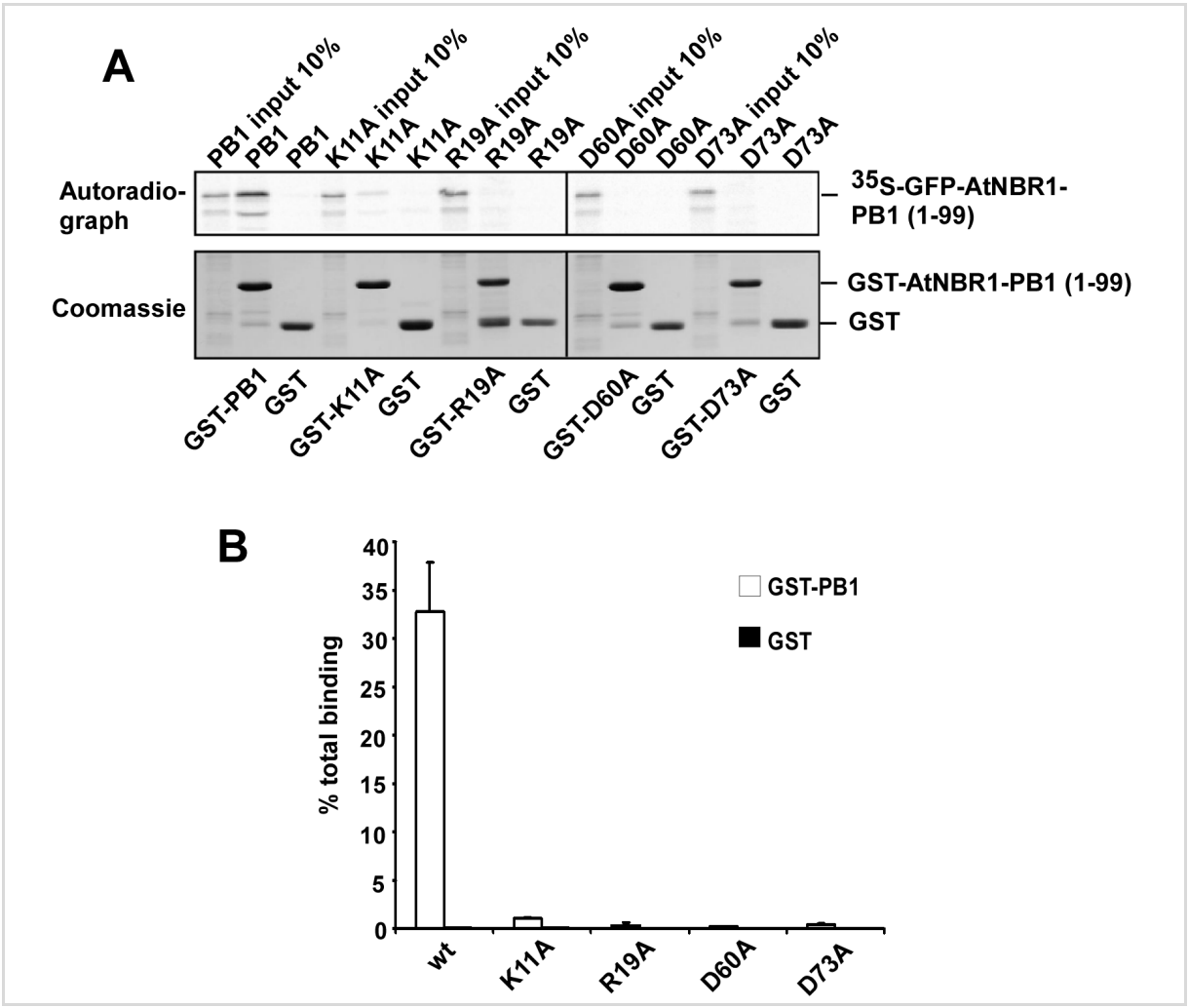

Figure 3.7: The PB1-domain of AtNBR1 self-interacts through acidic residues of the OPCA motif and residues of the basic cluster. A: GST-pulldown assay using in-vitro translated [35]S-GFP-PB1 (wt or the indicated mutants) and GST- PB1 (wt or the indicated mutants) produced by coupled in vitro transcription and translation in the presence of [35]S-methionine and bacterial expression respectively. GST-tagged proteins and pulled-down proteins as well as in vitro translated proteins corresponding to 10% of the input were resolved by SDS-PAGE, stained using coomassie, and detected by autoradiography. **B:** quantitative representation of the interaction data shown in *A*. Y-axis values are set to percent total binding, based on input x 10. Results are mean values of three independent experiments with standard deviations indicated as bars.

Results shown in figure 3.7 are clearly suggestive of PB1 self-interaction through interaction between the positively and negatively charged interaction surfaces. While all four point mutants completely lost the ability to self-interact, the wild type PB1 domain showed a strong self-interaction. Based on the 10% input, the total amount of precipitated protein is calculated to approximately 30%.

3.2 Only one of the two UBA domains of AtNBR1 binds ubiquitin

AtNBR1 contains two predicted UBA domains in the C-terminal region and both these UBAs cantain the conserved amino acids predicted to create the Ub binding hydrophobic patch (see figure 3.8). A secondary structure prediction reveals that the position of the three helix bundle of both UBA domains is similar to that found in the UBA domain of p62 (see figure 3.9).

```
Sc Rad23A UBA2    374    -DDQAISRLCELGF--ERDLVIQVYFACDKNEEAAANILFS----------   394
Sc GTS1   UBA     195    -YSRQLAELKDMGFG-DTNKNLDALSSAHGNINRAIDYLEK----------   233
Hs p62    UBA     392    RLIESLSQMLSMGFSDEGGWLTRLLQTKNYDIGAALDTIQYSKHPPPL----   440
Hs UPB5   UBA2    724    -PEDCVTTIVSMGF--SRDQALKALRATNNSLERAVDWIFS----------   761
Hs NBR1   UBA     915    QTAALMARLFEMGFC-DRQLNLRLLKKHNYNILQVVTELLQLNNNDWYSQRY  966
At Rad23A UBA2    333    -EREAIERLEGMGF--DRAMVLEVFFACNKNEELAANYLLD----------   370
At KIN10  UBA     317    -DEEILQEVINMGF--DRNHLIESLRNRTQNDGTVTYYLIL----------   354
At Nbr1   UBA1    617    VEITMLKELEEMGFK-EIDLNKEILRDNEYNLEQSVDALC----------   656
At Nbr1   UBA2    659    EWDPILEELQEMGFC-DDVTNKRLLKKNNGSIKGVVMDLLTGEKEA------  704
```

Figure 3.8: Amino acid sequence of selected UBA domains from human (Hs), Yeast (Sc) and Arabidopsis (At). The two bottom rows are the predicted UBA domains of AtNBR1. Highlighted in yellow are some of the amino acids that are conserved in all domains, and that have been found to constitute the hydrophobic binding patch (based on a comparison with other UBA sequences, see appendix, figure 6.4).

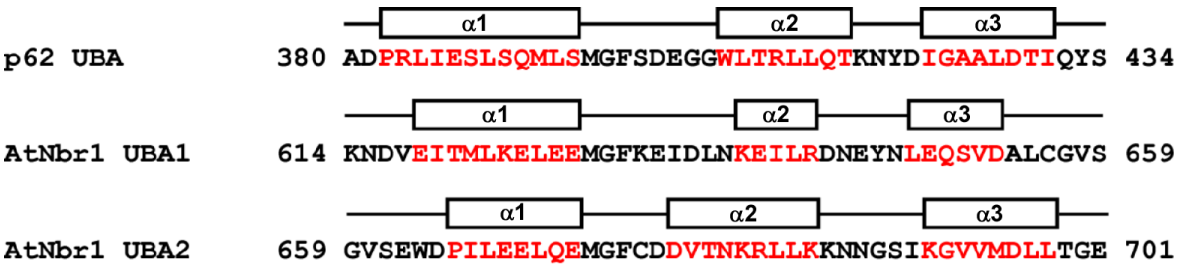

Figur 3.9: Secondary structure prediction of UBA domains in AtNBR1. Amino acid sequence and schematic illustration of the predicted three helix bundle that constitutes the UBA domains of AtNBR1. Prediction was made using JPRED (http://www.compbio.dundee.ac.uk/www-jpred/). Also included is the sequence and location of the three α helix structures in the UBA domain of p62. (Evans *et al.* 2008).

The main hypothesis about AtNBR1 having two UBA domains is that it binds poly-Ub stronger than a single UBA domain would. Also, having two domains might aid in selection of specific Ub-chains. To test this, GST pulldown was performed with in vitro translated AtNBR1 and GST-Ub and GST-4xUb (see figure 3.10). Deletion constructs of AtNBR1 was made to test if the binding of Ub could be attributed to one of the UBA domains, or if both

contribute to the binding. In addition, a monomeric D60A mutant of AtNBR1 was tested since polymerization of AtNBR1 may affect the binding properties of AtNBR1.

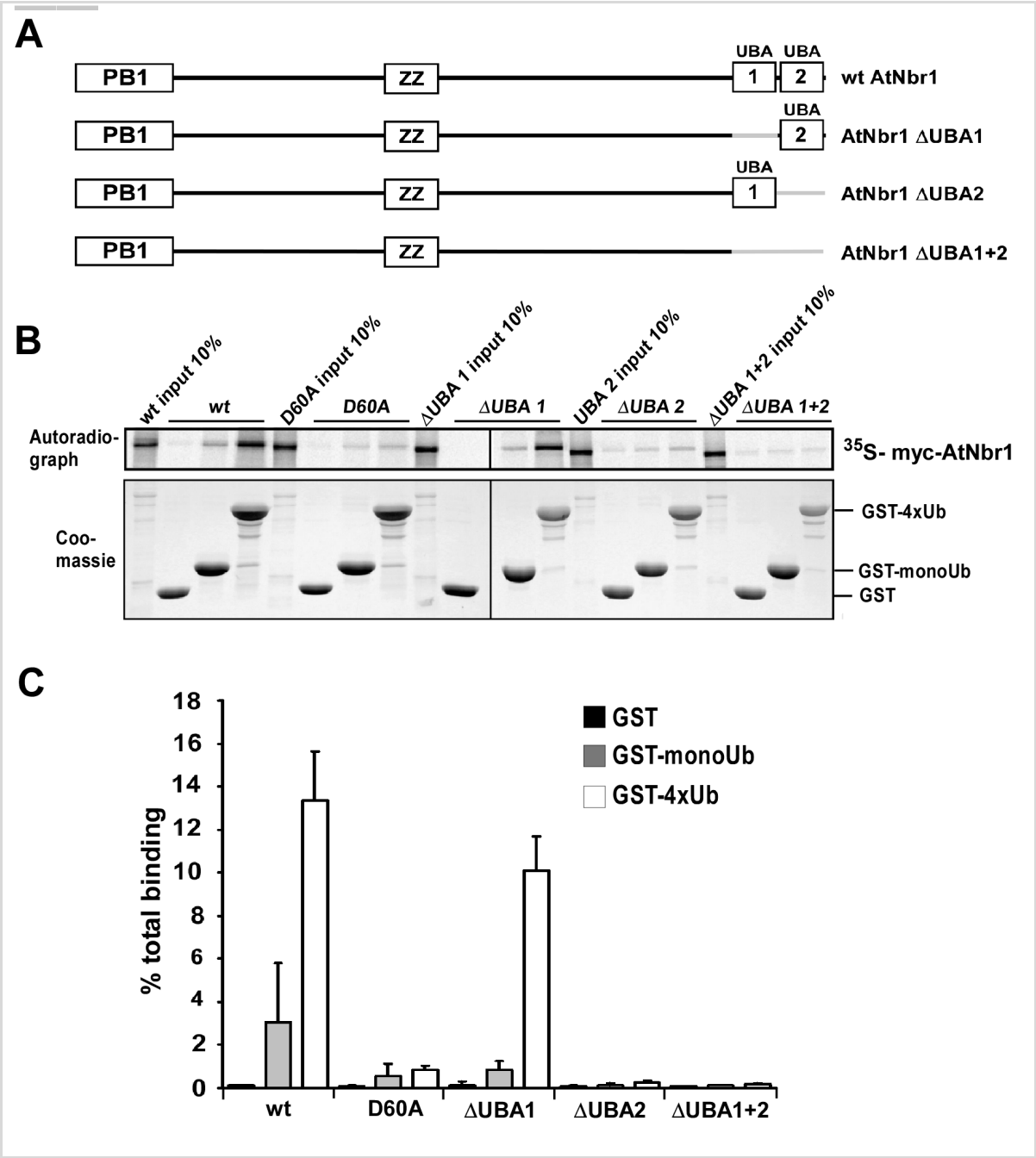

Figure 3.10: AtNBR1 binds 4xUb and mono-Ub through UBA2. A: Structural representation of AtNBR1 and UBA deletion constructs (grey regions are deleted). **B:** GST-pulldown assay using in-vitro translated [35]S-Myc-AtNBR1 (wt or the indicated mutants) and GST-Ub (mono and tetra) produced by coupled in vitro transcription and translation in the presence of [35]S-methionine and bacterial expression respectively. GST-tagged proteins and pulled-down proteins as well as in vitro translated proteins corresponding to 10% of the input were resolved by SDS-PAGE, stained using coomassie, and detected by autoradiography. **C:** quantitative representation of the interaction data shown in *A*. Y-axis values are set to percent total binding, based on input x 10. Results are mean values of three independent experiments with standard deviations indicated as bars.

The results from figure 3.10 show that AtNBR1 has the ability to bind Ub, and that the UBA2 domain is responsible for this binding. Deletion of the UBA2-domain completely eliminates interaction with Ub, while deletion of the UBA1 domain has no significant negative effect on Ub binding. However, the strong binding observed between wt-AtNBR1 and 4xUb is reduced almost tenfold when using a monomeric point-mutant (D60A), indicating that polymerization is an important element in determining binding affinity to 4xUb. It was therefore necessary to verify these results by testing the binding capacity of the isolated UBA-domains, which would exclude the effect of polymerization. The results from this experiment are shown in figure 3.11. Monomeric UBA2 is able to bind Ub while monomeric UBA1 does not show significant binding. Compared to full-length AtNBR1, the Ub binding capacity of UBA2 is considerably lower, and monomeric UBA2 binds more strongly to GST-Ub than to GST-4xUb. When comparing the binding efficiency of monomeric AtNBR1 and the isolated UBA1+2 domain, the binding is approximately the same (results not shown). This indicates that the UBA domains alone are required for Ub binding, and that no other part of the protein partakes in this interaction.

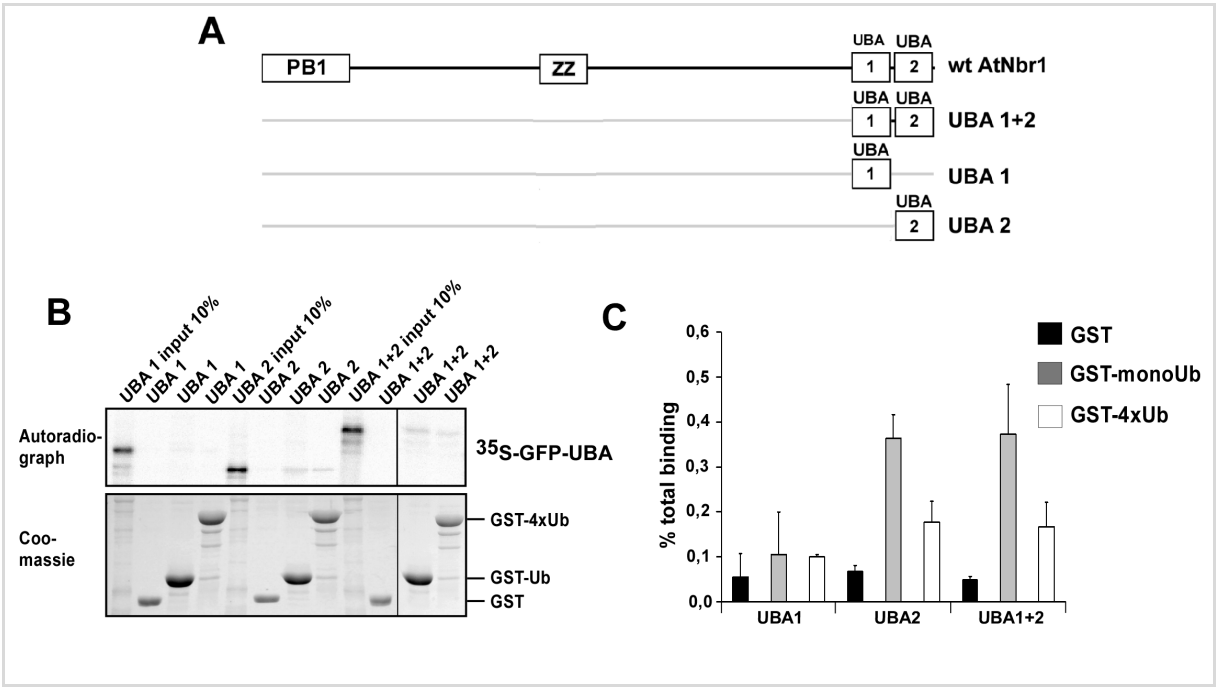

Figure 3.11: The isolated UBA2-domain of AtNBR1 binds Ub. A: Structural representation of AtNBR1 and UBA deletion constructs (grey regions are deleted). **B:** GST-pulldown assay using in-vitro translated [35]S-GFP-UBA (UBA1, UBA2 or UBA1+2) and GST-Ub (mono and tetra) produced by coupled in vitro transcription and translation in the presence of [35]S-methionine and bacterial expression respectively. GST-tagged proteins and pulled-down proteins as well as in vitro translated proteins corresponding to 10% of the input were resolved by SDS-PAGE, stained using coomassie, and detected by autoradiography. **C:** quantitative representation of the interaction data shown in *A*. Y-axis values are set to percent total binding, based on input x 10. Results are mean values of three independent experiments with standard deviations indicated as bars.

3.3 AtNBR1 interacts with Arabidopsis homologues of ATG8.

It has previously been shown that p62 and NBR1 are recruited to autophagosomes by binding to the LC3 and GABARAP family proteins (Kirkin, et al. 2009b, Pankiv, et al. 2007). Arabidopsis contains a family of nine ATG8 homologues (A-I), which all show sequence similarity to mammalian and yeast ATG8, and have been linked to the autophagic machinery of plants (see section 1.3). The following figure shows a phylogram of ATG8-orthologues from different organisms.

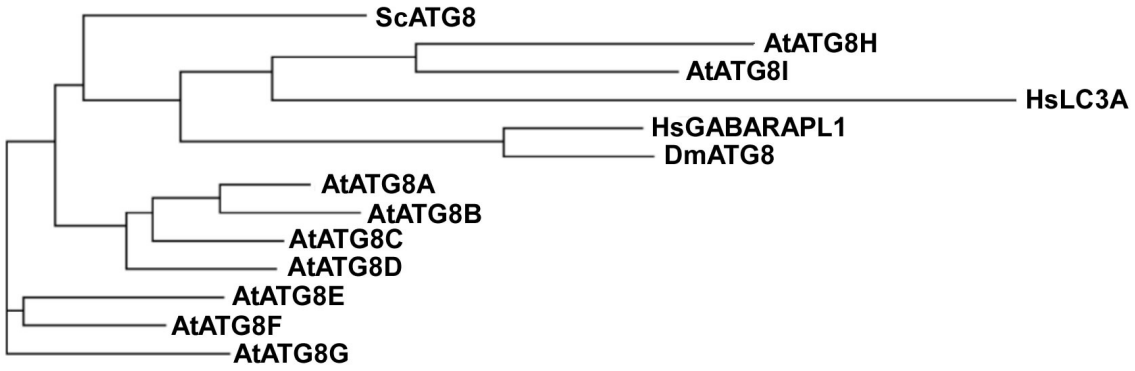

Figur 3.12: Phyologram of ATG8 orthologues. Sc- *Saccharomyces cerevisiae,* Hs- *Homo sapiens*, Dm- *Drosphila melanogaster*, At- *Arabidopsis thaliana*. Generated using ClustalW.

Given that AtNBR1 is the plant-counterpart of mammalian NBR1 and p62, it is assumed that AtNBR1 is able to bind AtATG8. This was tested by GST-pulldown assays using *in vitro* translated AtNBR1 against GST-coupled AtATG8 (see figure 3.13).

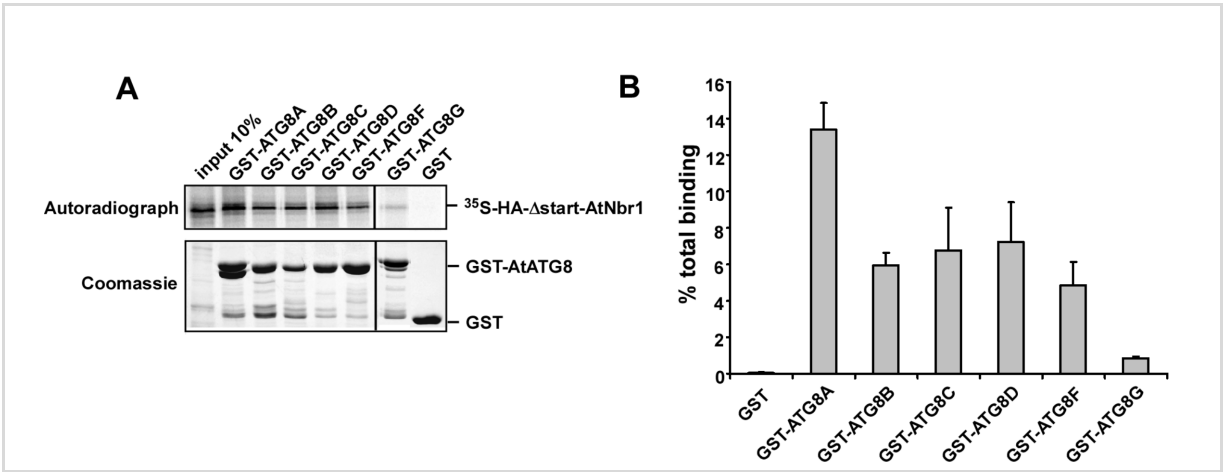

Figure 3.13: AtNBR1 binds to AtATG8. A: GST-pulldown assay using in-vitro translated $^{[35S]}$HA-AtNBR1 and GST-AtATG8 (A,B,C,D,F,G) produced by coupled in vitro transcription and translation in the presence of $^{[35S]}$-methionine and bacterial expression respectively. GST-tagged proteins and pulled-down proteins as well as in vitro translated proteins corresponding to 10% of the input were resolved by SDS-PAGE, stained using coomassie, and detected by autoradiography. **C:** quantitative representation of the interaction data shown in *A*. Y-axis values are set to percent total binding, based on input x 10. Results are mean values of three independent experiments with standard deviations indicated as bars.

AtATG8A, B, C, D, F and G were tested and found to bind AtNBR1. Out of these, AtATG8A showed the strongest binding, but B, C, D and F were also strong binders. AtATG8G and H (results not shown for AtATG8H) both showed significantly lower binding than all the other AtATG8s tested. The coomassie staining shows that AtATG8A comes out as two separate bands on the gel (figure 3.13, lane 2). Each of these bands is as strong as the individual bands of the other AtATG8s, and this may partially explain the difference in binding. The strong interaction between AtNBR1 and AtATG8A is not dependent on PB1 interaction, as a point mutation in the PB1 domain (D60A) did not affect binding (see figure 3.14 A).

In order to further examine the role of AtNBR1 in autophagy it was necessary to map the AtATG8 interaction site. This would enable the creation of mutated AtNBR1 that is unable to bind AtATG8. If AtNBR1 is degraded by autophagy, losing the ability to bind ATG8 is expected to abolish any autophagic degradation of AtNBR1, as it can no longer associate with the autophagosome. To map the exact region of AtNBR1 that contains the ATG8-binding site, various deletion and isolation constructs of AtNBR1 were created. These constructs were then used in GST-pulldown assays with GST-AtATG8A (figure 3.14).

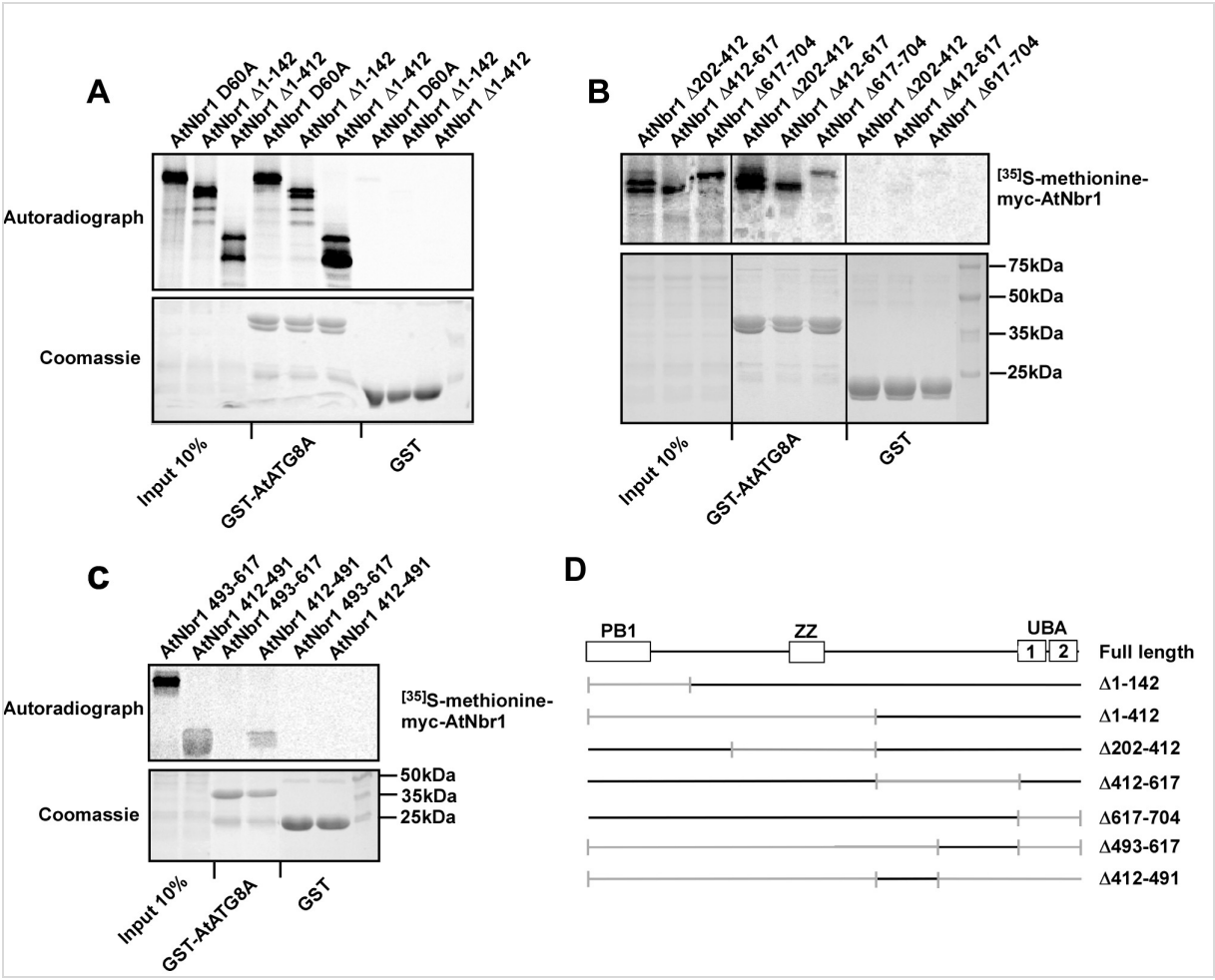

Figure 3.14: The region spanning amino acids 412-491 of AtNBR1 is sufficient for interaction with AtATG8A. GST-pulldown assay using in-vitro translated [35]S-myc-AtNBR1 (indicated mutant or truncated constructs) and GST-AtATG8A produced by coupled *in vitro* transcription and translation in the presence of [35]S-methionine and bacterial expression, respectively. GST-tagged proteins and pulled-down proteins as well as in ivtro translated proteins corresponding to 10% of the input were resolved by SDS-PAGE, stained using coomassie, and detected by autoradiography. **A:** GST-pulldown assay with monomeric deletion constructs of AtNBR1. **B:** GST-pulldown assay with polymeric deletion constructs of AtNBR1. **C:** GST-pulldown assay with isolated regions of AtNBR1. **D:** Structural representation of AtNBR1 constructs.

The data presented in figure 3.14 is tentative, as only one set of data is included. None of the AtNBR1 deletion constructs failed to interact with ATATG8A, but two deletion constructs (Δ412-617 and Δ617-704) displayed a weaker interaction (figure 3.14 A and B), indicating that there is more than one AtATG8 interaction region in AtNBR1. Deletion of amino acids 1-412 did not result in loss of binding (figure 3.14 A), further indicating that the binding site was present between amino acid 412 and 704. An isolation construct of amino acids 493-617 did not show binding, which mapped down the binding site to amino acids 412-493 and 617-704 (figure 3.14 C). A fragment containing amino acids 412 and 491 was created, and this

piece of 79 amino acids was able to bind AtATG8A (figure 3.14 C). The UBA domains (617-704) have not been tested separately for binding to AtATG8 and could possibly represent a second interaction surface.

3.4 Experiments with AtNBR1 and ATATG8 in HeLa cells

All transfections of HeLa cells were done using the Metafectene® system. Cells were fixed 24 hours after transfection and all pictures were taken using a laser scanning confocal microscope (Zeiss).

Mammalian p62 and NBR1 form aggregates when overexpressed in autophagy-deficient HeLa cells, and the aggregation is caused by a combination of self-polymerization and binding of ubiquitinated proteins (Bjørkøy, et al. 2005, Kirkin, et al. 2009b). The p62-containing aggregates are seen as round punctuate dots when visualized in HeLa cells, and upon deletion of the PB1 or UBA domain these structures are lost. Given that AtNBR1 is distinctly similar in structure to p62 and NBR1, and is able to self-polymerize and bind Ub, it is expected that AtNBR1 may be able to form similar structures when overexpressed in HeLa cells. To test this, AtNBR1 was expressed in HeLa cells using an N-terminal EGFP expression vector.

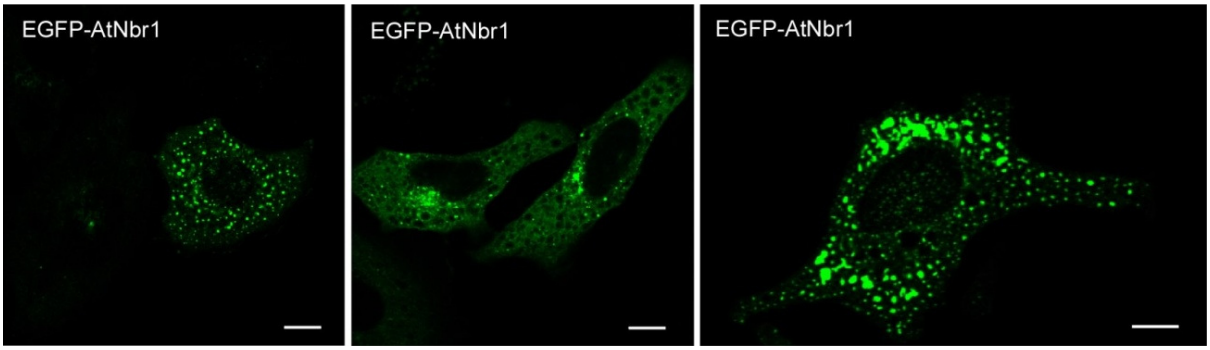

Figure 3.15: EGFP-AtNBR1 forms cytosolic aggregates when overexpressed in HeLa cells. HeLa cells transfected with EGFP-AtNBR1 show a large cytosolic accumulation of AtNBR1 containing aggregates. No signal can be detected in the nucleus. Bars are 10µm.

As seen in figure 3.15, EGFP-tagged wt AtNBR1 forms cytosolic aggregates in HeLa cells. Having confirmed that AtNBR1 is able to form aggregates, the next step was to verify that the aggregation is dependent on the self-polymerization and Ub binding of AtNBR1. A PB1 point mutant and a UBA1+2 deletion mutant of AtNBR1 was tagged with N-terminal EGFP and expressed in HeLa cells (see figure 3.16 and 3.17).

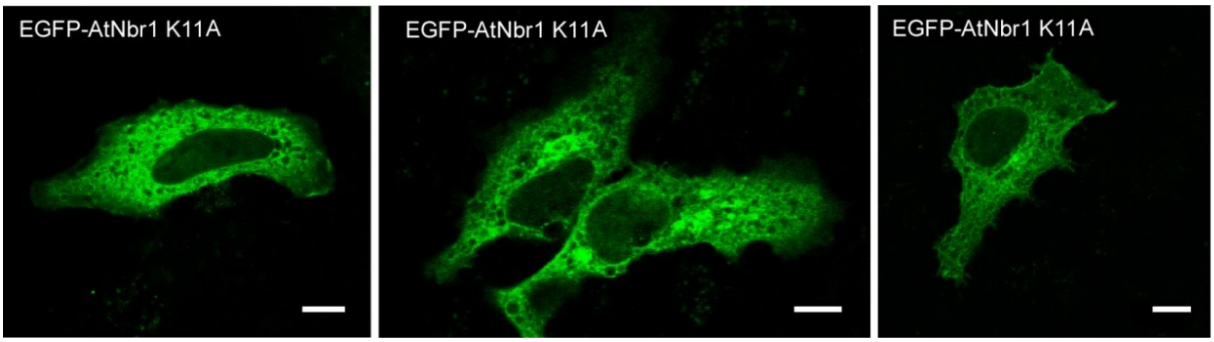

Figure 3.16: EGFP-AtNBR1-K11A is diffusely distributed in the cytosol of transfected HeLa cells. N-terminal EGFP-tagged AtNBR1 with a point mutation in the basic cluster of the PB1 domain (lysine to alanine) lose the ability to form cytosolic aggregates in HeLa cells. No signal can be detected in the nucleus. Bars are 10µm.

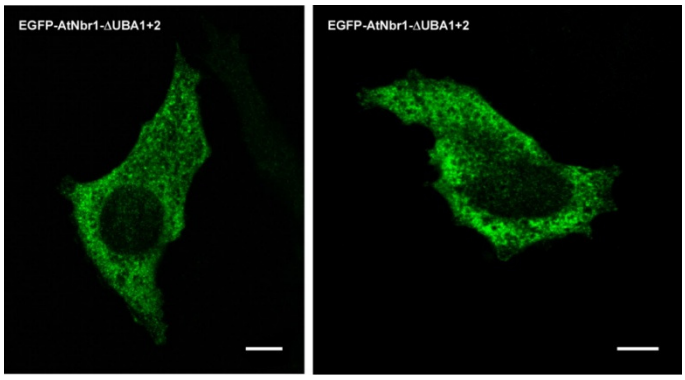

Figure 3.17: EGFP-AtNBR1-ΔUBA1+2 is diffusely distributed in the cytosol of transfected HeLa cells. N-terminal EGFP-tagged AtNBR1 lacking both UBA domains lose the ability to form cytosolic aggregates in HeLa cells. No signal can be detected in the nucleus. Bars are 10µm.

The results presented in figure 3.16 show that AtNBR1 lost the ability to form cytosolic aggregates in HeLa cells when the PB1 domain is non-functional. Polymerization is necessary for aggregate formation. Removing the two UBA domains also results in loss of aggregate formation (figure 3.17), indicating that Ub binding is also necessary for aggregate formation.

Mammalian lysosomes contain acid hydrolases that require a low pH to function. GFP is acid labile, with a pK_a of 6.0 (Shaner *et al.* 2005). This results in a loss of fluorescence when GFP enters acidified compartments. The red fluorescent protein mCherry is more acid-stabile than GFP, and can therefore be used to visualize proteins that are recruited to acidic environments (Pankiv, et al. 2007, Shaner, et al. 2005). In a recently described approach to fluorescent tagging, combing GFP and the red fluorescent protein mCherry in a double tag made it possible to deduce whether a protein is present in neutral or acidic compartments. In a neutral environment like the cytosol, both GFP and mCherry is functional and the emission spectra will overlap, while in an acidic environment the GFP will stop fluorescing leaving only the

red fluorescence of mCherry (Bjørkøy *et al.* 2009). This was used to demonstrate that p62 and NBR1 containing aggregates are sequestered to acidic lysosomes in HeLa cells (Kirkin, et al. 2009b, Pankiv, et al. 2007).

AtATG8 is known to be associated with autophagic bodies in plant cells, and considering the high degree of homology between plant and mammalian ATG8, it is reasonable to believe that AtATG8 can associate with autophagic bodies in a mammalian system. To test this, AtATg8A was expressed with an N-terminal mCherry-tag in HeLa cells.

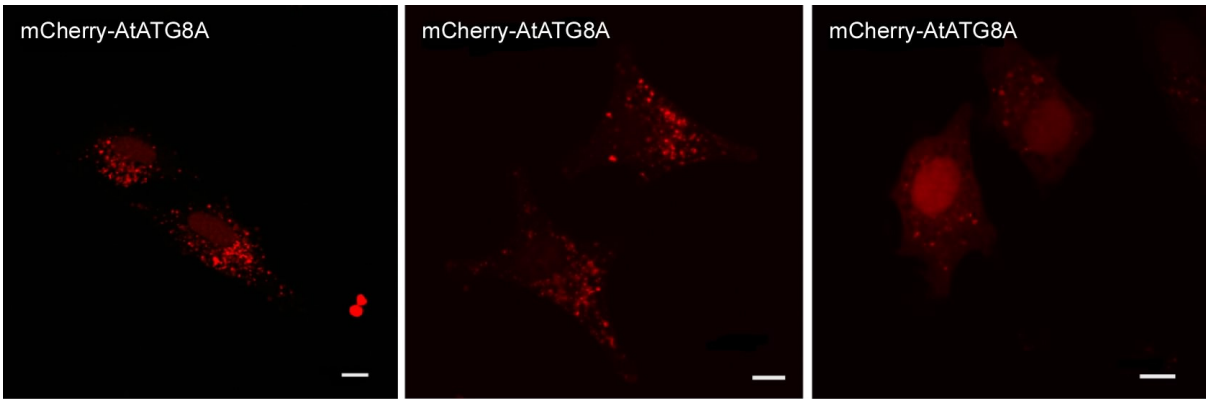

Figure 3.18: mCherry-ATATG8A is found in cytosolic aggregates and ubiquitously localized in the nucleus when overexpressed in HeLa cells. HeLa cells transfected with Cherry-AtATG8A show cytosolic accumulation of AtTG8 containing aggregates and a diffuse expression of AtATG8 within the nucleus. The aggregates are mainly centered around the periphery of the nucleus. Bars are 10 µm.

AtATG8 appear in cytosolic punctuated structures when expressed in HeLa cells (figure 3.18). A diffuse staining can also be seen in the nucleus, suggesting that AtATG8 is transported to the nucleus. The biochemical experiments show a strong interaction between AtNBR1 and AtATG8, and to test this interaction in vitro, HeLa cells were cotransfected with Cherry-AtATG8A and EGFP-AtNBR1.

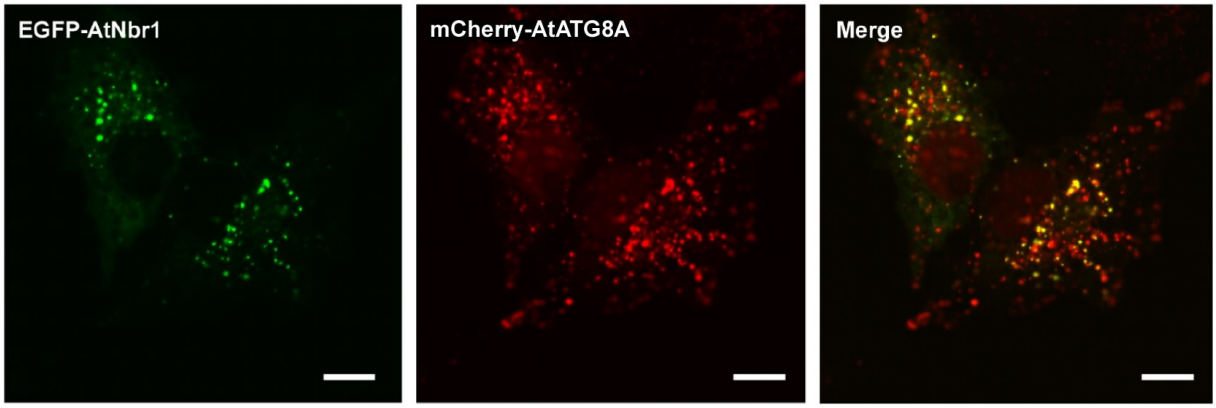

Figure 3.19: B: AtNBR1 colocalize with AtATg8A in HeLa cells. HeLa cells Co-transfected with EGFP-AtNBR1 and mCherry-AtATG8 show accumulation of cyosolic aggregates containing both AtNBR1 and AtATG8A. Green fluorescent aggregates completely overlap with red fluorescence, but most aggregates show only red fluorescence. Bars are 10 µm.

AtNBR1 colocalize with AtATG8 in HeLa cells (figure 3.19). Furthermore, red dotted structures are seen that might represent acidified autophagosomes. The red fluorescent signal of AtATG8 is maintained within these autophagosome, but it is not possible to say if the autophagosomes also contain AtNBR1, since the GFP signal is lost in acidic compartments.

A tandem EGFP-mCherry double-tag was used to test if AtNBR1 containing aggregates are sequestered to acidified autophagosomes in HeLa cells. As can be seen in figure 3.13, the double-tagged AtNBR1 accumulated in large cytosolic aggregates, but the red and green fluorescent signal was completely overlapping. This means that that AtNBR1 containing aggregates are not acidified and therefore not recognized as an autophagic substrate in a mammalian system (within the time-frame of this experiment). Having seen that AtATG8A might be associated with autophagosomes (see figure 3.19) it was reasonable to think that AtATG8 was needed to link AtNBR1 with the autophagosome. This was tested by cotransfecting HeLa cells with EGFP-Cherry-AtNBR1 and myc-AtATG8.

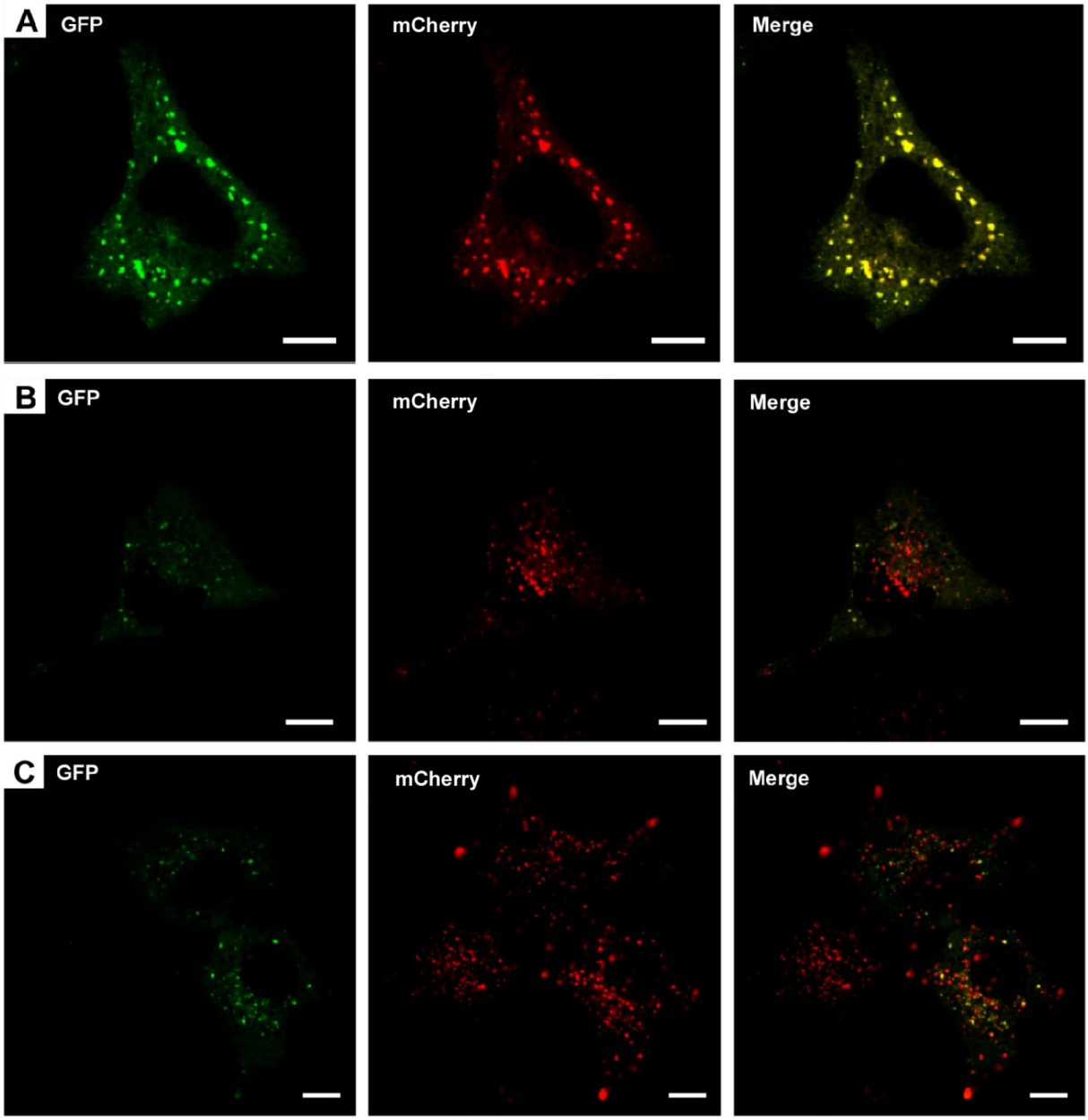

Figure 3.120: AtNBR1 containing structures are acidified in the presence of AtATG8. A: Double-tagged EGFP-Cherry-AtNBR1 forms cytosolic aggregates when overexpressed in HeLa cells, green and red fluorescent signals are completely overlapping. **B and C:** HeLa cells contransfected with EGFP-Cherry-AtNBR1 and myc-AtATG8A/B show accumulation of punctuated structures. The green fluorescent signal is almost completely lost, and most structures are only emitting red fluorescence. Bars are 10 µm.

As seen in figure 3.20, AtNBR1 containing structures are acidified when cotransfected with AtATG8. This indicates that AtNBR1 does not recognize mammalian ATG8 and can therefore not be sequestered to autophagosomes without AtATg8.

3.5 Experiments with AtNBR1 in Arabidopsis protoplasts

Results from biochemical experiments suggest that AtNBR1 has the same capability as p62 and NBR1 to polymerize and bind Ub (see section 3.2). *In vitro* experiments in HeLa cells showed that wild type AtNBR1 forms cytosolic aggregates that colocalize with AtATG8, and the aggregation was dependent on polymerization by PB1 and Ub binding by the two UBA domains (see section 3.4). However, AtNBR1 is a plant protein, and it is therefore necessary to verify these results in a plant model system. The following experiments have all been carried out in Arabidopsis protoplasts. All protoplast transformations were performed using PEG-mediated transformation and pictures were taken 24-48 hours after transformation.
To determine the cellular localization of wild type AtNBR1 in Arabidopsis protoplasts, wild-type AtNBR1 was expressed with an N-terminal YFP-tag (figure 3.14).

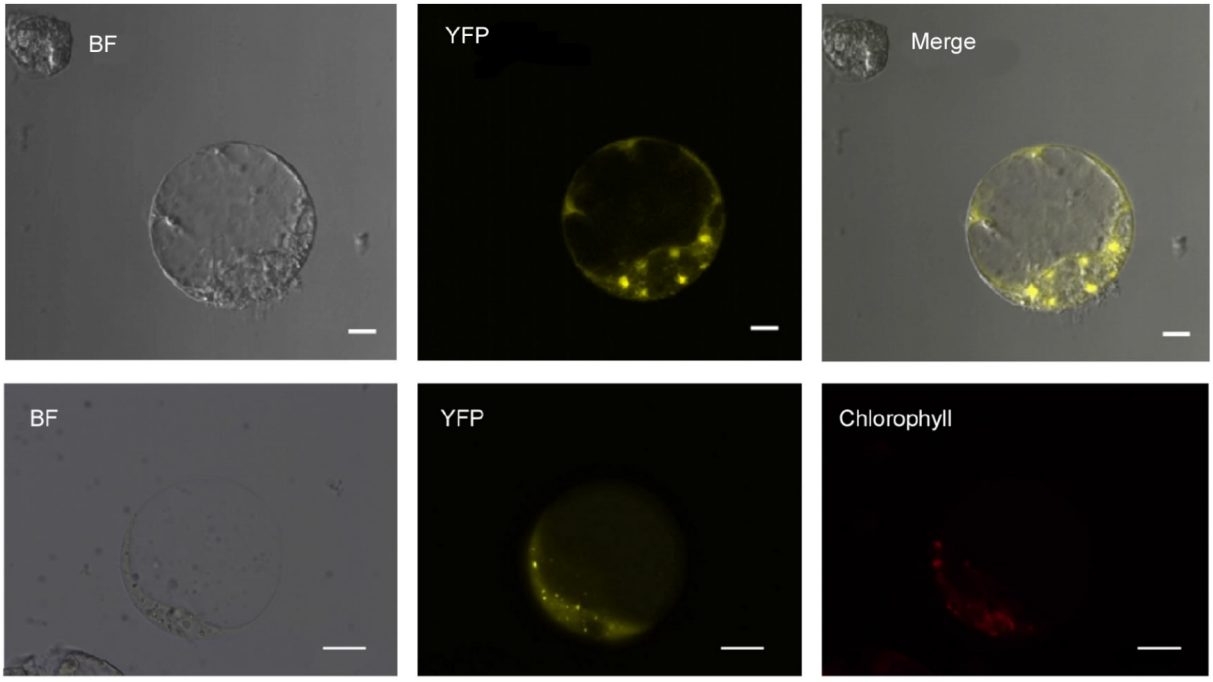

Figure 3.14: YFP-AtNBR1 forms cytosolic aggregates in living protoplasts. Arabidopsis protoplasts transformed with YFP-AtNBR1 show dotted structures with YFP-fluorescence. **Top:** Pictures taken in LSCM (Leica). **Bottom:** Pictures taken in fluorescence microscope (Zeiss). The chlorophyll autofluorescence indicate that the cells are healthy. Bars are 100 µm.

The results presented in figures 3.14 indicate that AtNBR1 has the ability to form cytosolic aggregates in living Arabidopsis protoplasts. AtNBR1 contains two C-terminal UBA-domains, of which the UBA2-domain is responsible for Ub binding. AtNBR1 lost the ability to form aggregates in HeLa cells when lacking both UBA domains (see figure 3.10). Having established that wt AtNBR1 forms aggregates in protoplasts the next step was to express

truncated AtNBR1 lacking both UBA-domains to investigate which affect this would have on the formation of aggregates in (see figures 3.15).

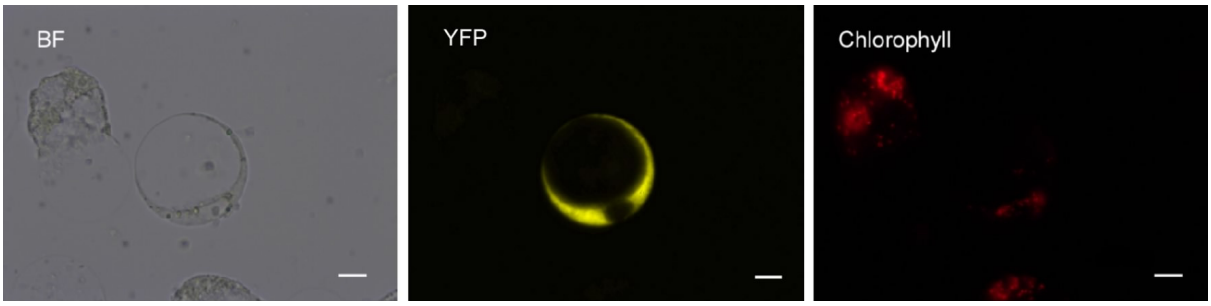

Figure 3.15: YFP-AtNBR1-DUBA1+2 does not form aggregates in living protoplasts. Protoplasts transformed with YFP-AtNBR1-DUBA1+2 show YFP-fluorescence that is diffuse, filling the entire cytoplasm of the cell. Chlorophyll autofluorescence indicate that the cells are healthy. No AtNBR1 can be seen in the nucleus. Pictures taken in fluorescence microscope (Zeiss). Bars are 100 µm.

AtNBR1 lacking both UBA domains show a diffuse distribution in Arabidopsis protoplasts, indicating that the UBA domains are required for aggregation (figure 3.15).
The PB1 domain is also important for the formation of aggregates. In HeLa cells, p62 lose the ability to form aggregates when the PB1 domain is mutated or deleted (Lamark, et al. 2003). The PB1 domain of AtNBR1 is required for AtNBR1 to aggregate *in vitro* (see figure 3.1), and the point mutant K11A of AtNBR1 also showed a diffuse expression in HeLa cells (see figure 3.9). The point mutant AtNBR1D60A as well as a PB1-deletion mutant (AtNBR1 Δ1-142) was expressed in living protoplast with N-terminal YFP tags (results not shown), but no conclusive data could be obtained.

To verify that AtNBR1 is involved in autophagy it is necessary to show that AtNBR1-containing aggregates are transported to the vacuole. The central vacuole is an acidified organelle that fills almost the entire plant cell, and it has previously been shown that autophagic substrates are being transported to the vacuole for degradation (Ishida, et al. 2008, Wada, et al. 2009, Yano, et al. 2007). The RFP is more acid stable that any of the other fluorescent proteins, and has been used to track autophagic substrates in the plant vacuole (Ishida, et al. 2008, Wada, et al. 2009). Using a double-tagged YFP-mCherry-AtNBR1 it should be possible to distinguish between AtNBR1 containing aggregates in the cytosol and the vacuole. In the following experiment, protoplasts were transformed with double tagged AtNBR1 to examine if AtNBR1containing aggregates could be visualized within the central vacuole of the protoplast.

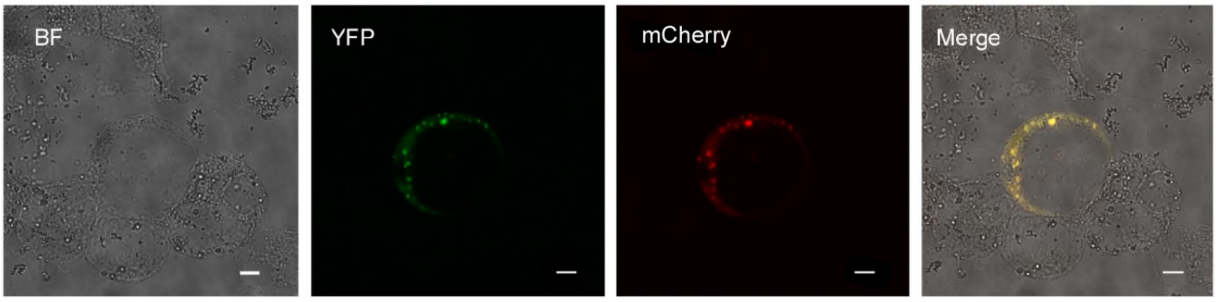

Figure 3.16: Cherry-YFP-AtNBR1 forms cytosolic aggregates in living protoplasts. Double tagged AtNBR1 forms aggregates in the cytosol of living protoplasts. No signal can be detected within the vacuole. The inclusion bodies are exhibiting completely overlapping yellow and red fluorescence. Cherry-fluorescence was detected using Far-Red settings, which excludes chlorophyll autofluorescence. Pictures are taken in confocal microscope (Zeiss). Bars are 10 µm.

The results presented in figure 3.16 show that double-tagged AtNBR1 containing aggregates are not found to the central vacuole. Red and green fluorescent signals were completely overlapping, which means that no aggregates were acidified. This experiment was also performed in onion epidermal cells by ballistic transformation (results not shown). Some aggregates containing AtNBR1 could also be seen in the onion cells, but the red and green fluorescent signal is completely overlapping, which means that no AtNBR1 was transported to the vacuole.

3.6 Agrobacterium-mediated transformation of *Arabidopsis thaliana*

In vitro experiments with cell systems give an indication of how a protein works, but this does not represent the complexity of a whole organism. *In vivo* experiments represent a natural setting in which a protein can be expressed and observed. The main goal of the experiments with transgenic Arabidopsis was to determine if fluorescently tagged AtNBR1 could be visualized within the vacuole of plant cells *in vivo*. This would be a clear indication of autophagic degradation of ATNBR1. Also, these plants will provide stably transfected protoplasts that can be used for co-expression studies with AtATG8.

Wt Arabidopsis (Columbia) was transformed with AtNBR1 fused to four different combinations of fluorescent tags. A standard N-terminal YFP-tag, and a C-terminal EGFP tag to check if the protein behaves differently when the tag is C-terminal. Also, the two double tagged constructs YFP-Cherry and YFP-ECFP-AtNBR1are included to visualize AtNBR1-containing inclusion bodies in the vacuole. mCherry and ECFP is more acid stabile than YFP and GFP, and should therefore continue to fluoresce after the protein has entered the vacuole. ECFP is also easier to distinguish from chlorophyll autofluorescence. Two mutant variants of AtNBR1 were also included. The ΔUBA1+2 mutation had a strong effect on AtNBR1

localization in protoplasts, and is used in plant transformation with an N-terminal YFP tag and an N-terminal Double tag (YFP-ECFP). The PB1 point mutant (D60R) was used for transformation with an N-terminal YFP tag. Results from transformed Arabidopsis protoplasts showed that both p62 and NBR1 was able to form cytosolic aggregates (results not shown), and it is expected that both proteins will form visible inclusion bodies in plant cells. p62 and NBR1 was used for plant transformation with an N-terminal YFP-tag and in separate constructs with a C-terminal EGFP tag.

All constructs were transformed into Agrobacterium and then used for transformation of wild type A. *thaliana* (Colombia). The seedlings of seeds collected from the T0 generation were treated with glyfosinate (see figure 3.17)

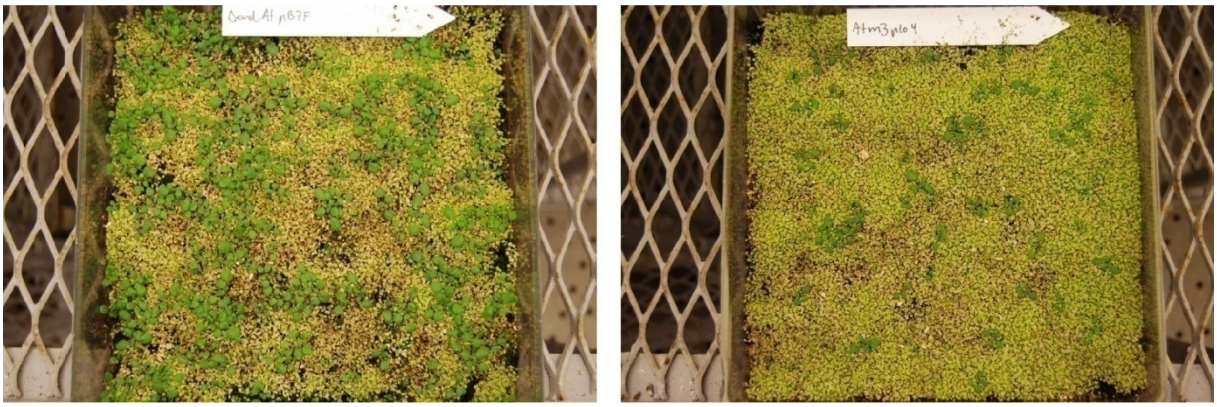

Figur 3.17: Glyfosinate treatment of T1 generation. Surviving transformants appear healthy green, while untransformed seedlings are killed.

Out of the seedlings that survived the glyfosinate treatment, 40 were selected for further growth. Surviving the glyfosinate treatment does not guarantee that expression of recombinant protein is high, and only about 1 out of 10 plants will have sufficient expression of recombinant protein. When using fluorescently tagged proteins the plants are normally analyzed by microscopy, but due to a large number of plants (approximately 440) and limited amount of time, a higher throughput screening method had to be used. After about 2 weeks, leaf material was collected from all plants and a western blot was performed with αGFp antibody. The following figure shows a model of the membrane used in the Dot-blot system.

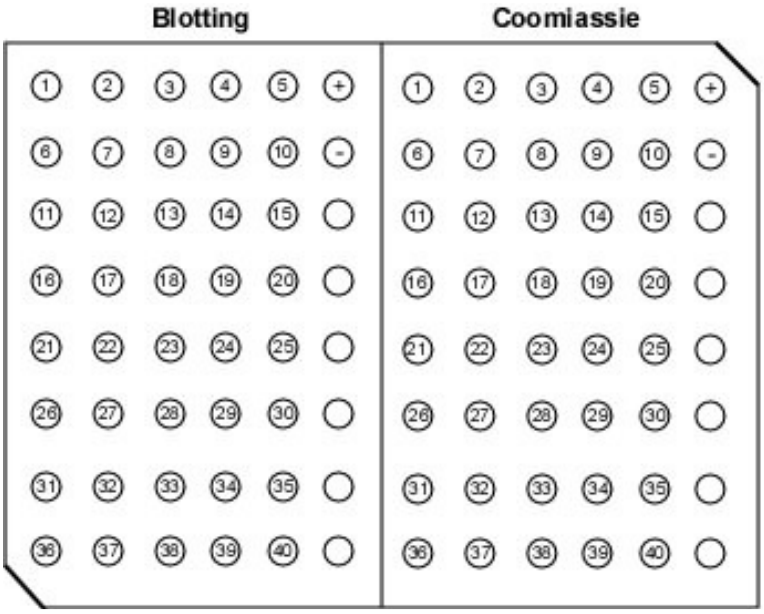

Figur 3.22: Blotting of leaf protein extracts on a PVDF membrane. Plant sample numbers are indicated in the dots, as well as negative and positive control. Left membrane: Immunostaining. Right membrane: Coomassie staining.

Results from the western blots were somewhat varied, but good enough to select candidates to parent the T2 generation. Figure 3.23 shows a blot of plants transformed with end-p62-pB7FWG2.0, where plant 12, 23 and 27 showed a clear GFP signal and were selected further.

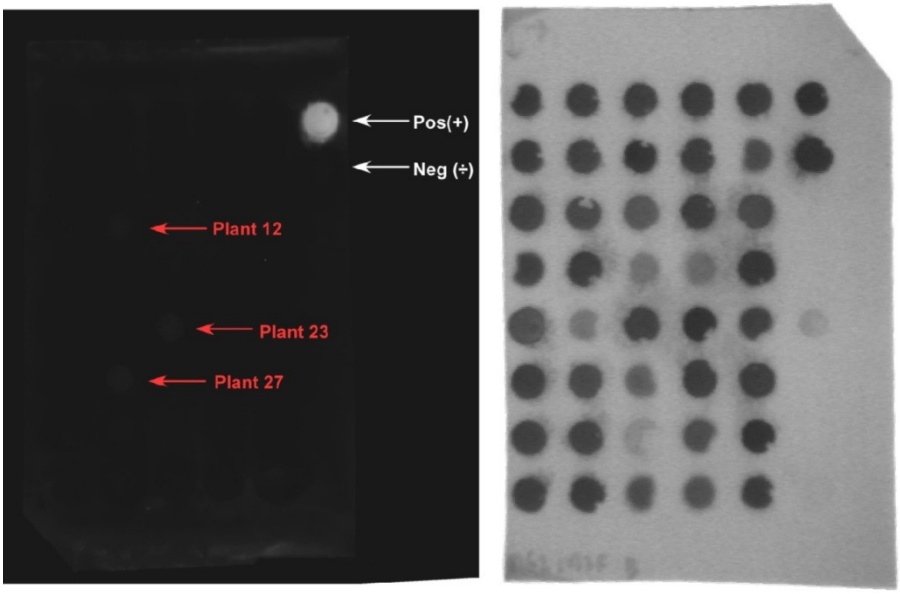

Figur 3.23: Plants expressing C-terminal EGFP-tagged p62. Left: Western blot with protein extracts from T1 generation plants transformed with Δend-p62-pB7FWG2,0 using αGFP primary antibody and αRabbit IgG HRP conjugated secondary antibody. Positive control: Stably transformed Arabidopsis expressing Chloroplast targeted GFP. Negative control: Wild type Arabidopsis (Colombia). Controls are indicated with white arrows and p62-EGFP expressing plants indicated with red arrows. **Right:** Coomassie staining of protein extracts in parallel to blot.

Based on the results from the western blot, between 3 and 8 plants from each batch of transformants were selected further. Seeds collected from these plants are expected to provide plants that express the fusion proteins strongly enough to be visualized. The majority of these results will not be available before after this thesis is submitted.

4.0 Discussion

It is now well established that p62 and NBR1 are selectively degraded by autophagy and can act as cargo receptors or adaptors for the autophagic degradation of ubiquitinated substrates (reviewed in Kirkin *et al.* 2009c, Lamark, et al. 2009). Research on autophagy in plants is also well under way, but the mechanism by which target substrates are sequestered for autophagic degradation has not been elucidated. This study has revealed that the plant protein Q9SB64 shares several important functional properties with p62 and NBR1, which indicates that it could act as a cargo receptor for the autophagic degradation of ubiquitinated substrates in plants.

4.1 AtNBR1 polymerizes through an N-terminal PB1 domain

AtNBR1 was shown in this study to interact with itself through an N-terminal type I/II PB1 domain. Molecular modeling suggest that the surface potential of the globular PB1 domain was clearly divided into one acidic and one basic side. It was therefore expected that each PB1 domain can interact with two other PB1 domains, thus forming polymers. The strength of the interaction between two isolated PB1 domains is an indication of polymerization. In this case the amount of precipitated protein exceeds the input by a ratio of 3:1, clearly suggesting that polymerization occurs. Point mutations that affect the basic cluster or the acidic OPCA-motif of the PB1 domain completely abolish the ability of AtNBR1 to self-interact. The effect is very clear, as the binding drops to zero as a result of a single point mutation. A protein with a mutation in the acidic OPCA-motif can interact with a protein that is mutated in the basic cluster, but this can only lead to dimerization, as each protein is only capable of binding to a single potein. The fact that AtNBR1 has no coiled coil domain and polymerizes through a type I/II PB1 domain makes it more functionally related to p62 than NBR1 in terms of PB1-PB1 interaction- and polymerization properties.

4.2 The C-terminal UBA domain (UBA2) of AtNBR1 binds ubiquitin

By sequence analysis, two putative UBA domains were identified in AtNBR1. This study has shown that AtNBR1 binds strongly to 4xUb. Surprisingly, only the second UBA domain (UBA2) is responsible for the binding, while no function for the UBA1 domain has been established so far. So what is the purpose of having two UBA domains as we see in AtNBR1?

Several other proteins also contain two, and even three UBAs, but only the tandem UBA-containing DNA repair proteins human HR23a and yeast Rad23 have so far been studied. hHR23a has been shown to bind K48-linked 4xUb stronger when it contains both UBA domains as opposed to only one (Raasi and Pickart 2003). In ScRad23, both UBA domains have the ability to bind Ub (Chen *et al.* 2001), and the second UBA domain protects the protein from proteosomal degradation (Heessen *et al.* 2005). However, both hHR23a and ScRad23 contain a stretch of 100- and 170 amino acids, respectively, between the two UBAs, and the two UBAs have the possibility to bind separate Ub-chains. In AtNBR1 the two domains are juxtaposed, and any correlation with hHR23a and ScRad23 would therefore be tentative.

The 4x-Ub chains used for GST-pulldown do not represent the full spectra of different Ub-modifications that exist in the cell. It is possible that the two UBA domains of AtNBR1 have affinities for specific Ub-chains, and that the UBA1 domain is able to recognize Ub-chains that have not been tested. In addition to the many type of Ub-modifications, a new group of Ub-like proteins have gradually emerged that also controls the activity of other proteins (Welchman *et al.* 2005). NEDD8 and Ufm are small Ub-like proteins, while ISG15 and FAT10 resemble Ub-chains (Downes and Vierstra 2005a). All the Ub-like proteins contain the Ub superfold, but most of them have little sequence homology to Ub (Kiel and Serrano 2006). Due to the structural similarity to Ub, many of the classical Ub binding domains also recognize a variety of Ub-like proteins (Grabbe and Dikic 2009). The Ub-like proteins are present in plants (Downes and Vierstra 2005a), and represent potential binding partners for the UBA1 domain of AtNBR1.

The binding affinity of polymeric AtNBR1 for 4xUb is 10-fold stronger than monomeric AtNBR1 (D60A) and isolated UBA2. Single UBA-ubiquitin interactions are commonly weak, but can be enhanced physiologically to high-affinity interactions by polymerization of the UBA domain containing protein (Hurley *et al.* 2006). This correlates well with the observed effect of PB1 polymerization on the Ub binding capacity of AtNBR1. A decline in binding capacity is also seen when using monomeric NBR1 (ΔCC1) and monomeric p62 (Kirkin, et al. 2009b) A recent article suggest that non-UBA domains/sequences within the full-length p62 can influence Ub recognition, and consequently the isolated UBA domain binds poorly (Long *et al.* 2008). Monomeric AtNBR1 and the isolated UBA2 domain have the same binding capacity, which suggests that apart from PB1-mediated polymerization, no

other part of AtNBR1 contributes to the binding. An interesting correlation is that the isolated UBA domain of NBR1 seems to bind 4xUb stronger than the full-length protein, while full-length p62 binds better than the isolated UBA domain. The Ub- binding capacity of polymeric p62 is also better that full-length NBR1 (Kirkin, et al. 2009b). Taken together with the results on AtNBR1, this further suggests a closer functional relationship between AtNBR1 and p62 than between AtNBR1 and NBR1.

4.3 AtNBR1 interacts with Arabidopsis homologues of ATG8

The interaction between AtNBR1 and AtATG8 has been investigated in this study, and the best binding was achieved with ATG8-A, B, C, D, and F. Out of the six AtATG8 that were tested, AtATG8A was the best binder. However, the coomassie staining revealed that AtATG8A is represented by two bands that each are approximately as strong as the single band of the other AtATG8s. This means that the amount of AtATG8A is significantly higher, which may also explain the increased amount of co-precipitated AtNBR1. A phylogenetic analysis of ATG8 family protein sequences (see figure 3.12) shows that the nine AtATG8 homologues forms two distinct groups. AtATG8H-I is placed among the mammalian ATG8s, while AtATG8A-G forms a separate group. This shows that the AtATG8 proteins can be separated into subfamilies. This was also reflected in the results obtained from GST-pulldown assays. With the exception of AtATG8G, all the members of the largest subgroup (AtATG8A-G) bound well to AtNBR1. Out of the two members of the small group, AtATH8H was tested and found to bind very weakly to AtNBR1. This indicates that the nine AtATG8 homologues may be separated by function, which is consistent with the results from a comprehensive study on all the AtATG8 homologues (Slavikova, et al. 2005).

An effort to map down the AtATG8-interacting region in AtNBR1 has shown that amino acids 412-491 are sufficient for binding. The LC3-interacting region in p62, NBR1 and yeast ATG19 is a small region of about 10 amino acids that contains a conserved hydrophobic motif, W/Y/F XX L/I/V, which is surrounded by acidic residues. Within the 412-491 region of AtNBR1 there are two possible interaction surfaces based on sequence similarity to previously described LIRs (see figure 4.1). The sequence alignment of plant NBR1 shows that only the second region is conserved in all 9 species, which strongly favors the second region. It consists of a very hydrophobic core motif (WVLI), surrounded by some acidic residues and a conserved arginine. It is expected that this motif may bind in a hydrophobic pocket of the C-

terminal Ub-like domain of AtATG8 proteins. The conserved Arg may be important in specifying the interaction by binding to the N-terminal arm of AtATG8.

Figur 4.1: Putative ATATG8-binding regions in plant NBR1. Amino acid 412-491 of AtNBR1 is sufficient for binding to AtATG8 and based on similarity to known LIR domains in p62, NBR1 and yeast ATG19, two plausible interaction regions have been identified. The second motif is highly conserved in NBR1 from 9 different plant species.

However, this putative binding site is located at the end of a much conserved region that forms a globular domain of unknown function (see figure 3.2). Also, a deletion construct from amino acid 412-617 could still bind ATG8, and the interaction was only slightly weakened by this deletion. This indicates the presence of another interaction region, as we see in mammalian NBR1. It is possible that the interaction region identified between aa 412 and 491 is hidden within the globular domain when AtNBR1 is correctly folded (in vivo), and that truncation of the protein exposes the region and mediates a weak binding to AtATG8. The only deletion construct that showed a significantly weaker interaction to AtATG8 is the construct lacking the two UBA domains. AtATG8 is an Ub-like protein and could possibly interact with one of the UBA domains. Having found that the UBA1 domain does not bind Ub, one could speculate that it might partake in the interaction with AtATG8.

4.4 AtNBR1 is sequestered to acidified compartments in HeLa cells by AtATG8

When AtNBR1 was overexpressed in HeLa cells it accumulated in large cytosolic aggregates due to polymerization and Ub binding. The same accumulation was seen when p62 or NBR1 is overexpressed in autophagy deficient cells (Bjørkøy, et al. 2005, Kirkin, et al. 2009b). This means that AtNBR1 containing aggregates were not sequestered for autophagic degradation in HeLa cells. There are two possible explanations for this. The overexpression of AtNBR1 could be too much for the endogenous ATG8 to handle, and the accumulated aggregates become too big to be degraded by autophagy. The second explanation is that AtNBR1-containing aggregates are not recognized by mammalian ATG8, and consequently not sequestered into autophagosomes. Overexpressing AtATG8 together with AtNBR1 led to

acidification of AtNBR1-containing aggregates. Hence, this may suggest that that AtNbr1 does not bind mammalian ATG8 proteins. This shows that AtATG8 is needed for lysosomal sequestration of AtNBR1-containing aggregates in HeLa cells.

AtNBR1 also formed cytosolic aggregates when expressed in Arabidopsis protoplasts. This is consistent with the results from HeLa cells, and is thought to reflect the ability of AtNBR1 to polymerize and interact with ubiquitinated proteins. Supporting this, a UBA deletion construct of AtNBR1 lost the ability to form aggregates. The double-tagged EGFP-mCherry-AtNBR1 formed cytosolic aggregates, but the sequestration of these aggregates to the vacuole could not be observed in Arabidopsis protoplasts. One possible explanation is that AtANBR1 is not involved in autophagy, and therefore not transported to the vacuole. However, the strong binding to AtATG8 argues against this conclusion, as AtATG8 is present in autophagic bodies that are transported to the central vacuole (Thompson, et al. 2005). The second alternative is that overexpression of AtNBR1 is out of proportion to the amount of ATATG8 in the cell, causing accumulation of cytosolic aggregates. The same construct was used in transformation of onion epidermal cells. Aggregates did form in these cells as well, but no aggregates were acidified.

4.5 Concluding remarks and future perspectives

The biochemical experiments show a clear interaction between AtNBR1 and AtATG8, which is a strong indication that AtNBR1 may be degraded by autophagy. The results from HeLa cells further indicate that AtNBR1 can be sequestered to acidified structures by binding to AtATG8. However, it remains to be seen that AtNBR1 can also enter the central vacuole of plant cells.

Nonetheless, the results indicate that AtNBR1 is an Arabidopsis thaliana homologue of both NBR1 and p62 with respect to the functional properties studied here. AtNBR1 is functionally more like p62, but from sequence comparison it is clearly the orthologue of NBR1. The latest results on p62 and NBR1 suggest that the two proteins are working together in targeting substrates for autophagic degradation (Kirkin, et al. 2009a), and since AtNBR1 has properties of both p62 and NBR1 one could speculate that AtNBR1 can perform the tasks that p62 and NBR1 work together in doing. Data from knockout mutants indicate that NBR1 and p62 can complement each other as backup systems (Kirkin, et al. 2009b), and an Arabidopsis

knockout mutant of AtNBR1 is required to determine whether AtNBR1 is essential for plant survival, or if there are other systems/proteins that serve the same function as AtNBR1.

In mammalian cells, we know more about the proteins involved in making the aggregate structures that are degraded by autophagy. Ub is an essential component of the aggregates, and is thought to target proteins for autophagic degradation by binding to p62/NBR1 (Kirkin, et al. 2009a). Having found that AtNBR1 binds Ub and that aggregation of AtNBR1 in vitro is dependent on Ub binding, the next step would be to verify that the cytosolic inclusions also contain Ub. Moreover, recent papers have shown that chloroplasts can be degraded by autophagy in plant cells (Ishida, et al. 2008, Wada, et al. 2009) and p62 is known to mediate autophagic degradation of ubiquitinated peroxisomes (Kim, et al. 2008). Based on this, one could speculate if AtNBR1 may assist in target recognition of ubiquitinated organelles in Arabidopsis destined for autophagic degradation. However, the most important question is whether AtNBR1 is recognized as an autophagic substrate in Arabidopsis. The transgenic Arabidopsis strains generated in this study will hopefully provide an answer to this. To aid in the study of AtNBR1 biochemically and *in vivo* it will also be necessary to make an antibody against AtNBR1. This will allow detection of AtNBR1 by western blot and staining of endogenous AtNBR1. Continued study of the interaction between AtNBR1 and AtATG8 is also necessary. Mapping the exact binding site is priority number one, as well as completing the interaction studies on the different AtATG8 homologues.

5.0 References

Avery, O.T., MacLeod, C.M. and McCarty, M. (1944) Studies on the chemical nature of the substance inducing transformation of pneumococcal types: Induction of transformation by a deoxyribonucleic acid fraction isolated from pneumococcus type III. *J. Exp. Med.*, 79, 137-158.

Bassham, D.C. (2009) Function and regulation of macroautophagy in plants. *Biochimica et Biophysica Acta (BBA) - Molecular Cell Research*, In Press, Corrected Proof.

Bassham, D.C., Laporte, M., Marty, F., Moriyasu, Y., Ohsumi, Y., Olsen, L.J. and Yoshimoto, K. (2006) Autophagy in Development and Stress Responses of Plants. *Autophagy*, 2, 2-11.

Beck, K. and Brodsky, B. (1998) Supercoiled Protein Motifs: The Collagen Triple-Helix and the [alpha]-Helical Coiled Coil. *Journal of Structural Biology*, 122, 17-29.

Bellu, A.R., Komori, M., van der Klei, I.J., Kiel, J.A.K.W. and Veenhuis, M. (2001) Peroxisome Biogenesis and Selective Degradation Converge at Pex14p. *J. Biol. Chem.*, 276, 44570-44574.

Bimboim, H.C. and Doly, J. (1979) A rapid alkaline extraction procedure for screening recombinant plasmid DNA. *Nucl. Acids Res.*, 7, 1513-1523.

Bjørkøy, G., Lamark, T., Brech, A., Outzen, H., Perander, M., Overvatn, A., Stenmark, H. and Johansen, T. (2005) p62/SQSTM1 forms protein aggregates degraded by autophagy and has a protective effect on huntingtin-induced cell death. *J. Cell Biol.*, 171, 603-614.

Bjørkøy, G., Lamark, T., Pankiv, S., Øvervatn, A., Brech, A., Johansen, T. and Daniel, J.K. (2009) Monitoring Autophagic Degradation of p62/SQSTM1. In *Methods in enzymology*: Academic Press, pp. 181-197.

Bundock, P., den Dulk-Ras, A., Beijersbergen, A. and P.J., H. (1995) Trans-kingdom T-DNA transfer from Agrobacterium tumefaciens to Saccharomyces cerevisiae. *EMBO*, 14, 3206–3214.

Burnette, W. (1981) "Western blotting": electrophoretic transfer of proteins from sodium dodecyl sulfate--polyacrylamide gels to unmodified nitrocellulose and radiographic detection with antibody and radioiodinated protein A. *Analytical biochemistry*, 112, 195-203.

Chalfie, M., Tu, Y., Euskirchen, G., Ward, W. and Prasher, D. (1994) Green fluorescent protein as a marker for gene expression. *Science*, 263, 802-805.

Chau, V., Tobias, J., Bachmair, A., Marriott, D., Ecker, D., Gonda, D. and Varshavsky, A. (1989) A multiubiquitin chain is confined to specific lysine in a targeted short-lived protein. *Science*, 243, 1576-1583.

Chen, L., Shinde, U., Ortolan, G.T. and Madura, K. (2001) Ubiquitin-associated (UBA) domains in Rad23 bind ubiquitin and promote inhibition of multi-ubiquitin chain assembly *EMBO reports*, 10, 933–938

Crick, F.H.C. (1953) The packing of -helices: simple coiled coils. *Acta Crystallographica*, 6, 689–697.

Crowle, A. (1956) A simplified agar electrophoretic method for use in antigen separation and serologic analysis. *The journal of laboratory and clinical medicine*, 48, 642-648.

De Duve, C. and Wattiaux, R. (1966) Functions of lysosomes. *Annual review of physiology*, 28, 435-492.

de Groot, M.J.A., Bundock, P., Hooykaas, P.J.J. and Beijersbergen, A.G.M. (1998) Agrobacterium tumefaciens-mediated transformation of filamentous fungi. *Nat Biotech*, 16, 839-842.

Doelling, J.H., Walker, J.M., Friedman, E.M., Thompson, A.R. and Vierstra, R.D. (2002) The APG8/12-activating Enzyme APG7 Is Required for Proper Nutrient Recycling and Senescence in Arabidopsis thaliana. *J. Biol. Chem.*, 277, 33105-33114.

Downes, B. and Vierstra, R.D. (2005a) Post-translational regulation in plants employing a diverse set of polypeptide tags. *Biochemical Society Transactions*, 33, 393-399.

Downes, B. and Vierstra, R.D. (2005b) Post-translational regulation in plants employing a diverse set of polypeptide tags. *Biochemical Society Transactions* 33, 393-399.

Dreher, K. and Callis, J. (2007) Ubiquitin, Hormones and Biotic Stress in Plants. *Annals of Botany*, 99, 787-822.

Duran, A., Linares, J.F., Galvez, A.S., Wikenheiser, K., Flores, J.M., Diaz-Meco, M.T. and Moscat, J. (2008) The Signaling Adaptor p62 Is an Important NF-[kappa]B Mediator in Tumorigenesis. *Cancer Cell*, 13, 343-354.

Evans, C.-L., Long, J.E., Gallagher, T.R.A., Hirst, J.D. and Searle, M.S. (2008) Conformation and dynamics of the three-helix bundle UBA domain of p62 from experiment and simulation. *Proteins: Structure, Function, and Bioinformatics*, 71, 227-240.

Fujioka, Y., Noda, N.N., Fujii, K., Yoshimoto, K., Ohsumi, Y. and Inagaki, F. (2008) In Vitro Reconstitution of Plant Atg8 and Atg12 Conjugation Systems Essential for Autophagy. *J. Biol. Chem.*, 283, 1921-1928.

Gagne, J.M., Downes, B.P., Shiu, S.-H., Durski, A.M. and Vierstra, R.D. (2002) The F-box subunit of the SCF E3 complex is encoded by a diverse superfamily of genes in Arabidopsis. *Proceedings of the National Academy of Sciences*, 99, 11519-11524.

Gamerdinger, M., Hajieva, P., Kaya, A.M., Wolfrum, U., Hartl, F.U. and Behl, C. (2009) Protein quality control during aging involves recruitment of the macroautophagy pathway by BAG3. *EMBO J*, 28, 889-901.

Gong, J., Xu, J., Bezanilla, M., Huizen, R.v., Derin, R. and Li, M. (1999) Differential Stimulation of PKC Phosphorylation of Potassium Channels by ZIP1 and ZIP2. . *Science*, 285, 1565-1569.

Grabbe, C. and Dikic, I. (2009) Functional Roles of Ubiquitin-Like Domain (ULD) and Ubiquitin-Binding Domain (UBD) Containing Proteins. *Chemical Reviews*, 109, 1481-1494.

Han, L., Mason, M., Risseeuw, E.P., Crosby, W.L. and Somers, D.E. (2004) Formation of an SCFZTL complex is required for proper regulation of circadian timing. *The Plant Journal*, 40, 291-301.

Hara, T., Nakamura, K., Matsui, M., Yamamoto, A., Nakahara, Y., Suzuki-Migishima, R., Yokoyama, M., Mishima, K., Saito, I., Okano, H. and Mizushima, N. (2006) Suppression of basal autophagy in neural cells causes neurodegenerative disease in mice. *Nature*, 441, 885-889.

He, H., Dang, Y., Dai, F., Guo, Z., Wu, J., She, X., Pei, Y., Chen, Y., Ling, W., Wu, C., Zhao, S., Liu, J.O. and Yu, L. (2003) Post-translational Modifications of Three Members of the Human MAP1LC3 Family and Detection of a Novel Type of Modification for MAP1LC3B. *J. Biol. Chem.*, 278, 29278-29287.

Heessen, S., Masucci, M.G. and Dantuma, N.P. (2005) The UBA2 Domain Functions as an Intrinsic Stabilization Signal that Protects Rad23 from Proteasomal Degradation. *Molecular Cell*, 18, 225-235.

Heim, R., Cubitt, A.B. and Tsien, R.Y. (1995) Improved green fluorescence. *Nature*, 373, 663-664.

Herman, E. and Schmidt, M. (2004) Endoplasmic Reticulum to Vacuole Trafficking of Endoplasmic Reticulum Bodies Provides an Alternate Pathway for Protein Transfer to the Vacuole. *Plant Physiol.*, 136, 3440-3446.

Hershko, A. and Ciechanover, A. (1998) The ubiquitin system. *Annual Review of Biochemistry*, 67, 425-479.

Hershko, A., Ciechanover, A. and Varshavsky, A. (2000) The ubiquitin system. *Nature Medicine*, 6, 1073 - 1081

Hicke, L. (2001) A New Ticket for Entry into Budding Vesicles--Ubiquitin. *Cell*, 106, 527-530.

Higuchi, R., Krummel, B. and Saiki, R. (1988) A general method of in vitro preparation and specific mutagenesis of DNA fragments: study of protein and DNA interactions. *Nucl. Acids Res.*, 16, 7351-7367.

Hirano, Y., Yoshinaga, S., Ogura, K., Yokochi, M., Noda, Y., Sumimoto, H. and Inagaki, F. (2004) Solution Structure of Atypical Protein Kinase C PB1 Domain and Its Mode of Interaction with ZIP/p62 and MEK5. *J. Biol. Chem.*, 279, 31883-31890.

Hirano, Y., Yoshinaga, S., Takeya, R., Suzuki, N.N., Horiuchi, M., Kohjima, M., Sumimoto, H. and Inagaki, F. (2005) Structure of a Cell Polarity Regulator, a Complex between Atypical PKC and Par6 PB1 Domains. *J. Biol. Chem.*, 280, 9653-9661.

Hochrainer, K. and Lipp, J. (2007) Ubiquitylation within signaling pathways in- and outsideof inflammation. *Thrombosis and Haemostasis* 97, 370-377.

Hoecker, U. (2005) Regulated proteolysis in light signaling. *Current Opinion in Plant Biology*, 8, 469-476.

Hoege, C., Pfander, B., Moldovan, G.-L., Pyrowolakis, G. and Jentsch, S. (2002) RAD6-dependent DNA repair is linked to modification of PCNA by ubiquitin and SUMO. *Nature*, 419, 135-141.

Honbou, K., Minakami, R., Yuzawa, S., Takeya, R., Suzuki, N.N., Kamakura, S., Sumimoto, H. and Inagaki, F. (2007) Full-length p40phox structure suggests a basis for regulation mechanism of its membrane binding. *The EMBO journal*, 26, 1176–1186.

Hurley J, Sangho, L. and Gali, P. (2006) Ubiquitin-binding domains. *The Journal of Biochemistry*, 399, 361–372.

Hurley, J.H., Lee, S. and Prag, G. (2006) Ubiquitin-binding domains. *Biochemical journal*, 399, 361–372.

Hutchison, C.r., Phillips, S., Edgell, M., Gillam, S., Jahnke, P. and Smith, M. (1978) Mutagenesis at a specific position in a DNA sequence. *The journal of biological chemistry*, 253, 6551-6560.

Ichimura, Y., Kumanomidou, T., Sou, Y.-s., Mizushima, T., Ezaki, J., Ueno, T., Kominami, E., Yamane, T., Tanaka, K. and Komatsu, M. (2008) Structural Basis for Sorting Mechanism of p62 in Selective Autophagy. *J. Biol. Chem.*, 283, 22847-22857.

Imaizumi, T., Schultz, T.F., Harmon, F.G., Ho, L.A. and Kay, S.A. (2005) FKF1 F-Box Protein Mediates Cyclic Degradation of a Repressor of CONSTANS in Arabidopsis. *Science*, 309, 293-297.

Inoue, Y., Suzuki, T., Hattori, M., Yoshimoto, K., Ohsumi, Y. and Moriyasu, Y. (2006) AtATG Genes, Homologs of Yeast Autophagy Genes, are Involved in Constitutive Autophagy in Arabidopsis Root Tip Cells. *Plant Cell Physiol.*, 47, 1641-1652.

Inouye, S. and Tsuji, F.I. (1994) Aequorea green fluorescent protein: Expression of the gene and fluorescence characteristics of the recombinant protein. *FEBS Letters*, 341, 277-280.

Ishida, H., Yoshimoto, K., Izumi, M., Reisen, D., Yano, Y., Makino, A., Ohsumi, Y., Hanson, M.R. and Mae, T. (2008) Mobilization of Rubisco and Stroma-Localized Fluorescent Proteins of Chloroplasts to the Vacuole by an ATG Gene-Dependent Autophagic Process. *Plant Physiol.*, 148, 142-155.

Ito, T., Matsui, Y., Ago, T., Ota, K. and Sumimoto, H. (2001) Novel modular domain PB1 recognizes PC motif to mediate functional protein–protein interactions. *The EMBO journal*, 20, 3938–3946.

Kaelin, W.G., Pallas, D.C., DeCaprio, J.A., Kaye, F.J. and Livingston, D.M. (1991) Identification of cellular proteins that can interact specifically with the T/ElA-binding region of the retinoblastoma gene product. *Cell*, 64, 521-532.

Kalbin, G., Strid, A. and Frohnmeyer, H. (1999) Transcriptional activation of the parsley chalcone synthase promoter in heterologous pea and yeast systems. *Plant Physiol Biochem*, 37, 821-829.

Kaledin, A.S., Sliusarenko, A.G. and Gorodetskii, S.I. (1980) Isolation and properties of DNA polymerase from extreme thermophylic bacteria Thermus aquaticus YT-1. *Biokhimiia*, 45, 644-651.

Kanki, T. and Klionsky, D.J. (2008) Mitophagy in Yeast Occurs through a Selective Mechanism. *J. Biol. Chem.*, 283, 32386-32393.

Karimi, M., Inzé, D. and Depicker, A. (2002) GATEWAY(TM) vectors for Agrobacterium-mediated plant transformation. *Trends in Plant Science*, 7, 193-195.

Keith W. Earley, J.R.H., Olga Pontes, Kristen Opper, Tom Juehne, Keming Song, Craig S. Pikaard, (2006) Gateway-compatible vectors for plant functional genomics and proteomics. *The Plant Journal*, 45, 616-629.

Ketelaar, T., Voss, C., Dimmock, S.A., Thumm, M. and Hussey, P.J. (2004) Arabidopsis homologues of the autophagy protein Atg8 are a novel family of microtubule binding proteins. *FEBS Letters*, 567, 302-306.

Kiel, C. and Serrano, L. (2006) The Ubiquitin Domain Superfold: Structure-based Sequence Alignments and Characterization of Binding Epitopes. *Journal of molecular biology*, 355, 821-844.

Kim, J. and Klionsky, D.J. (2000) Autophagy, Cytoplasm-to-vacuole targeting pathway, and pexophagy in yeast and mammalian cells. *Annual Review of Biochemistry*, 69, 303.

Kim, P.K., Hailey, D.W., Mullen, R.T. and Lippincott-Schwartz, J. (2008) Ubiquitin signals autophagic degradation of cytosolic proteins and peroxisomes. *Proc Natl Acad Sci U S A*, 105, 20567-20574.

Kimura, S., Fujita, N., Noda, T., Yoshimori, T. and Daniel, J.K. (2009) Chapter 1 Monitoring Autophagy in Mammalian Cultured Cells through the Dynamics of LC3. In *Methods in enzymology*: Academic Press, pp. 1-12.

Kirkin, V., Lamark, T., Johansen, T. and Dikic, I. (2009a) NBR1 co-operates with p62 in selective autophagy of ubiquitinated targets. *Autophagy*, 5, 1-2.

Kirkin, V., Lamark, T., Sou, Y.-S., Bjørkøy, G., Nunn, J.L., Bruun, J.-A., Shvets, E., McEwan, D.G., Clausen, T.H., Wild, P., Bilusic, I., Theurillat, J.-P., Øvervatn, A., Ishii, T., Elazar, Z., Komatsu, M., Dikic, I. and Johansen, T. (2009b) A Role for NBR1 in Autophagosomal Degradation of Ubiquitinated Substrates. *Molecular Cell*, 33, 505-516.

Kirkin, V., McEwan, D.G., Novak, I. and Dikic, I. (2009c) A Role for Ubiquitin in Selective Autophagy. 34, 259-269.

Kleppe, K., Ohtsuka, E., Kleppe, R., Molineux, I. and Khorana, H.G. (1971) Studies on polynucleotides. XCVI. Repair replications of short synthetic DNA's as catalyzed by DNA polymerases. *Journal of molecular biology*, 56, 341-361.

Klercker, J. (1892) Eine Methode zur isoleirung lebender protoplasten. *Ofversigt af Kungliga Vetenskaps Akademiet Förhandlingar Stockholm*, 463-475.

Klionsky, D., Cuervo, A., Dunn, W.A., Levine, B., van der Klei, J. and Seglen, P.O. (2007) How shall I eat thee. *Autophagy*, 3, 413-416.

Klionsky, D.J. (2007) Autophagy: from phenomenology to molecular understanding in less than a decade. *Nat Rev Mol Cell Biol*, 8, 931-937.

Klionsky, D.J., Cregg, J.M., Dunn Jr, W.A., Emr, S.D., Sakai, Y., Sandoval, I.V., Sibirny, A., Subramani, S., Thumm, M., Veenhuis, M. and Ohsumi, Y. (2003) A Unified Nomenclature for Yeast Autophagy-Related Genes. *Developmental Cell*, 5, 539-545.

Komatsu, M., Ueno, T., Waguri, S., Uchiyama, Y., Kominami, E. and Tanaka, K. (2007a) Constitutive autophagy: vital role in clearance of unfavorable proteins in neurons. *Cell Death Differ*, 14, 887-894.

Komatsu, M., Waguri, S., Koike, M., Sou, Y.S., Ueno, T., Hara, T., Mizushima, N., Iwata, J., Ezaki, J., Murata, S., Hamazaki, J., Nishito, Y., Iemura, S., Natsume, T., Yanagawa, T., Uwayama, J., Warabi, E., Yoshida, H., Ishii, T., Kobayashi, A., Yamamoto, M., Yue, Z., Uchiyama, Y., Kominami, E. and Tanaka, K. (2007b) Homeostatic levels of p62 control cytoplasmic inclusion body formation in autophagy-deficient mice. *Cell*, 131, 1149-1163.

Koncz, C. and Schell, J. (1986) The promoter of the T_L-DNA 5 gene controls the tissue specific expression of chimeric gene carried by a novel type of *Agrobacterium* binary vector. *Molecular genetics and genomics*, 204, 383–396.

Kristensen, A.R., Schandorff, S., Hoyer-Hansen, M., Nielsen, M.O., Jaattela, M., Dengjel, J. and Andersen, J.S. (2008) Ordered Organelle Degradation during Starvation-induced Autophagy. *Mol Cell Proteomics*, 7, 2419-2428.

Kuma, A., Hatano, M., Matsui, M., Yamamoto, A., Nakaya, H., Yoshimori, T., Ohsumi, Y., Tokuhisa, T. and Mizushima, N. (2004) The role of autophagy during the early neonatal starvation period. *Nature*, 432, 1032-1036.

Kurihara, N., Hiruma, Y., Zhou, H., Subler, M.A., Dempster, D.W., Singer, F.R., Reddy, S.V., Gruber, H.E., Windle, J.J. and Roodman, G.D. (2007) Mutation of the sequestosome 1 (p62) gene increases osteoclastogenesis but does not induce Paget disease. *The journal of clinical investigation*, 117, 133–142.

Kuusisto, E., Salminen, A. and Alafuzoff, I. (2001) Ubiquitin-binding protein p62 is present in neuronal and glial inclusions in human tauopathies and synucleinopathies. *Neuroreport*, 12, 2085-2090.

Kvam, E. and Goldfarb, D.S. (2007) Nucleus-vacuole junctions and piecemeal microautophagy of the nucleus in S. cerevisiae. *Autophagy*, 3, 85-92.

Lamark, T., Kirkin, V., Dikic, I. and Johansen, T. (2009) NBR1 and p62 as cargo receptors for selective autophagy of ubiquitinated targets. *Cell cycle*, 8, 1-5.

Lamark, T., Perander, M., Outzen, H., Kristiansen, K., Overvatn, A., Michaelsen, E., Bjorkoy, G. and Johansen, T. (2003) Interaction Codes within the Family of Mammalian Phox and Bem1p Domain-containing Proteins. *J. Biol. Chem.*, 278, 34568-34581.

Lange, S., Xiang, F., Yakovenko, A., Vihola, A., Hackman, P., Rostkova, E., Kristensen, J., Brandmeier, B., Franzen, G., Hedberg, B., Gunnarsson, L.G., Hughes, S.M., Marchand, S., Sejersen, T., Richard, I., Edstrom, L., Ehler, E., Udd, B. and Gautel, M. (2005) The Kinase Domain of Titin Controls Muscle Gene Expression and Protein Turnover. *Science*, 308, 1599-1603.

Lemasters, J.J. (2005) Selective Mitochondrial Autophagy, or Mitophagy, as a Targeted Defense Against Oxidative Stress, Mitochondrial Dysfunction, and Aging. *Rejuvenation Research*, 8, 3-5.

Levine, B. and Kroemer, G. (2008) Autophagy in the pathogenesis of disease. *Cell*, 132, 27-42.

Liu, Y., Schiff, M., Czymmek, K., Tallóczy, Z., Levine, B. and Dinesh-Kumar, S.P. (2005) Autophagy Regulates Programmed Cell Death during the Plant Innate Immune Response. *Cell*, 121, 567-577.

Long, J., Gallagher, T.R.A., Cavey, J.R., Sheppard, P.W., Ralston, S.H., Layfield, R. and Searle, M.S. (2008) Ubiquitin Recognition by the Ubiquitin-associated Domain of p62 Involves a Novel Conformational Switch. *J. Biol. Chem.*, 283, 5427-5440.

Lupas, A., Van Dyke, M. and Stock, J. (1991) Predicting Coled Coils from Protein Sequences. *Science* 252, 1162-1164.

Majeski, A.E. and Dice, F.J. (2004) Mechanisms of chaperone-mediated autophagy. *The International Journal of Biochemistry & Cell Biology*, 36, 2435-2444.

Marques, J.P., Schattat, M.H., Hause, G., Dudeck, I. and Klösgen, R.B. (2004) In vivo transport of folded EGFP by the DeltapH/TAT-dependent pathway in chloroplasts of Arabidopsis thaliana. *Journal of experimental botany*, 55, 1697-1706.

Matsuoka, K. and Klionsky, D., J. (2008) Chimeric Fluorescent Fusion Proteins to Monitor Autophagy in Plants. In *Methods in Enzymology*: Academic Press, pp. 541-555.

Matsuoka, K.a.K., D.J. (2008) Chimeric Fluorescent Fusion Proteins to Monitor Autophagy in Plants. In *Methods in enzymology*: Academic Press, pp. 541-555.

Maxam, A.M. and Gilbert, W. (1977) A new method for sequencing DNA. *Proceedings of the National Academy of Sciences of the United States of America*, 74, 560-564.

Meselson, M. and Yuan, R. (1968) DNA Restriction Enzyme from E. coli. *Nature*, 217, 1110-1114.

Meusser, B., Hirsch, C., Jarosch, E. and Sommer, T. (2005) ERAD: the long road to destruction. *Nat Cell Biol*, 7, 766-772.

Meyerowitz, E.M. (2001) Prehistory and history of Arabidopsis research. *Plant Physiol*, 125, 15-19.

Mizushima, N., Levine, B., Cuervo, A.M. and Klionsky, D.J. (2008) Autophagy fights disease through cellular self-digestion. *Nature*, 451, 1069-1075.

Mizushima, N., Noda, T., Yoshimori, T., Tanaka, Y., Ishii, T., George, M.D., Klionsky, D.J., Ohsumi, M. and Ohsumi, Y. (1998) A protein conjugation system essential for autophagy. *Nature*, 395, 395-398.

Moscat, J., Diaz-Meco, M.T. and Wooten, M.W. (2007) Signal integration and diversification through the p62 scaffold protein. 32, 95-100.

Mueller, T.D. and Feigon, J. (2002) Solution Structures of UBA Domains Reveal a Conserved Hydrophobic Surface for Protein-Protein Interactions. *Journal of Molecular Biology*, 319, 1243-1255.

Mullis, K.B. and Faloona, F.A. (1987) Specific synthesis of DNA in vitro via a polymerase-catalyzed chain reaction. *Methods in enzymology*, 155, 335-350.

Müller, S., Kursula, I., Zou, P. and Wilmanns, M. (2006) Crystal structure of the PB1 domain of NBR1. *FEBS Letters*, 580, 341-344.

Nakamura, T. and Lipton, S. (2007) Molecular mechanisms of nitrosative stress-mediated protein misfolding in neurodegenerative diseases. *Cellular and Molecular Life Sciences (CMLS)*, 64, 1609-1620.

Nezis, I.P., Simonsen, A., Sagona, A.P., Finley, K., Gaumer, S., Contamine, D., Rusten, T.E., Stenmark, H. and Brech, A. (2008) Ref(2)P, the Drosophila melanogaster homologue of mammalian p62, is required for the formation of protein aggregates in adult brain. *J. Cell Biol.*, 180, 1065-1071.

Noda, N.N., Kumeta, H., Nakatogawa, H., Satoo, K., Adachi, W., Ishii, J., Fujioka, Y., Ohsumi, Y. and Inagaki, F. (2008) Structural basis of target recognition by Atg8/LC3 during selective autophagy. *Genes to Cells*, 13, 1211-1218.

Noda, T. and Ohsumi, Y. (1998) Tor, a Phosphatidylinositol Kinase Homologue, Controls Autophagy in Yeast. *J. Biol. Chem.*, 273, 3963-3966.

Noda, Y., Kohjima, M., Izaki, T., Ota, K., Yoshinaga, S., Inagaki, F., Ito, T. and Sumimoto, H. (2003) Molecular Recognition in Dimerization between PB1 Domains. *J. Biol. Chem.*, 278, 43516-43524.

Ohsumi, Y. (2001) Molecular dissection of autophagy: two ubiquitin-like systems. *Nat Rev Mol Cell Biol*, 2, 211-216.

Orvedahl, A. and Levine, B. (2008) Viral evasion of autophagy. *Autophagy*, 4, 280-285.

P. Zambryski, H.J., C. Genetello, J. Leemans, M. Van Montagu, and J. Schell (1983) Ti plasmid vector for the introduction of DNA into plant cells without alteration of their normal regeneration capacity. *EMBO*, 2, ø2143–2150

Pandey, U.B., Nie, Z., Batlevi, Y., McCray, B.A., Ritson, G.P., Nedelsky, N.B., Schwartz, S.L., DiProspero, N.A., Knight, M.A., Schuldiner, O., Padmanabhan, R., Hild, M., Berry, D.L., Garza, D., Hubbert, C.C., Yao, T.-P., Baehrecke, E.H. and Taylor, J.P. (2007) HDAC6 rescues neurodegeneration and provides an essential link between autophagy and the UPS. *Nature*, 447, 860-864.

Pankiv, S., Clausen, T.H., Lamark, T., Brech, A., Bruun, J.-A., Outzen, H., Overvatn, A., Bjorkoy, G. and Johansen, T. (2007) p62/SQSTM1 Binds Directly to Atg8/LC3 to Facilitate Degradation of Ubiquitinated Protein Aggregates by Autophagy. *J. Biol. Chem.*, 282, 24131-24145.

Park, J.C., Walsh, C., Yun, Y., Strominger, J. and Shin, J. (1995) Phosphotyrosine-independent binding of a 62-kDa protein to the src homology 2 (SH2) domain of p56lck and its regulation by phosphorylation of Ser-59 in the lck unique N-terminal region. *Procedings of the National Academy of Sciences*, 92, 12338-12342.

Pohl, C. and Jentsch, S. (2009) Midbody ring disposal by autophagy is a post-abscission event of cytokinesis. *Nat Cell Biol*, 11, 65-70.

Prasher, D.C., Eckenrode, V.K., Ward, W.W., Prendergast, F.G. and Cormier, M.J. (1992) Primary structure of the Aequorea victoria green-fluorescent protein. *Gene*, 111, 229-233.

Pujol, C., Klein, K.A., Romanov, G.A., Palmer, L.E., Cirota, C., Zhao, Z. and Bliska, J.B. (2009) Yersinia pestis can reside in autophagosomes and avoid xenophagy in murine macrophages by preventing vacuole acidification. *Infect. Immun.*, IAI.00068-00009.

Puls, A., Schmidt, S., Grawe, F. and Stabel, S. (1997) Interaction of protein kinase C zeta with ZIP, a novel protein kinase C-binding protein. *Proceedings of the National Academy of Sciences*, 94, 6191-6196.

Pursiheimo, J.P., Rantanen, K., Heikkinen, P.T., Johansen, T. and Jaakkola, P.M. (2009) Hypoxia-activated autophagy accelerates degradation of SQSTM1/p62. *Oncogene*, 28, 334-344.

Raasi, R.V., Fushman, D. and Pickart, C.M. (2005) Diverse polyubiquitin interaction properties of ubiquitin-associated domains. *Nature structural & molecular biology*, 12, 708 - 714.

Raasi, S. and Pickart, C.M. (2003) Rad23 Ubiquitin-associated Domains (UBA) Inhibit 26 S Proteasome-catalyzed Proteolysis by Sequestering Lysine 48-linked Polyubiquitin Chains. *Journal of Biological Chemistry*, 278, 8951-8959.

Raymond, S. and Weintraub, L. (1959) Acrylamide Gel as a Supporting Medium for Zone Electrophoresis. *Science*, 130, 711-.

Reinstein, E. and Ciechanover, A. (2006) Narrative Review: Protein Degradation and Human Diseases: The Ubiquitin Connection. *Ann Intern Med*, 145, 676-684.

Rose, T.L., Bonneau, L., Der, C., Marty-Mazars, D. and Marty, F. (2006) Starvation-induced expression of autophagy-related genes in Arabidopsis. *Biology of the Cell*, 98, 53-67.

Rubinsztein, D.C. (2006) The roles of intracellular protein-degradation pathways in neurodegeneration. *Nature*, 443, 780-786.

Saiki, R.K., Gelfand, D.H., Stoffel, S., Scharf, S.J., Higuchi, R., Horn, G.T., Mullis, K.B. and Erlich, H.A. (1988) Primer-directed enzymatic amplification of DNA with a thermostable DNA polymerase. *Science*, 239, 487-491.

Sakai, Y., Koller, A., Rangell, L.K., Keller, G.A. and Subramani, S. (1998) Peroxisome Degradation by Microautophagy in Pichia pastoris: Identification of Specific Steps and Morphological Intermediates. *J. Cell Biol.*, 141, 625-636.

Sanchez, P., De Carcer, G., Sandoval, I.V., Moscat, J. and Diaz-Meco, M.T. (1998) Localization of Atypical Protein Kinase C Isoforms into Lysosome-Targeted Endosomes through Interaction with p62. *Mol. Cell. Biol.*, 18, 3069-3080.

Sanger, F. and Coulson, A.R. (1975) A rapid method for determining sequences in DNA by primed synthesis with DNA polymerase. *J Mol Biol*, 94, 441-448.

Schlesinger, D., Goldstein, G. and Niall, H. (1975) The complete amino acid sequence of ubiquitin, an adenylate cyclase stimulating polypeptide probably universal in living cells. *Biochemistry*, 14, 2214-2218.

Schwechheimer, C. and Schwager, K. (2004) Regulated proteolysis and plant development. *Plant Cell Rep*, 23, 353-364.

Scott, S.V., Baba, M., Ohsumi, Y. and Klionsky, D.J. (1997) Aminopeptidase I Is Targeted to the Vacuole by a Nonclassical Vesicular Mechanism. *J. Cell Biol.*, 138, 37-44.

Seibenhener, M.L., Babu, J.R., Geetha, T., Wong, H.C., Krishna, N.R. and Wooten, M.W. (2004) Sequestosome 1/p62 Is a Polyubiquitin Chain Binding Protein Involved in Ubiquitin Proteasome Degradation. *Molecular and Cellular Biology*, 24, 8055-8068.

Shaner, C., Steinbach, A. and Tsien, Y. (2005) A guide to choosing fluorescent proteins. *Nature methods*, 2, 905-909.

Shieh, H.-L. and Chiang, H.-L. (1998) In Vitro Reconstitution of Glucose-induced Targeting of Fructose-1,6-bisphosphatase into the Vacuole in Semi-intact Yeast Cells. *J. Biol. Chem.*, 273, 3381-3387.

Shimomura, O., Johnson, F. and Saiga, Y. (1962) Extraction, purification and properties of aequorin, a bioluminescent protein from the luminous hydromedusan, Aequorea. *Journal of cellular and comparative physiology*, 223-239.

Slavikova, S., Shy, G., Yao, Y., Glozman, R., Levanony, H., Pietrokovski, S., Elazar, Z. and Galili, G. (2005) The autophagy-associated Atg8 gene family operates both under favourable growth conditions and under starvation stresses in Arabidopsis plants. *J. Exp. Bot.*, 56, 2839-2849.

Smith, E. and Townsend, C. (1907) A plant tumor of bacterial origin. *Science*, 15, 671 - 673.

Smith, L.M., Sanders, J.Z., Kaiser, R.J., Hughes, P., Dodd, C., Connell, C.R., Heiner, C., Kent, S.B.H. and Hood, L.E. (1986) Fluorescence detection in automated DNA sequence analysis. *Nature*, 321, 674-679.

Somers, D.E. and Fujiwara, S. (2009) Thinking outside the F-box: novel ligands for novel receptors. *Trends in Plant Science*, 14, 206-213.

Sosuke, Y., Motoyuki, K., Kenji, O., Masashi, Y., Ryu, T., Takashi, I., Hideki, S. and Fuyuhiko, I. (2003) The PB1 domain and the PC motif-containing region are structurally similar protein binding modules. *The EMBO journal*, 22, 4888–4897.

Strnad, P., Zatloukal, K., Stumptner, C., Kulaksiz, H. and Denk, H. (2008) Mallory-Denk-bodies: Lessons from keratin-containing hepatic inclusion bodies. *Biochimica et Biophysica Acta (BBA) - Molecular Basis of Disease*, 1782, 764-774.

Sugawara, K., Suzuki, N.N., Fujioka, Y., Mizushima, N., Ohsumi, Y. and Inagaki, F. (2004) The crystal structure of microtubule-associated protein light chain 3, a mammalian homologue of Saccharomyces cerevisiae Atg8. *Genes Cells*, 9, 611-618.

Sumimoto, H., Kamakura, S. and Ito, T. (2007) Structure and Function of the PB1 Domain, a Protein Interaction Module Conserved in Animals, Fungi, Amoebas, and Plants. *Science STKE*, 2007, re6-.

Suzuki, N.N., Yoshimoto, K., Fujioka, Y., Ohsumi, Y. and Inagaki, F. (2005) The Crystal Structure of Plant ATG12 and its Biological Implication in Autophagy. *Autophagy*, 1, 119 - 126

T. Ito, Y.M., T. Ago, K. Ota, H. Sumimoto (2001) Novel modular domain PB1 recognizes PC motif to mediate functional protein-protein interactions. *EMBO Journal*, 20, 3938–3946

Takeshige, K., Baba, M., Tsuboi, S., Noda, T. and Ohsumi, Y. (1992) Autophagy in yeast demonstrated with proteinase-deficient mutants and conditions for its induction. *J. Cell Biol.*, 119, 301-311.

Talloczy, Z., Virgin, H. and Levine, B. (2006) PKR-Dependent Xenophagic Degradation of Herpes Simplex Virus Type 1. *Autophagy*, 2, 24 - 29.

Thompson, A.R., Doelling, J.H., Suttangkakul, A. and Vierstra, R.D. (2005) Autophagic Nutrient Recycling in Arabidopsis Directed by the ATG8 and ATG12 Conjugation Pathways. *Plant Physiol.*, 138, 2097-2110.

Thompson, A.R. and Vierstra, R.D. (2005) Autophagic recycling: lessons from yeast help define the process in plants. *Current Opinion in Plant Biology*, 8, 165-173.

Thorne, H. (1966) Electrophoretic separation of polyoma virus DNA from host cell DNA. *Virology*, 2, 234-239.

Towbin, H., Staehelin, T. and Gordon, J. (1979) Electrophoretic transfer of proteins from polyacrylamide gels to nitrocellulose sheets: procedure and some applications. *PNAS*, 4350-4354.

Utako Nagaoka, K.K., Nihar Ranjan Jana, Hiroshi Doi, Mieko Maruyama, Kenichi Mitsui, Fumitaka Oyama, Nobuyuki Nukina, (2004) Increased expression of p62 in expanded polyglutamine-expressing cells and its association with polyglutamine inclusions. *Journal of Neurochemistry*, 91, 57-68.

Vadlamudi, R.K., Joung, I., Strominger, J.L. and Shin, J. (1996) p62, a Phosphotyrosine-independent Ligand of the SH2 Domain of p56lck, Belongs to a New Class of Ubiquitin-binding Proteins. *J. Biol. Chem.*, 271, 20235-20237.

van Doorn, W.G. and Woltering, E.J. (2005) Many ways to exit? Cell death categories in plants. *Trends in plant science*, 10, 117–122.

Vogelstein, B. and Gillespie, D. (1979) Preparative and analytical purification of DNA from agarose. *Proceedings of the National Academy of Sciences of the United States of America*, 76, 615-619.

Wada, S., Ishida, H., Izumi, M., Yoshimoto, K., Ohsumi, Y., Mae, T. and Makino, A. (2009) Autophagy Plays a Role in Chloroplast Degradation during Senescence in Individually Darkened Leaves. *Plant Physiol.*, 149, 885-893.

Wang, W.a.M., B.A. (1999) Two-stage PCR protocol allowing introduction of multiple mutations, deletions and insertions using QuikChange Site-Directed Mutagenesis. *Biotechniques*, 26, 680-682.

Wang, Y., Weiss, L. and Orlofsky, A. (2009) Host cell autophagy is induced by Toxoplasma gondii and contributes to parasite growth. *Journal of Biological Chemistry*, 284, 1694-1701.

Welchman, R.L., Gordon, C. and Mayer, R.J. (2005) Ubiquitin and ubiquitin-like proteins as multifunctional signals. *Nat Rev Mol Cell Biol*, 6, 599-609.

Wiebe, H., Meijer, I., van der Klei, J., Veenhuis, M. and Kiel, J.A.K.W. (2007) ATG Genes Involved in Non-Selective Autophagy are Conserved from Yeast to Man, but the Selective Cvt and Pexophagy Pathways also Require Organism-Specific Genes. *Autophagy*, 3, 106 - 116.

Wilson, M.I., Gill, D.J., Perisic, O., Quinn, M.T. and Williams, R.L. (2003) PB1 Domain-Mediated Heterodimerization in NADPH Oxidase and Signaling Complexes of Atypical Protein Kinase C with Par6 and p62. *Molecular Cell*, 12, 39-50.

Xie, Z. and Klionsky, D.J. (2007) Autophagosome formation: core machinery and adaptations. *Nat Cell Biol*, 9, 1102-1109.

Xie, Z., Nair, U. and Klionsky, D.J. (2008) Atg8 Controls Phagophore Expansion during Autophagosome Formation. *Molecular biology of the Cell*, 19, 3290–3298.

Xin, Y., Yu, L., Chen, Z., Zheng, L., Fu, Q., Jiang, J., Zhang, P., Gong, R. and Zhao, S. (2001) Cloning, Expression Patterns, and Chromosome Localization of Three Human and Two Mouse Homologues of GABAA Receptor-Associated Protein. *Genomics*, 74, 408-413.

Xiong, Y., Contento, A.L. and Bassham, D.C. (2007) Disruption of Autophagy Results in Constitutive Oxidative Stress in Arabidopsis. *Autophagy*, 3, 257 - 258.

Yano, K., Suzuki, T. and Moriyasu, Y. (2007) Constitutive Autophagy in Plant Root Cells. *Autophagy*, 3, 360 - 362.

Zatloukal, K., Stumptner, C., Fuchsbichler, A., Heid, H., Schnoelzer, M., Kenner, L., Kleinert, R., Prinz, M., Aguzzi, A. and Denk, H. (2002) p62 Is a Common Component of Cytoplasmic Inclusions in Protein Aggregation Diseases. *Am J Pathol*, 160, 255-263.

6.0 Appendix

Table 6.1. Description of the different types of autophagy (Klionsky, et al. 2007).

Name	Description
Aggrephagy	The selective autophagic sequestration of protein aggregates.
Autophagy	Any process involving degradative delivery of aportion of the cytoplasm to the lysosome or vacuole that does notinvolve direct transport through the endocytic or vacuolar protein sorting, Vps, pathways.
Chaperone-mediated autophagy (CMA)	Import and degradation of soluble cytosolic proteins by chaperone-dependent, direct translocation across the lysosomal membrane.
Crinophagy	Direct fusion of secretory vesicles with lysosomes.
Cytoplasm to vacuole targeting (Cvt)	A biosynthetic pathway in yeast that transports resident hydrolases to the vacuole (the yeast lysosome) through a selective autophagy-related process.
Macroautophagy	The largely nonspecific autophagic sequestration of cytoplasm into a double- or multiple-membrane-delimited compartment (an autophagosome) of nonlysosomal/vacuolar origin.
Microautophagy	Uptake and degradation of cytoplasm by invagination of the lysosomal/vacuolar membrane.
Mitophagy	Selective autophagic sequestration and degradation of mitochondria.
Pexophagy	Selective type of autophagy involving the sequestration and degradation of peroxisomes; can occur by a micro- or macropexophagic process.
Piecemeal microautophagy of the nucleus	Intrusion of portions of the nucleus into the vacuole, followed by scission and degradation.
Reticulophagy	Selective autophagic sequestration and degradation of endoplasmic reticulum.
Vacuole import and degradation	Selective uptake of cytosolic fructose-1,6-bisphosphatase, and possibly other proteins, within 30 nm single membrane vesicles, followed by fusion with the vacuole
Xenophagy	Selective degradation of microbes (e.g., bacteria, fungi, parasites and/or viruses) through an autophagy-related mechanism.

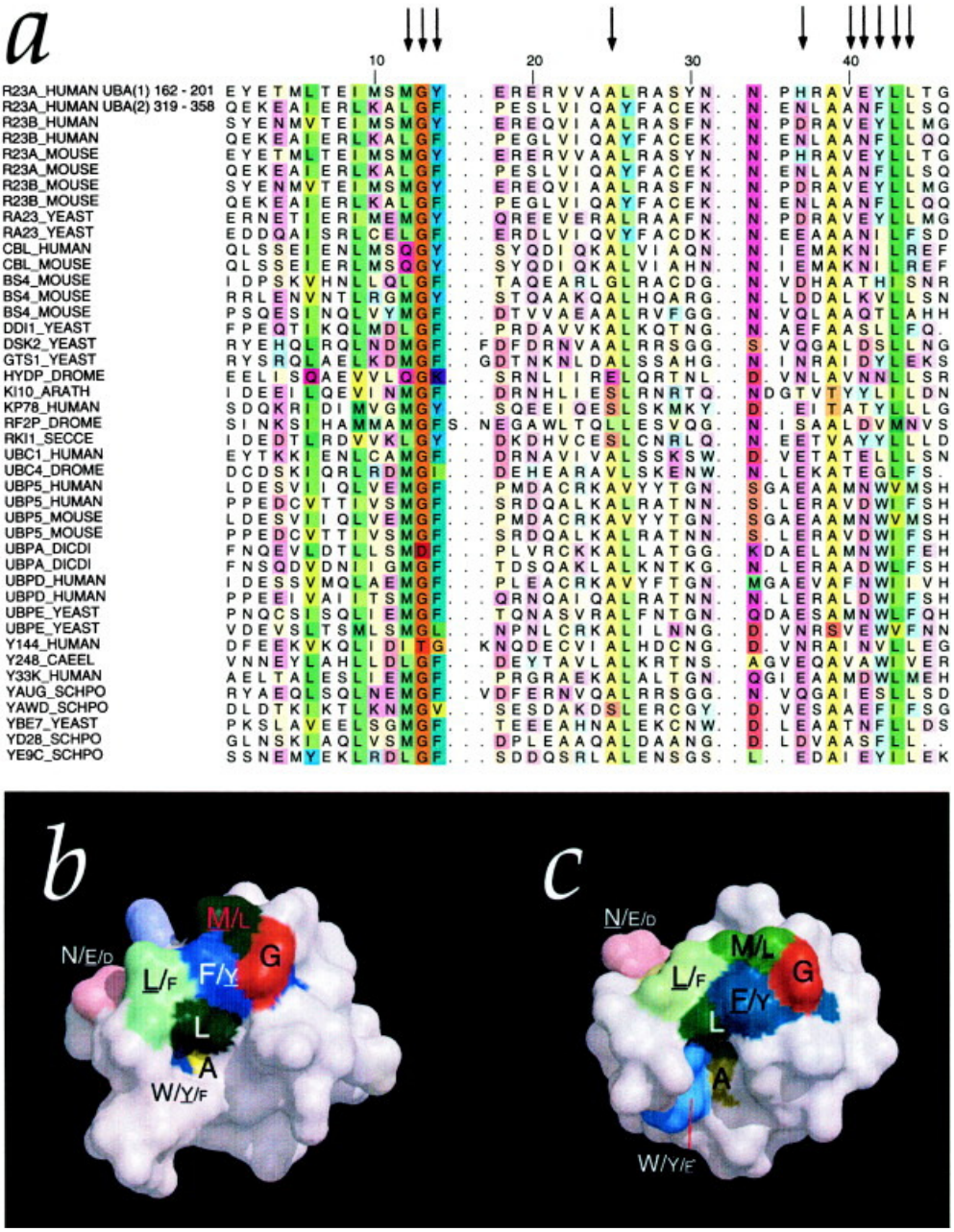

Figur 6.1: Sequence comparison of selected UBA domains. Very conserved aa are shown in the brightest colors. Arrows point to the amino acid residues that are shown labeled in the surface representations, constituting the hydrophobic patch that binds ubiquitin. (From (Mueller and Feigon 2002).

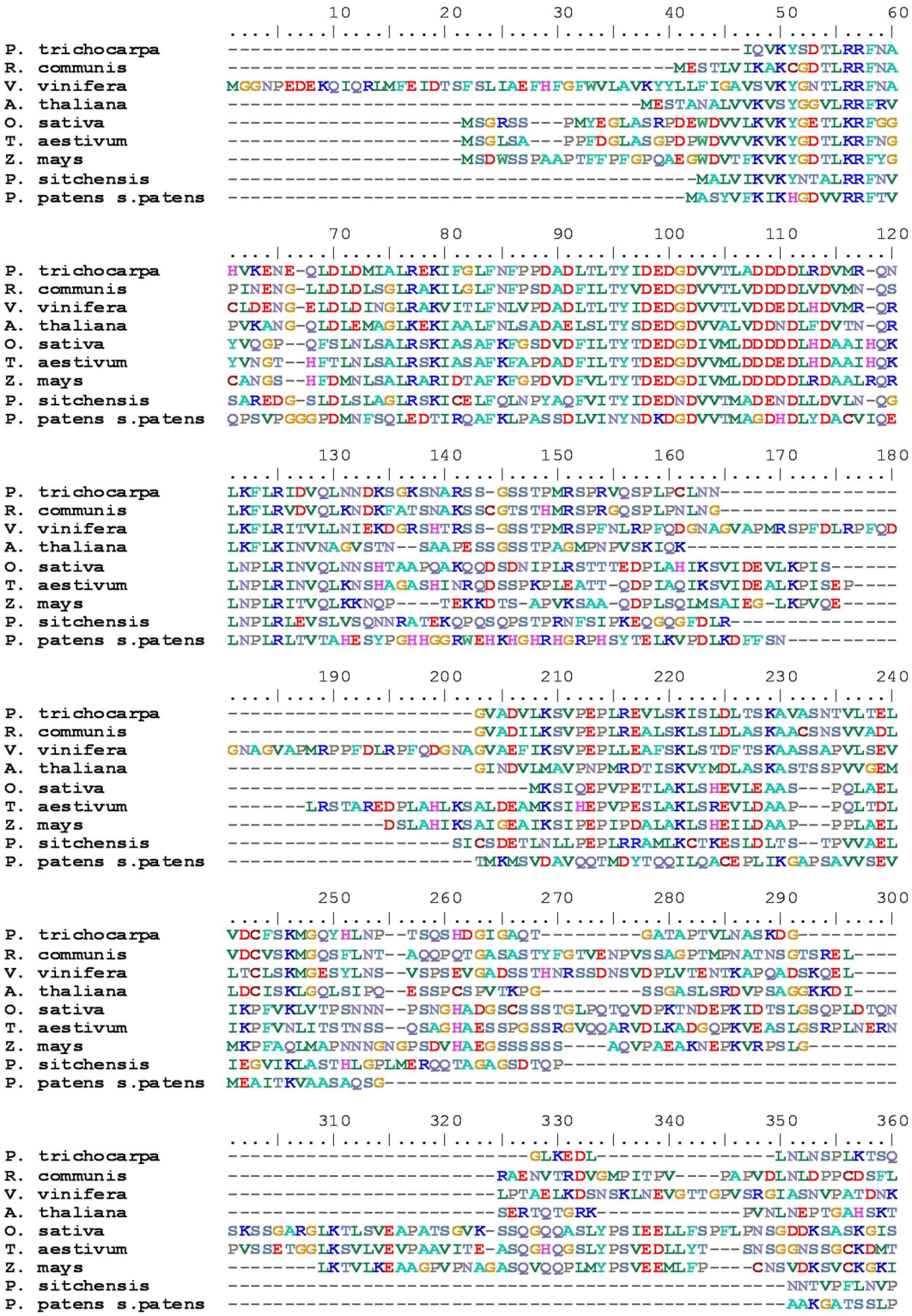

Figur 6.2: Multiple sequence alignment of Nbr1 homologues from nine different plant species. Species: Populus trichocarpa (Black cottonwood), Ricinus communis (Castor oil plant), Vitis vinifera (Common grape vine), Arabidopsis thaliana (Thale cress), Oryza sativa (Common rice), Triticum aestivum (Common wheat), Zea mays (maize), Picea sitchensis (Sitka spruce), Physcomitrella patens subsp. Patens (moss). Aligned using ClustalW (BLOSUM30 matrix)

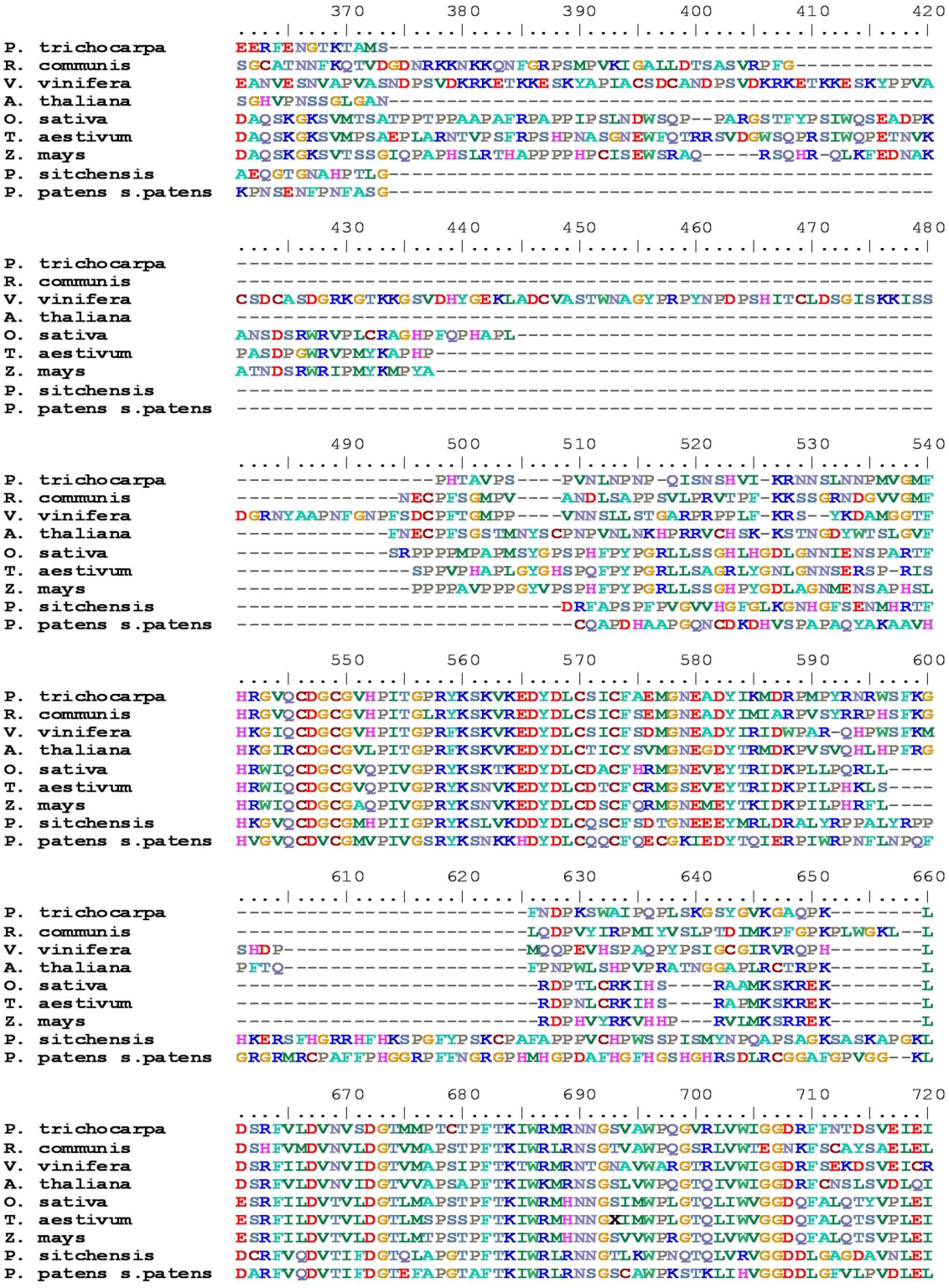

Figure 6.2 continued: Multiple sequence alignment of Nbr1 homologues from nine different plant species. Species: Populus trichocarpa (Black cottonwood), Ricinus communis (Castor oil plant), Vitis vinifera (Common grape vine), Arabidopsis thaliana (Thale cress), Oryza sativa (Common rice), Triticum aestivum (Common wheat), Zea mays (maize), Picea sitchensis (Sitka spruce), Physcomitrella patens subsp. Patens (moss). Aligned using ClustalW (BLOSUM30 matrix)

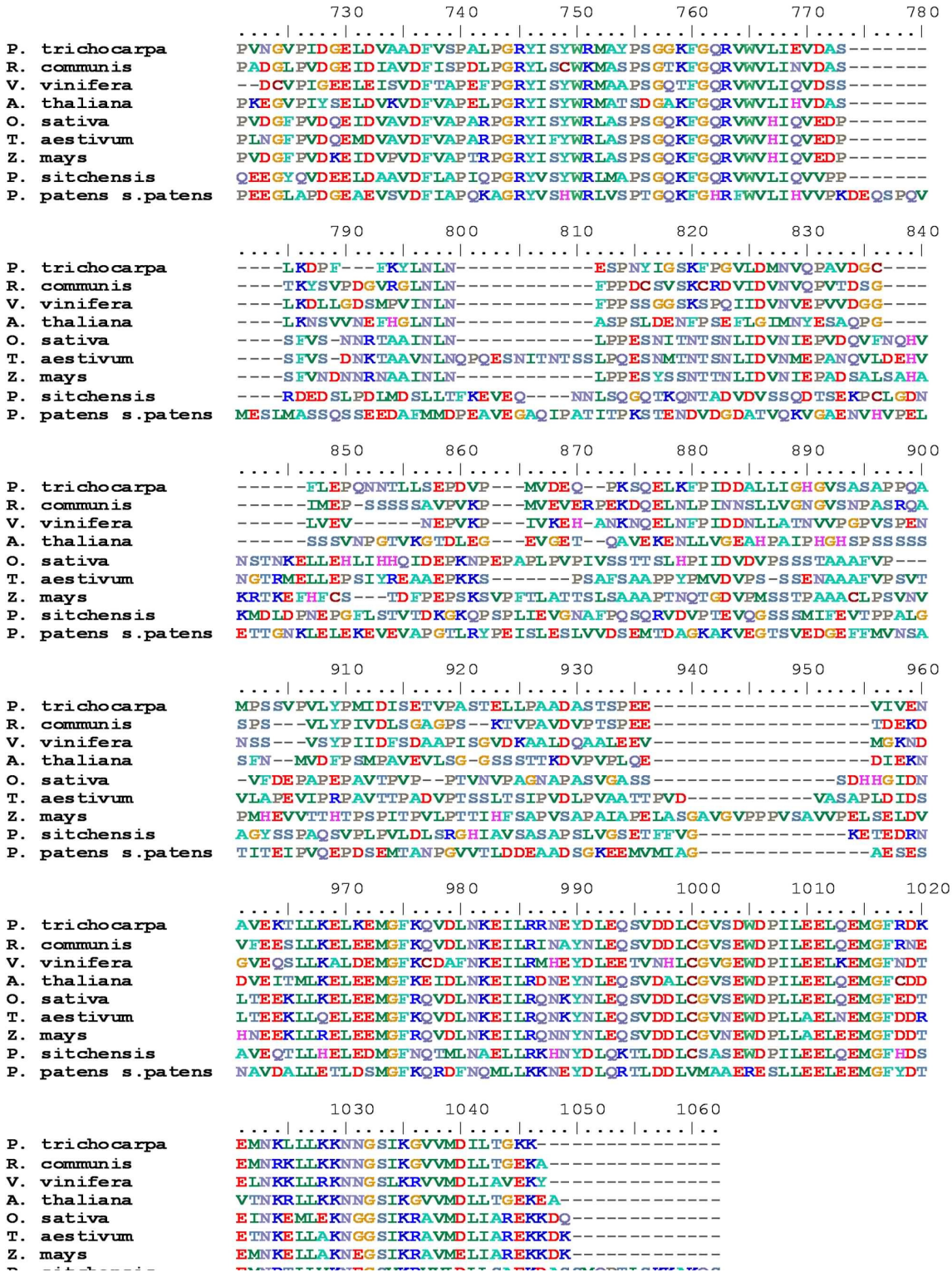

Figure 6.2 continued: Multiple sequence alignment of Nbr1 homologues from nine different plant species. Species: Populus trichocarpa (Black cottonwood), Ricinus communis (Castor oil plant), Vitis vinifera (Common grape vine), Arabidopsis thaliana (Thale cress), Oryza sativa (Common rice), Triticum aestivum (Common wheat), Zea mays (maize), Picea sitchensis (Sitka spruce), Physcomitrella patens subsp. Patens (moss). Aligned using ClustalW (BLOSUM30 matrix)